The Role of Inhibitor of Apoptosis Proteins (IAPs) and Receptor Interacting Protein Kinases (RIPKs) in Cancer

---

Dissertation

zur

Erlangung der naturwissenschaftlichen Doktorwürde

(Dr.sc.nat.)

vorgelegt der

Mathematisch-Naturwissenschaftlichen Fakultät der

Universität Zürich

von

Kay Franz Hänggi

aus

Balgach SG

Promotionskommitee

Dr. W.Wei-Lynn Wong (Vorsitz und Leitung der Dissertation)

Prof. Dr. Christian Münz (Vorsitz)

Prof. Dr. Anne Müller

Prof. Dr. Burkhard Becher

Zürich, 2017

I. Table of Contents

II. Acknowledgements

First of all I want to thank my Ph.D supervisor Lynn Wong who has guided me with great passion through the past four and a half years of my Ph.D. I was able to learn so many things from you, both scientifically and ethically in order to be a good scientist. You have always set a high Standard on these things and because of that I have a high opinion about you. I estimate as well that you gave me the trust and freedom to follow my ideas for the project during my Ph.D, which really meant a lot to me. I will always be thankful for this time!

I want to thank Christian Münz for being the head of my Ph.D committee and for the helpful and excellent advices during the committee meetings, as well as during the institute meetings. I am also very grateful that you supported me for my future career in science.

Another big thank goes to the remaining committee members Anne Müller and Burkhard Becher for their good advice and shared expertise, which helped my project.

Further I want to thank the following persons:

- My dear colleagues Janin, Lazaros and Lisanne for helping and working with me. It was really nice to have you as labmates. And Lazaros gets an extra thank for his help on my project and your reliability in doing things, at work and at home.
- Tom Hartwig as my best buddy from the institute. It was always good to talk to you and smoke on the balcony to release some stress. We discussed science as well as life, and for that I have enjoyed your company a lot, and I still do.
- Michael 'Miguel' Maurer und Isaak Quast for the support especially when I started at the institute. You made me feel welcome!

- Paulina Kulig from the Becher Group, who helped a lot in the beginning getting the tumor model started.
- Melanie Greter and Andrew 'Andy' Croxford for the great expertise and helpful advice that helped assessing the myeloid cells in the lung.
- The animal housing technicians Ondrej Klimes, Deborah Häfeli and Nicole Burkhalter
- Alex Sartori, that I could do a great master thesis in his lab and since then he always had an open ear and supportive advice.
- Mini lieb Fründin Martina
- Alli mini Fründe usm Rhyntl und vu Züri wo i grossartigi Zite ha chöne gnüsse.
- Zu gueter Letscht möcht I mi ganz herzlich bi mine liebste Eltere Marco und Rita bedanke. Ihr händ mir das ganze Studium ermöglicht und ohni eu wär das ganz sicher nöd möglich gsi. Ihr händ mi in allne Belange unterstützt und wenn I dahei in Balgach gsi bin ha i immer chöne alli Sorge vergässe und Energie uftanke. Danke für alles!

–

Meine Doktorarbeit ist meiner zukünftigen Tochter gewidmet

III. Abbreviations

IAP Inhibitor of Apoptosis Proteins
cIAP cellular Inhibitor of Apoptosis proteins
RIPK Receptor Interacting Protein Kinase
MLKL Mixed Lineage Kinase-domain Like
TNF Tumor Necrosis Factor
TNFR TNF Receptor
TAK1 Transforming Growth Factor Beta-activated Kinase 1
TAB1 TGF-β activated Kinase 1
VEGF Vascular Endothelial Growth Factor
VEGFR VEGF Receptor
FGF Fibroblast Growth Factor
FGFR FGF Receptor
PDGF Platelet-derived Growth Factor
MMP Matrix-metalloproteinase
HMGB1 High-Mobility Group 1
PD-1 Programmed Death 1
CTLA-4 Cytotoxic T Lymphocyte Associated protein 4
PMN Pre-Metastatic Niche
TME Tumor Microenvironment
TAM Tumor Associated Macrophages
TAN Tumor Associated Neutrophils
CAF Cancer Associated Fibroblast
EC Endothelial Cell
DC Dendritic Cells
T cell T lymphocyte
BMDM Bone Marrow Derived Macrophages
BMDC Bone Marrow Derived DC
PCD Programmed Cell Death
ICD Immunogenic Cell Death
PAMP Pathogen Associated Molecular Pattern
DAMP Danger Associated Molecular Patterns

CMV Cytomegalovirus

MCMV Mouse Cytomegalovirus

IFN Interferons

TLR Toll-like Receptor

PRR Pattern Recognition Receptor

DR Death Receptor

NSCLC Non-Small Cell Lung Carcinoma

NETs Neutrophil Extracellular Traps

ECM Extracellular Matrix

PDA Pancreatic Ductal Adenocarcinoma

PDEC Pancreatic Ductal Epithelial Cells

SMAC Second Mitochondria-derived Activator of Caspases

AML Acute myeloid leukemia

ALL Acute lymphoblastic leukemia

FLT3-ITD FLT3-internal tandem duplication

LIC Leukemia initiating cells

IV. General Summary

In comparison to apoptosis, programmed necrosis or necroptosis is a caspase-independent form of programmed cell death with proinflammatory properties due to uncontrolled release of intracellular contents upon membrane rupture and the concomitant secretion of danger associated molecular patterns (DAMPs) and proinflammatory cytokines. Programmed cell death is a crucial process involved in development and tissue homeostasis of organisms. The ability to induce programmed cell death is often disrupted in cancer cells and reveals an important strategy by which neoplastic cells promote survival and proliferation, as well as instead contributes to chemoresistance of cancer cells.

Inhibitor of apoptosis proteins (IAPs) and receptor interacting protein kinases (RIPKs) are central regulators at the decision point whether a cell survives, or dies by apoptosis or necroptosis. In this process, RIPK3 and its substrate MLKL are necessary to trigger necroptosis. In contrast to MLKL, however, RIPK3 has shown the ability to regulate inflammation independent of necroptosis. The relative contribution of necroptosis in cancer disease and how IAPs and RIPKs contribute *in vivo* to this is not well defined yet. Therefore, we aimed to understand the role of IAPs and RIPK in the pathology of cancer by using transplantable mouse tumor models, and how the ability of RIPKs to regulate inflammation in the tumor microenvironment alters tumor growth and progression.

My work contributed to understand how antagonizing the IAPs by Smac-mimetic compounds in combination with inhibition of p38 mitogen-activated protein kinase (MAPK) or MAPK-activated protein kinase MK2 enhanced autonomous leukemia cell killing. In more detail, simultaneous inhibition of p38 or MK2 in combination with Smac-mimetics significantly increased TNF production by leukemic cells mediated by ERK and JNK, which in turn resulted in enhanced TNF-induced autocrine cell killing by apoptosis. My work also showed that the loss of RIPK3 in the tumor microenvironment

decreased the ability of tumor cells to disseminate to the lung. In this process, RIPK3 in endothelial cells was responsible to promote tumor cell extravasation, which was surprisingly independent of MLKL-dependent necroptosis. Rather it was the case that in the absence of cell death, RIPK3 promoted extravasation by promoting tumor cell- and VEGF-induced vascular permeability, which was likely through altering vascular signaling via p38/HSP27 and ERK in endothelial cells. Therefore, my work provides a novel example, in which RIPK3 functions are of relevance *in vivo* independent of cell death.

In summary, the work in this manuscript assesses the differential roles of IAPs and RIPKs in the tumor and the tumor microenvironment, and to which degree necroptosis and RIPK3 alternative functions contribute to the outcome of cancer disease. Thereby, the role of IAPs and RIPKs is put in context to the literature and potential mechanism underlying the cell death independent functions of RIPK3 in endothelial cells are discussed. Further, by addressing the benefits and limitations, targeting the necroptosis machinery as a strategy for therapeutic intervention in cancer diseases is put in perspective.

V. Zusammenfassung

Im Vergleich zur Apoptose ist die Programmierte Necrose oder auch Necroptose genannt ein Caspasen-unabhängiger Prozess, bei welchem entzündliche Cytokine und 'Danger-associated molecular patterns' (DAMPs) sekretiert werden sobald die Zelle als Folge der Necroptose geplatzt ist. Programmierer Zelltod ist ein wichtiger Bestandteil während der Entwicklung und Homeostase. In Krebszellen sind diese Zelltod Prozesse oft gestört, welches fördernd auf Überlebensprogramme und die Zellteilung wirkt, aber auch wesentlich zur Chemoresistenz von Krebszellen beiträgt.

Hierbei spielen die 'Inhibitor of Apoptosis' Proteine (IAPs) und die 'Receptor-interacting Protein Kinasen' (RIPKs) eine zentrale Rolle, ob eine Zelle überlebt und proliferiert, oder durch Apoptose oder Necroptose stirbt. Dabei ist RIPK3 und MLKL, welches ein Substrat von RIPK3 darstellt, unablässig zur Ausführung von Necroptose. Im Gegensatz zu MLKL hat sich gezeigt dass RIPK3 Entzündungsreaktionen regulieren kann und dies unabhängig von der Necroptose Funktion. Der relative Beitrag von Necroptose zum Krankheitsverlauf in Krebs *in vivo* ist bis dato nur wenig verstanden. Deshalb war es unser Ziel die Rolle der IAPs und RIPKs im Tumor, sowie der Tumorumgebung anhand von Transplantierbaren Maus Tumormodellen, zu untersuchen.

Die Resultate meiner Arbeit haben gezeigt, dass die Antagonisierung von IAPs mit Hilfe von 'Smac-mimetics' in Kombination mit Inhibitoren gegen p38 oder MK2 Mitogen-aktivierter Protein Kinasen (MAPKs) die Krebszellen effizienter durch Apoptose Induktion getötet wurden. Dabei hat die Kombinationsbehandlung von Krebszellen mit Smac-mimetics und p38 oder MK2 Inhibitoren dazu geführt dass via ERK und JNK vermehrt autokrines TNF produziert wurde im Vergleich zur Einzelbehandlung, welches wiederum zur Folge hatte dass Krebszellen vermehrt durch autokrines TNF-induzierte Apoptose gestorben sind. Weiters hat meine Arbeit gezeigt dass der Verlust von RIPK3 in der Tumor Umgebung dazu geführt hat dass Tumorzellen sich

weniger verbreiten konnten um Ableger zu bilden. Dabei hat sich herausgestellt, dass RIPK3 in Endothelzellen dafür verantwortlich war. Hierbei unterstütze RIPK3 in Endothelzellen die Induzierung von vaskulärer Permeabilität durch Tumorzellen, wie auch durch den Angiogenese Faktor 'vascular endothelial growth factor' VEGF, welches für die Extravasierung von Tumorzellen nötig ist. Überraschend war, dass diese Prozesse unabhängig von MLKL-abhängiger Nekroptose war. Wir konnten diesen Effekt von RIPK3 darauf zurückführen dass RIPK3 die intrazellulären Signalwege via p38/HSP27 und ERK in Endothelzellen gestört hat. Deshalb ist diese Arbeit ein Beispiel für eine neue Funktion von RIPK3 welche unabhängig von der Zelltod-Funktion ist und so den Krankheitsverlauf von Krebs signifikant beeinflussen kann.

Zusammenfassend thematisiert diese Arbeit die Verschiedenen Funktionen der IAPs and RIPKs im Tumor und der Tumorumbegung, und zu welchem Grad Necroptose und RIPK3 die weitere Tumorprogression beeinflusst. Dabei wurden die Rolle der IAPs und RIPKs in den Kontext zur bekannten Literatur gesetzt und die möglichen Mechanismen, welche der Zelltod unabhängigen Funktion von RIPK3 in Endothelzellen unterliegen, diskutiert. Weiters wurde die Möglichkeit zur therapeutischen Nutzung durch gezielte Manipulierung von Necroptose in Perspektive gesetzt.

1. Introduction

1.1. The inhibitor of apoptosis protein (IAP) family

The inhibition of apoptosis is an important strategy for viruses to promote propagation or for cancer cells for survival. The inhibitor of apoptosis proteins (IAPs) were first discovered in baculovirus and were found to be shared in all metazoan organisms. There are eight IAP proteins found in humans (Figure 1) that include the neuronal apoptosis inhibitory protein NAIP (encoded by *birc1*), cellular IAP1 (cIAP1; encoded by *birc2*), cellular IAP2 (cIAP2 or BIRC3, X chromosome linked IAP (XIAP or BIRC4), Survivin (BIRC5), ubiquitin-conjugating BIR domain enzyme apollon (BIRC6), melanoma IAP (ML-IAP or BIRC7), and IAP-like protein 2 (ILP2 or BIRC8)[1,2]. The baculovirus IAP repeat (BIR) domain is shared within all members of the IAP family and IAP proteins contain one to three BIR domains. The mammalian IAPs are cIAP1, cIAP2 and XIAP and each protein contains three BIR domains for protein interaction, an Ubiquitin-associated domain (UBA) that mediates binding to poly-ubiquitin (poly-Ub) chains and a really interesting new gene (RING) domain that has E3 ubiquitin ligase activity. Furthermore, cIAP1 and cIAP2 but not XIAP have a caspase recruitment domain (CARD) that was shown to inhibit its E3 ligase activity[3-5]. Among the three IAPs, the cIAPs can bind caspases, but only XIAP can bind and inhibit caspase activity. XIAP binds to caspase-9 via the BIR3 domain and prevents formation of caspase-9 homodimerization and therefore blocks its activation for apoptosis execution[6-13]. The second mitochondria-derived activator of caspases (Smac) is encoded by the *DIABLO* gene and can inhibit XIAP by binding to the same pocket where caspases bind and therefore Smac is considered as a pro-apoptotic gene[1,2].

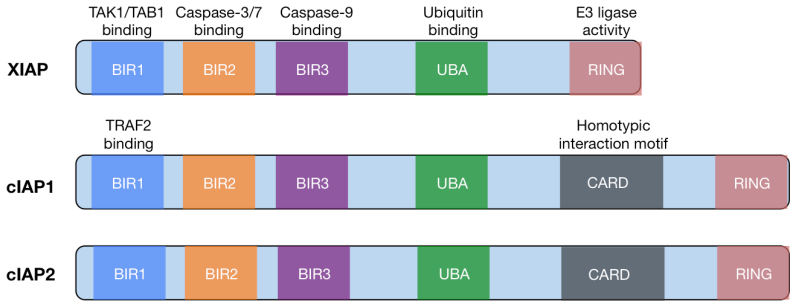

Figure 1: Structure and function of the mammalian inhibitor of apoptosis proteins (IAPs) (adapted from Bai et al, 2014)[3-5].

1.2. The receptor interacting Ser/Thr protein kinase (RIPK) family

The roles of the receptor-interacting protein (RIP) kinase (RIPK) family members are important modulators of cell death and inflammation[6-13]. The RIPK are known as serine/threonine kinases and consists of seven members (RIPK1-7). As illustrated (Figure 2), the kinase domain (KD) is relatively conserved throughout the seven RIP kinases while other functional domains are partially shared or unique. Among the gene family, only *Ripk1* and *Ripk3* contain a RIP homotypic interaction motif (RHIM) and the RHIM domain is necessary for protein-protein interaction to promote necroptosis. While RIPK1 contains a death domain (DD) at the C-term, RIPK3 does not obtain similarity in the C-terminus with any other known protein. Both, RIPK1 and RIPK3 have a prominent function in cell death signaling upon death receptor stimulation (e.g. TNFR1, Fas/CD95) at the decision point of survival and programmed cell death via either apoptosis or necrosis[14-19].

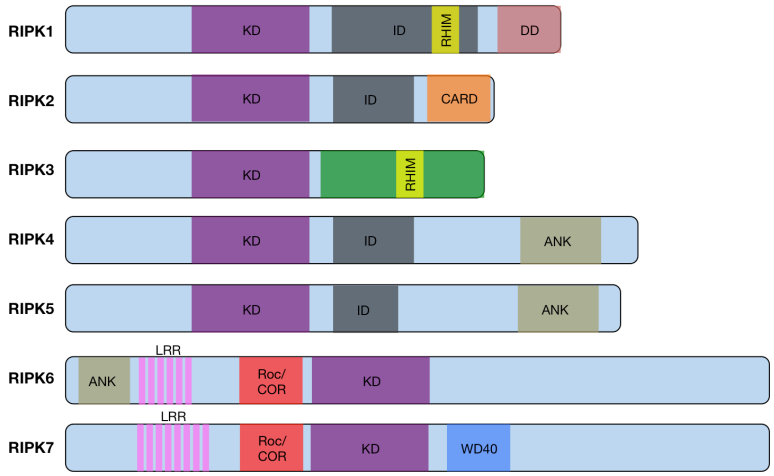

Figure 2: Structure and function of the RIPK protein family. Kinase domain (KD), intermediate domain (ID), death domain (DD), caspase activation and recruitment domain (CARD), RIP homotypic interaction motif (RHIM), ankryn repeat (ANK) domain, leucine rich repeat kinase (LRRK, protein kinase C-associated kinase, RIP-like-interacting caspase-like apoptosis-regulatory protein kinase and RIP-like-interacting caspase-like apoptosis-regulatory protein kinase (RICK) (adapted from Zhang et al., 2010)[20].

1.3. Regulation of cell death and immune responses by IAPs and RIPK

Any form of autonomous cell killing that is determined in a genetically regulated manner is termed "programmed cell death" (PCD). PCD fulfills fundamental functions in both metazoan and plants, and under physiological conditions PCD is necessary during development and tissue homeostasis but serves also important functions as part of the immune system. An overview of different forms of cell death is illustrated in Table 1.

Types of Cell Death:	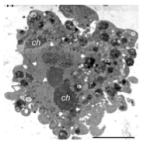 **Apoptosis**	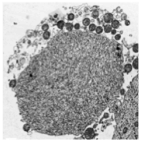 **Necroptosis**	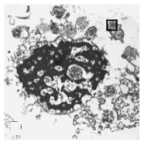 **Oncosis/Necrosis**	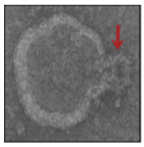 **Pyroptosis**
Morphology	• Chromatin condensation • Nuclear fragmentation • Apoptotic bodies	• Cellular swelling (nucleus and organelles) • Permeabilization and rupture of plasma membrane • Release of cellular content (DAMPs, inflammatory cellular components)	• Cytoplasmic swelling • Release of necrotic blebbs	• Cytosolic swelling • Nuclear fragmentation • Pore formation • Release of cellular content(DAMPs, inflammatory cytokines)
Signaling	Programmed	Programmed	accidental	Programmed
Triggers	• Death receptors • DNA-damage • Viral infection	• Death receptor ligands (TNF, FasL, TRAIL) • Infectious pathogens • Ischemic injury	• Toxins • Trauma • Inflammation	• DAMPs • Microbial infections
Mediators	• Initiator caspases: Caspase 8 (extrinsic), Caspase-9 (intrinsic) • Executer caspase-3/-6/-7	• TNFR signaling • RIPK1/RIPK3 necrosome		• Nod-like receptors • Inflammasome: Caspase-1/-11 dependent activation of gasdermin D
Lytic	No	Yes	Yes	Yes
Inflammation	No	Yes	Yes	Yes
Molecular markers	• α-Cleaved caspase 3/7 • Annexin-V • TUNEL	• Potentially α-Phospho-MLKL?	Not known	• Potentially Cleaved GasderminD ?

Table adapted from Kroemer et al., 2009, Inoue et al., 2013; Wallach et al, 2016
Images from Lane et al., 2005; Ziegler and Groscurth 2004; Naji et al., 2015;Liu et al., 2016

Table 1: Different forms of cell death.

1.3.1. Regulation of programmed cell death: apoptosis and necroptosis

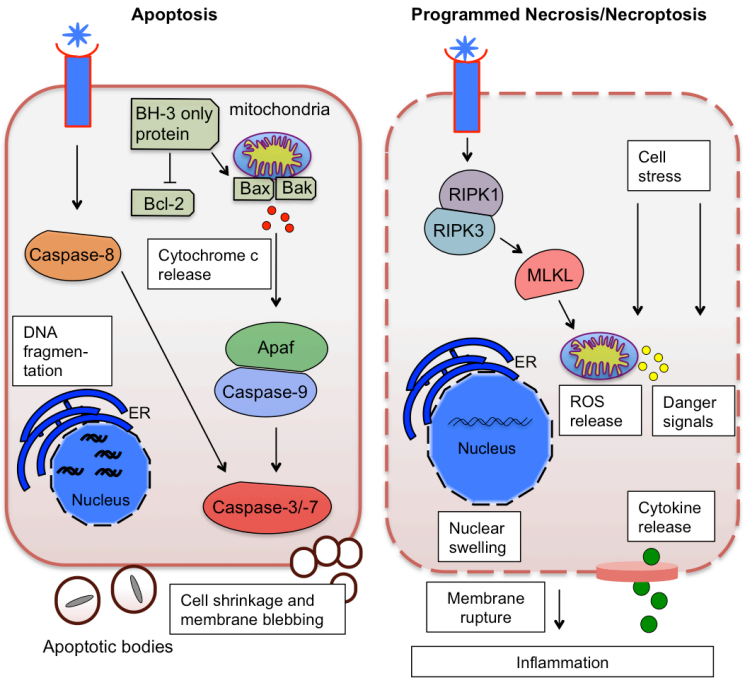

Figure 3: Differences between apoptosis and necroptosis (adapted from Ashida et al., 2011)[21].

1.3.2. Mechanisms of apoptosis execution

Apoptosis is the best described and understood form of PCD[22-25]. The process of apoptosis is defined by clear morphological aspects that include the rounding-up of the cell, retraction of pseudopods, decrease in cellular volume (pyknosis), chromatin condensation, nuclear fragmentation (karyorrhexis), plasma membrane blebbing and engulfment by phagocytic cells *in vivo*[26]. Apoptosis can be induced by a variety of stimuli, however they lead to the activation of initiator caspases, which induces signaling. A distinction is made into two main pathways, the extrinsic pathway that is Caspase-8 dependent and the intrinsic pathway, which is caspase-9 dependent. First, the extrinsic pathway can be induced by different extracellular stimuli activating death receptors (DRs), which are members of the TNF receptor (TNFR) superfamily such as TNFR1, CD95/Fas and TNF-related apoptosis-inducing ligand receptor-1 (TRAIL). Stimulation of these DRs cause procaspase-8 monomers to be recruited to the cytoplasmic

region of the DR leading to a complex formation which includes FAS-associated death domain (FADD), which in turn causes subsequent Caspase-8 dimerization. The intrinsic pathway is initiated upon factors released from the mitochondria which can occur upon DNA damage, cytoskeletal disruption, hypoxia and hormones during development[27,28]. Here, caspase-9 mediates downstream apoptosis signaling upon forming a dimer with the adapter protein apoptotic protease-activating factor-1 (APAF1)[29]. Both Caspase-8 (extrinsic) and caspase-9 (intrinsic) lead to downstream activation of the executioner caspases-3, -6 and -7 which are responsible to execute apoptosis by cleaving substrates such as Actin or Lamin, but also activate nucleases to cut the DNA between histones[30]. Activated executioner caspases can cleave themselves as well as other executioner caspases, that in fact leads to a positive feedback loop, which finally results in the execution of apoptosis[31]. In living animals, apoptotic cells are recognized by find me signals such as low levels of ATP or UTP, fractalkine, lysophosphatidylcholine, or sphingosine 1-phosphate and subsequent cognate receptor signaling mediates internalization of the dying cell by resident phagocytes such as macrophages. The phagocytic uptake of apoptotic cells is important to prevent secondary necrosis in order to remain healthy tissue homeostasis without promoting an inflammatory response[26].

1.3.3. Mechanisms of programmed necrosis or necroptosis

Necrosis is characterized by swelling of the cell and their organelles, and a loss of plasma membrane integrity which subsequently leads to membrane rupture and the leak of cellular content into the extracellular space (Figure 3). In the past, necrosis was described as a form of cell death that occurs accidentally. However, it became clear that necrosis can also be a genetically regulated process, and that programmed necrosis or necroptosis is clearly distinguishable from apoptosis as it is caspase-independent (Figure 3). It was observed in 1988 that TNF can also promote non-apoptotic cell death via necrosis in particular cell lines, however the mechanisms behind were still elusive for another decade[32]. It is now known that a variety of stimuli can

promote necroptosis such as TNF ligand family members (e.g. TNF, FasL), interferons (IFNs), or toll-like receptor 3 (TLR3) [9,10,33-37]. Initially it was found that Fas ligand induced necrosis and that this was blocked by the loss of receptor-interacting protein kinase-1 (RIPK1) function[9,10,33]. In addition, triggering of necroptosis has been described for TLR3 stimulation to occur independent of RIPK1 via the adaptor protein TRIF or by infection with mouse cytomegaloviruses (MCMV) via the IFN-induced protein DAI[38-40]. Furthermore, it has been identified that the function of RIPK3 and MLKL are essential to trigger necroptosis downstream of these different necroptotic stimuli whether they depend on RIPK1 or not[11-13].

TNF receptor stimulation is known to trigger RIPK1 recruitment, however the role of RIPK1 has been shown to be more complex and it has now been recognized that RIPK1 is important but not essential for cytokine induced NF-κB activation for survival [41] or cell death by either apoptosis or necroptosis[42-44]. Usually, necroptosis is triggered by RIPK1 interaction with RIPK3, RIPK3 dimerization, autophosphorylation of RIPK3 and subsequent phosphorylation of mixed lineage kinase domain-like protein (MLKL)[45-48]. Upon phosphorylation, MLKL forms a trimer that leads to the formation of a pore-complex that can compromise cell membrane integrity and lead to membrane permeability[48,49] Therefore, MLKL is currently considered as being the essential protein for the execution of necroptosis. More recent studies have also suggested additional roles for RIPK1 and RIPK3 in inflammation under pathological conditions [39,47,50-52].

Taken together, necroptosis is considered as an alternative form of PCD to apoptosis that is independent of caspases, and which is usually promoted when the function of caspases is compromised.

1.4. The role of IAPs and RIPKs in the regulation of TNFR1 mediated signaling

The role of TNF has been implicated to have pleiotropic functions in a variety of processes during immunity, cell death and inflammation. TNF can bind to TNF receptor 1 (TNFR1) as well as TNFR2, which can result in contradictory outcomes. TNFR1 can signal survival and cell death, while TNFR2 also signals survival and is generally not implicated in cell death signaling. The outcome upon TNFR1 activation depends strongly on the posttranslational modification of the key components in the complex.

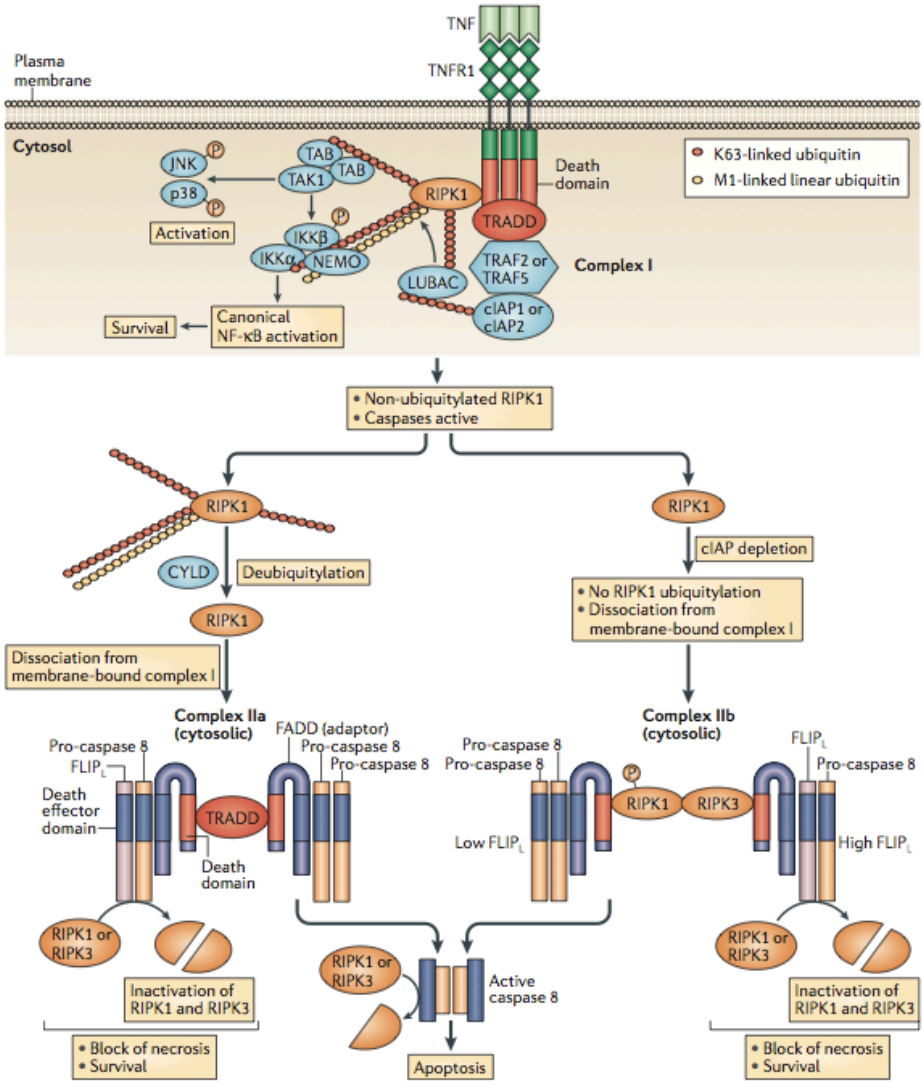

Figure 4: The role of RIPK1 and cIAP1/2 at the decision point of TNFR1 mediated survival, apoptosis or necroptosis (from Brenner et al., 2015).

1.4.1. TNFR1 mediated survival signaling

TNFR1 is a transmembrane receptor that consists of an extracellular cysteine-rich domain, which allows binding of TNF, and the cytoplasmic region, which owns a 'death domain', serves as a binding site for the adaptor protein TNFR1-associated death domain (TRADD). Once TRADD has bound, RIPK1 is recruited to the complex followed by the assembly of TRAF2 to TRADD, and TRAF2 can then bind cIAP1 and cIAP2. This receptor bound complex of TNF-TNFR1-TRADD-TRAF2-cIAP1/2 is termed as complex I and all the components central regulators of NF-κB signaling for survival[17]. The type and timing of ubiquitylation of RIPK1 is central for regulating the outcome of the cell. The process of ubiquitylation of a protein involves three steps that includes the E1 ubiquitin-activating, the E2 ubiquitin-conjugating and the E3 ubiquitin-ligating enzymes, which then attach ubiquitin-chains to a target protein. Depending on the length and the type of ubiquitin linkage attached to a protein, it can be either directed for proteasomal degradation (e.g. K11 or K48-linkage) or reinforce stabilization by preferentially K63-ubiquitin chains attached on a target protein but it also serves as a signaling platform by which other proteins can bind to form a complex[53,54] (Figure 4).

In the process of TNFR1 signaling and the formation of complex I, cIAPs have E3 ubiquitin-ligase activity that can mediate the attachment of K63-linked ubiquitin chains to RIPK1, while CYLD has been shown to deubiquitylate K63 and M1-linked polyubiquitin. K63-linked chains attached to RIPK1 mediate the recruitment of TAK1 kinase complex that consists of TAK1, TAB2 and TAB3, which subsequently activates IKK complex. Activated IKK then allows for the degradation of IκBα that in turn releases p50/p65 which allows for nuclear translocation of p50/p65 promoting survival via transcription of canonical NF-κB target genes[55-57].

1.4.2. TNFR1 mediated apoptosis signaling

In order to switch from a pro-survival phenotype to the cell death phenotype, the deubiquitinase cylindromatosis (CYLD) is responsible to remove K63

chains from RIPK1 in complex I. Thus, CYLD mediates RIPK1 dissociation from the membrane bound complex I in which the formation of the DISC complex or complex II[9,58]. The core components of the DISC complex are known to be Fas-associated protein with death domain (FADD), TRADD, RIPK3, Caspase-8 and FLIP. The complex II promotes apoptosis mediated Caspase-8 activation of downstream caspases, and in parallel complex II inhibits necroptosis by cleavage of RIPK1, RIPK3 and CYLD [16,59,60].

1.4.3. TNFR1 mediated necroptosis signaling

When complex II triggers cell death, this leads to apoptosis. However under conditions where the activity of Caspase-8 is compromised or absent, RIPK1 can bind RIPK3 (Figure 5). When RIPK1 interacts with RIPK3 under these conditions, subsequent RIPK1/RIPK3 and RIPK3/RIPK3 dimerization and autophosphorylation of RIPK3 occurs which forms the necrosome[61]. RIPK3 then directly phosphorylates MLKL which then results in the execution of necroptosis[45,46,48,49]. Recent evidence suggest that MLKL triggers necroptosis by directly forming pore-complexes consisting of trimers in the plasma-membrane, and thereby triggering the loss of membrane integrity as the final step of necroptosis[48,49].

In contrast to the membrane bound complex I, another complex called complex IIb can be formed when the function of cIAP1 and cIAP2 is lost. This leaves RIPK1 not being ubiquitylated by cIAPs, which in turn leads to assembly of RIPK1 with RIPK3, pro-caspase-8, FADD and FLIP-long isoform ($FLIP_L$) in the cytosol. Both complex IIa and complex IIb trigger apoptosis via activation of Caspase-8. However, $FLIP_L$ within complex IIb (also called ripoptosome) regulate whether complex IIb signals towards apoptosis rather than necroptosis. The form of cell death can be shifted toward necroptosis when levels of $FLIP_L$ are increased or the apoptotic machinery is compromised or inhibited upon formation of complex IIb[58,62-64].

Taken together, the example of TNFR1 stimulation mediated survival via NF-κB, or programmed cell death by either apoptosis or necroptosis reveals that

the induction of necroptosis is a separate pathway, in which RIPK1, RIPK3 and MLKL have essential roles.

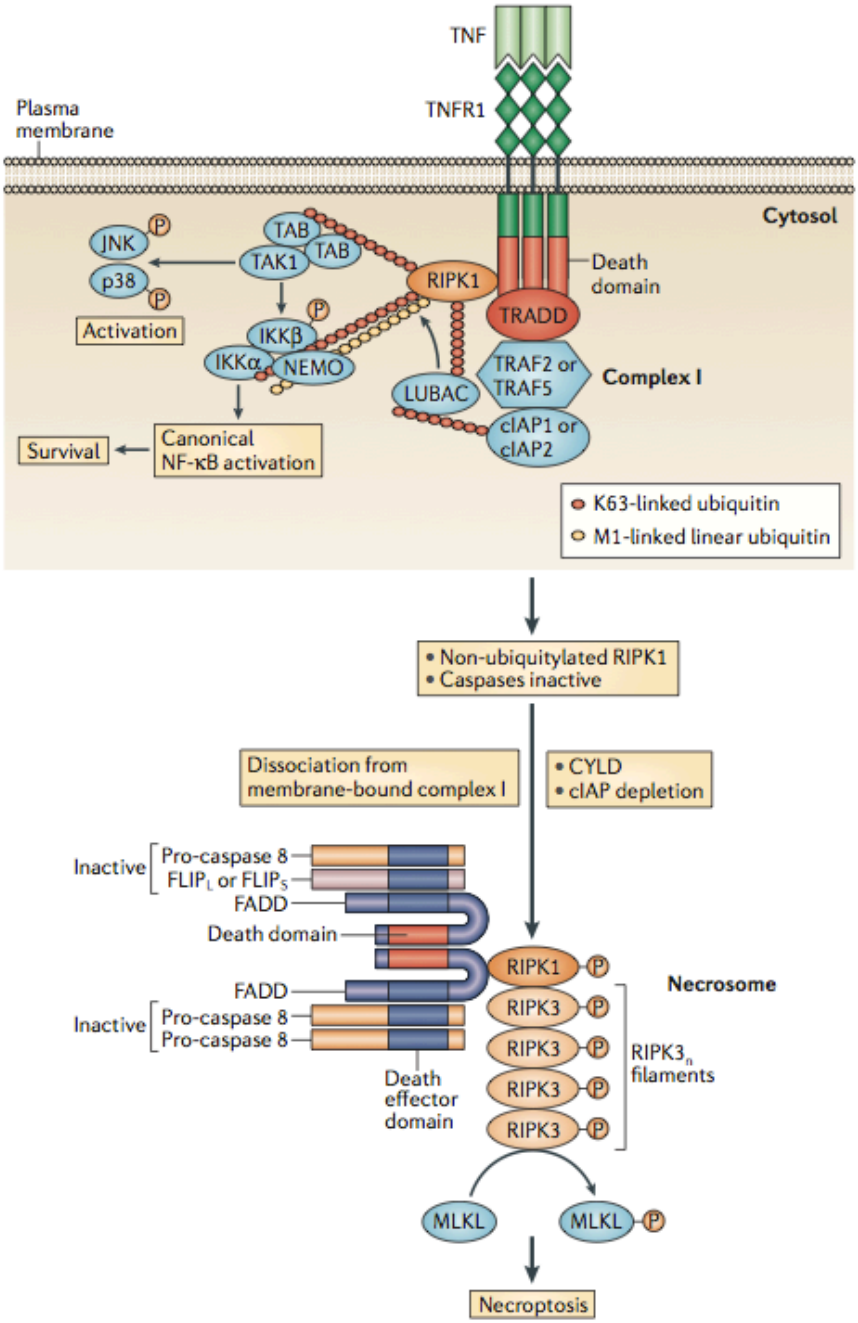

Figure 5: TNF-induced necroptosis requires non-ubiquitylated RIPK1 and Caspase-8 inactivation.

1.5. Characteristics of cancer disease

Cancer is defined as a disease in which abnormal cells divide without control and can invade nearby tissues, in which cancer cells can spread to other parts in the human body throughout the blood and lymph system. Cancers can be divided into five different categories by means of their tissue of origin.

The tumor tissue that has originally developed from normal tissue can arise from many specialized cell types throughout the body. However, the majority of tumors in humans arise from epithelial tissues – the carcinomas. They represent the most common human cancers that cause more than 80% of cancer-related deaths in the Western world.

Several lines of evidence support that the formation of a tumor (tumorigenesis) is a process that requires multiple steps, in which normal human cells acquire genetic alterations that drive the progressive transformation into highly malignant cells[65]. Therefore, Weinberg and Hanahan postulated the six hallmarks of cancers in order to provide a comprehensive scheme that allows understanding the heterogeneity and complexity of the disease by characterization of their common features. These steps include 1) sustaining proliferative signaling, 2) evading growth suppressors, 3) resisting cell death, 4) enabling replicative immortality, 5) Inducing angiogenesis and 6) Activation of invasion and metastasis. In the search of the cause of cancer, physical (e.g. UV, x-ray), chemical agents (carcinogens) and infectious sources (e.g. EBV, HPV) were identified.

1.5.1. Hallmarks of Cancer

Cancer research has illuminated the remarkable heterogeneity of neoplastic diseases and the mechanisms how normal cells acquire malignant behavior showed to be as complex and diverse. In order to understand and explain the complexity of cancer, Weinberg and Hanahan[65] wanted to provide an organizing principle that puts the different cancer diseases into a logical framework. Therefore they proposed six hallmarks of cancer suggesting the multistep development of human tumors. Neoplastic cells have acquired

distinctive and complementary capabilities in an evolving process that transforms normal cells to become tumorigenic and ultimately malignant.

1.5.2. Resistance to cell death

Cancer cells develop strategies to avoid signals that induce apoptosis in order to enhance their ability to survive and proliferate. In the course of cancer development as well as cancer treatment, tumor cells often show disrupted apoptotic machinery. For example, most cells that have a disrupted cell cycle due to oncogenic mutations will be eliminated by apoptosis[66,67]. Here, the protein TP53 or also termed as p53 plays a central role and inactivation of p53 allows for sporadic cancer formation, revealing p53 as a tumor suppressor. P53 is a sensor for a variety of stress signals such as DNA damage, replicative stress or hyperproliferative signals (e.g. Ras signaling) and is considered as the guardian of the genome, thereby critically controlling the induction of cell death[68]. Moreover, different strategies by which cancer cells acquire capabilities to circumvent apoptosis induction include the upregulation of anti-apoptotic genes (e.g. FLIP, IAPs, Bcl-2 or Bcl-xL) and mutation of pro-apoptotic genes (e.g. Bax, Fas, FADD or caspases).

1.5.2.1. The role of RIPKs in cancer

Necroptosis in cancer disease has recently emerged that the loss of necroptosis in the tumor cells associates with resistance and poor prognosis[12,69,70]. The loss of RIPK3 due to e.g. epigenetic silencing prevented MLKL activation and execution of necroptosis[71,72]. In CLL leukemia cells for example, RIPK3 and CYLD downregulation resulted in compromised necroptosis execution upon TNF and zVAD (caspase inhibitor)[73]. Validation of primary tumor samples showed high frequency of decreased RIPK3 expression at mRNA and protein level in colon carcinoma, AML and small-cell carcinoma[70,74,75]. The downregulation was often mediated by epigenetic silencing, due to hypermethylation of the RIPK3 promoter region [71,75]. Interestingly, it was observed in these examples that RIPK3 protein and

mRNA levels were significantly decreased, while RIPK1 levels remained unaffected[70,74].

Interestingly, neither RIPK1 or RIPK3 nor caspases were required for cell death upon traditional chemotherapeutic agents such as Doxorubicin, Etoposide, Oxaliplatin or 5-fluorouracil (5-FU)[70]. Such drugs induced cell death in epithelial cancer cell lines (HT29 and Colo205) and in lymphoma cell lines (Jurkat, H9, U937, BJAB) through non-caspase protease mediated cell death via cathepsins[70].

In summary, this suggests that cancer cells can compromise their necroptotic and mediate resistance to classical necroptosis inducing stimuli (TNF+zVAD+Smac-mimetics, FasL+zVAD, poly(I:C)+zVAD), but necroptosis deficiency did not affect the ability of clinically used chemotherapeutics such as the DNA damaging agents to kill tumor cells. However, necroptosis is a backup mechanism to apoptosis that is thought as a promising strategy for therapeutic intervention to overcome apoptosis resistance[76].

1.5.2.2. The role of inhibitor of apoptosis proteins in cancer

Mutations in the IAP genes have been found throughout different cancers that include hepatocellular carcinoma, cervical cancer, liver cancer, glioblastoma, medulloblastoma, non-small-cell lung cancer (NSCLC), esophageal cancer and pancreatic cancer[77-82]. The cellular IAPs are considered as proto-oncogenes due to common genetic aberrations in cancers. Several genetic alterations have been found such as the 11q21-q23 amplification or the t(11;18)(q21;q21) translocation that fuses the BIR domains of MALT1 with that of cIAP2 leading to constitutive activation of NF-κB[83,84]. Due to such genetic aberrations, IAP proteins show increase in their mRNA or protein levels, or the loss of the endogenous inhibitor Smac in many cancers. Among the three IAPs, cIAP2 proved to accurately predict overall survival in AML patients, but in childhood de novo AML, increased XIAP levels showed to correlate with poor prognosis[85-87].

1.5.2.3. Mechanisms of IAP inhibition by Smac-mimetic compounds

IAPs play an important role in cancer survival as they are often upregulated and/or altered, or expression of endogenous inhibitor second mitochondrial activator of caspases (Smac) is lost. Here, IAPs promote survival (via NF-κB) and are often found over-expressed in cancers. For this purpose, efforts were put to target the IAP proteins and a variety of inhibitory compounds against IAP family members have been generated by targeting different domains within the protein. Among several different targeting strategies, most attention has fallen on the small-molecule IAP antagonists and antisense oligonucleotides as indicated by the fact that several IAP antagonizing compounds are currently in clinical- and preclinical trials (e.g. MV1 and BV6 from Genentech; Comp A from TetraLogic Pharmaceuticals; LBW242 from Novartis;), while two have made it into the clinics (AT-406 from Ascenta Therapeutics/University of Michigan and TL32711 from Tetralogic Pharmaceuticals)[88-91].

Smac-mimetic compounds are antagonistic small-molecule inhibitors of IAPs (IAP antagonists) that mimic the endogenous inhibitor of IAPs Smac. The majority of Smac-mimetics target XIAP, cIAP1 and cIAP2 in parallel, which can be explained by their homology (Figure 1). IAP antagonists prevent caspases and Smac to bind to cIAP1, cIAP2 and XIAP. Here, XIAP is the only member that directly binds to Caspase-3/7/9, and which is blocked in the presence of IAP antagonists. Smac-mimetics binding to cIAPs in contrast, the mechanism turned out more complicated. As illustrated (Figure 6), Smac-mimetics bind to the BIR3 domain of cIAP1 or cIAP2 and induce a conformational change that enhances dimerization of cIAPs via the RING domain, which in turn results in an increased E3 ligase activity. cIAPs then auto-ubiquitylate, which in turn promotes their degradation via the proteasome.[88,92,93]

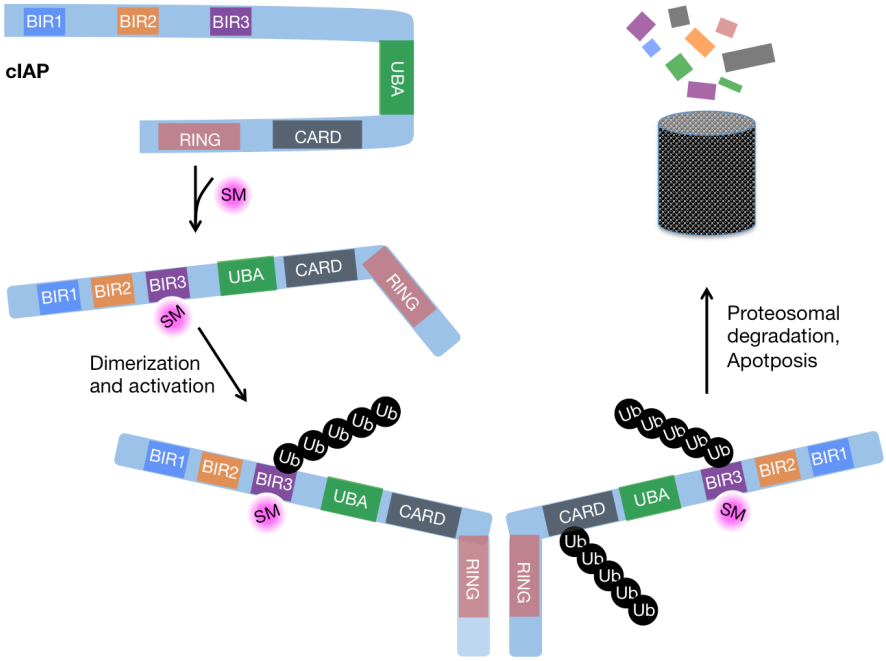

Figure 6: Smac mimetic compound work as IAP antagonists and lead to cIAP depletion via proteasomal degradation (adapted from Fulda 2012)[94].

1.5.2.4. The role of necroptosis immunogenic cell death and cancer immunity

Apoptotic cells are phagocytized by macrophages via eat-me signals usually before secondary necrosis occurs[42,95-98] that could potentially cause an inflammatory response. The term 'immunogenic' cell death refers to the consequence of an induction of expression of MHCII, CD40, CD80, and CD86 on DCs and the simultaneous release of inflammatory cytokines IL-1β, IL-6, IL-12 and TNF when a cell dies. However, in contrast to normal apoptosis, a form of immunogenic apoptosis is described in cancer cells treated with anthracycline chemotherapies and involves: 1) translocation of intracellular Calreticulin, and other endoplasmic reticulum proteins to cell surface; 2) secretion of ATP during the blebbing phase of apoptosis; and 3) release of the chromatin-binding protein high-mobility group box 1 (HMGB1)[99-103]. Interestingly, by binding of HMGB1 to T-cell immunoglobulin and mucin-domain containing (TIM)-3, DC activation within tumors can be suppressed, although this impacts tumor growth independently of a T cell response. Thus, enhancing immunogenic apoptosis in cancerous cells can

be very advantageous in a therapeutic setting because DAMPs induce a host anti-tumor immune response.

More recent studies have tested the immunogenicity of necroptosis in NIH 3T3 fibroblasts and CT26 cells and evaluated its potential as an alternative approach in cancer therapy. In order to cause cancer cells to undergo necroptosis, a system to induce dimerization of RIPK and/or FADD in cancer cells was used[104-107]. Necroptotic cancer cells released DAMPs (ATP and HMGB1), induce maturation of DCs and production of IFN-g by T cells and were therefore able to elicit DC activation and effective cross-priming of cytotoxic CD8+ T cells *in vivo* and *in vitro*, and mediated anti-tumor immunity. [104,105,107-109]

1.5.3. Induction of angiogenesis

Every cell requires nutrients and oxygen as well as the ability to evacuate metabolic wastes and carbon dioxide. Therefore, tumor cells acquire the ability to induce angiogenesis and neovascularization of hypoxic tumor tissue in order to grow. Angiogenesis and vasculogenesis in adults are mainly quiescent, with the exception of the wound healing process or the female reproductive cycling. In growing tumors, however, the angiogenic switch remains on, causing permanent sprouting of new blood vessels in order to support and maintain expanding neoplastic growth[110].

The most prominent regulators of angiogenesis that act with opposing effects are vascular endothelial growth factor-A (VEGF-A) and thrombospondin-1 (TSP-1). The ligands decoded from the VEGF-A gene that signal via tyrosine kinase receptors (VEGFR1-3) are well known in orchestrating new blood vessel growth during embryonic and postnatal development as well as during homeostatic survival of endothelial cells. Moreover, the fibroblast growth factor (FGF) gene family is also well known to be involved in wound healing and is also implicated as a proangiogenic signal during tumor angiogenesis. In contrast, TSP-1 is a counteracting

protein to the VEGF-A induced angiogenic switch by binding transmembrane receptors and therefore elevating suppressive signals.

1.5.4. Activating invasion and metastasis

The loss or decrease of extracellular matrix (ECM) integrity and with it the alteration in cell shape adhesive behavior with neighboring cells is typically obtained in carcinomas which coincides with increased invasiveness and progressing of a tumor to a more malignant state. E-cadherin is known to be critical key suppressor of this process by remaining the assembly of epithelial sheets and sustain quiescence of the cells within a tissue[111]. The process of invasion and metastasis has been characterized by series of steps that includes cell biologic changes with increasing local invasion of cancer cells, followed by intravasation into nearby blood and lymphatic vessels, travel through the lumen and by transmigrating through endothelial cells, the cell escapes into the parenchyma (extravasation). At distant tissue sites, small tumor nodules can be formed (micrometastases) that usually further grow into a macroscopic tumor nodule (colonization).

1.5.4.1. The invasion-metastasis cascade

Metastasis is a multistep cell-biological process that is characterized by the spread of malignant cells to distant organs. This is a result of an evolutionary process that is driven by genetic and/or epigenetic alteration within tumor cells, which includes the modulation of adjacent stromal cells or even distant pre-metastatic non-neoplastic cells. To overcome the different hurdles for a tumor cell from the primary tumor to the metastatic site and establish macroscopic metastasis, the completion of several steps was accomplished that is termed the invasion-metastatic cascade (Figure 7). During this process, carcinoma cells deviate from their primary growth site (local invasion, intravasation), disseminate systemically via circulation through the lymphatic or vascular system (survival, arrest at distant site, extravasation), and adapt to survive and establish a microenvironment (micrometastasis formation, metastatic colonization).

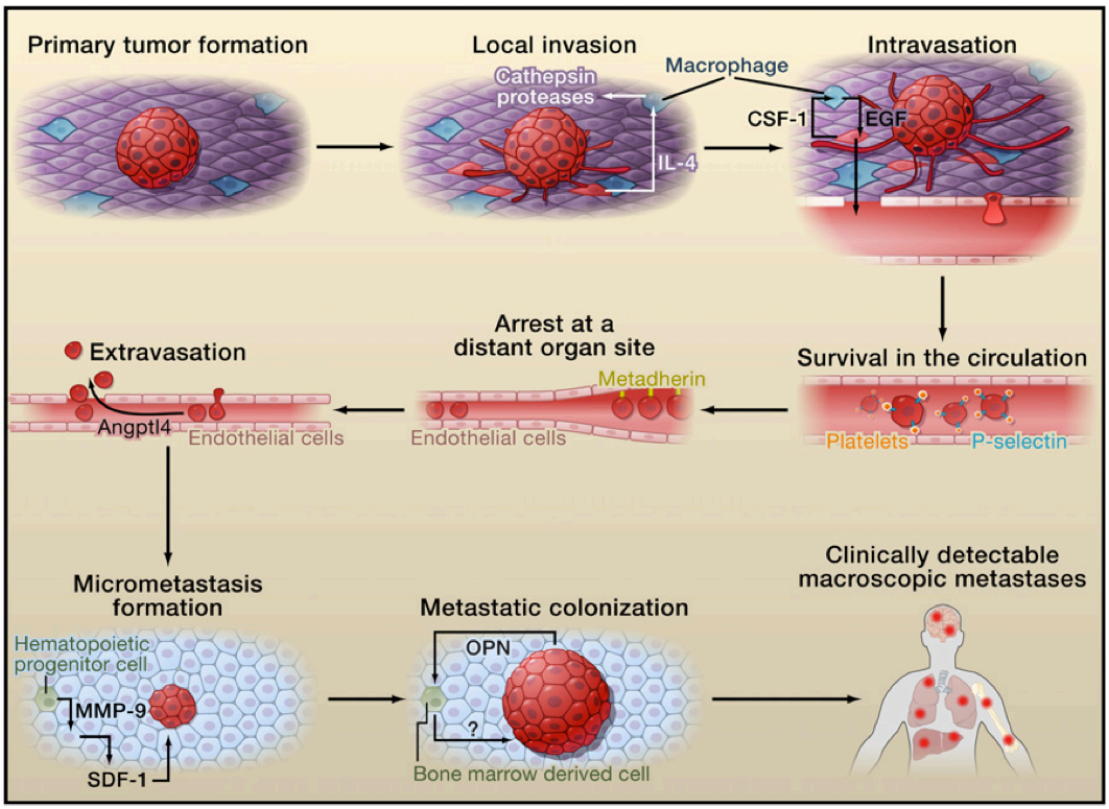

Figure 7: Stromal Cells are altered to aid during the Invasion-Metastasis Cascade (S. Valastyan and R.A. Weinberg, 2011).

1.5.4.2. The role of myeloid during invasion and metastasis

Among the immune cells, only macrophages, neutrophils and platelets were shown to aid in the processes of malignant cell invasion and metastasis, while leukocytes have not been reported to be of importance. Macrophages or their monocyte precursor cells have been demonstrated as regulators at all stages of the metastatic disease by aiding tumor cells for local invasion, intravasation to the blood- or lymphatic vessels, escape of the lumen and extravasation to peripheral tissues. Microscopy studies of metastatic lungs showed that tumor cells directly contact macrophages during extravasation and depletion of macrophages resulted in dramatic reduction of the number of cancer cells that migrated out of the blood vessels. The recruitment of monocytes to sites of extravasation or intravasation was shown to occur in a CCL2/CCR dependent manner. Thus, tumor associated macrophages are recognized to enhance tumor angiogenesis, promote tumor growth and enhance tumor cell migration and invasion[112-114]

Moreover, clinical studies propose that increased numbers of circulating neutrophils are correlative of poor prognosis, which has been shown in lung and gastric cancers[115-117]. Mechanistically, neutrophils are considered pro-metastatic by increasing ability of cancer cells to extravasate via adhesion of neutrophils via ICAM-1 on cancer cells[118,119]. Another specific feature of neutrophils is the formation of neutrophil extracellular traps (NETs). A study using syngeneic tumor mouse model has indicated that circulating tumor cells were trapped within NETs that surprisingly lead to an increase in micrometastasis formation by promoting tumor cell adhesion at distant sites [120]. However, formation of metastases is a rare event considering the millions of cells entering into the blood stream only very few tumor cells are able to form micrometastasis, which makes it difficult to assess experimentally *in vivo*. Therefore, the way myeloid cells aid in the process of metastasis is thought to be diverse and mechanism are still not fully understood.

Initially discovered about a decade ago, it has been discovered that (VEGFR1)-expressing bone-marrow derived cells, mainly derived from the myeloid lineage, home to distant tissue sites before malignant cells derived from a primary tumor colonize this pre-metastatic niche (PMN) to form a new metastasis[121]. The formation of PMNs is a result of the crosstalk between factors released from a primary tumor and the microenvironment of a secondary organ. In the process, besides tumor released factors such as cytokines, chemokines, growth factors and extracellular matrix remodeling enzymes, exosomes have been recognized as being critical for the formation of the pre-metastatic niche (PMN). Exosomes are small membrane vesicles (30-100nm) derived from the luminal membranes of multivesicular bodies that are released by cell membrane fusion. Exosomes showed the ability to facilitate local and systemic communication between cells via exosomal transfer of proteins, mRNAs and microRNAs. Exosomes can directly reprogram bone marrow-derived to home to a pre-metastatic spot[122-129]. Here, a pro-inflammatory milieu is created that promotes for additional recruitment of myeloid cells into the tumor (mainly macrophage/monocytes and neutrophils), and consequently enhancement of vascular permeability as

well as re-education of stromal cells. All these processes aid to create a successful PMN and consequentially metastasis.

1.5.4.3. The role of vascular endothelial cells during invasion and metastasis

The vascular endothelium is structurally different depending on the organ. In theory, the vasculature consists of a continuous and non-fenestrated endothelial monolayer in the skin, lung heart and brain. The extravasation of leukocytes in lung and liver endothelium occurs in the microvasculature, while in lymphoid organs this occurs at the higher endothelial venules In contrast, leukocytes that extravasate into skin, muscle and mesentery do that via the postcapillary venules[130,131]. This variability therefore leads to functional differences in homeostasis, permeability and leukocyte trafficking.

The microvasculature created by tumor cells and the absence of broad pericyte coverage is indicated to promote intravasation. Moreover, the capability to enhance breast carcinoma intravasation by the remodeling enzymes MMP-1 and MMP-2 and growth factor epiregulin was strongly connected to their ability to promote permeability of tumor vasculature[132]. To the latter, the stimulation of vascular permeability is not only of importance for intravasation, but is considered as a prerequisite for a cancer cell to extravasate. However, in comparison to leukocyte trafficking that is well understood, the mechanisms described for tumor cell transmigration vary. The process of rolling, adhesion and transmigration (diapedesis) are at least partially shared between leukocytes and tumor cells, because malignant cells mimic leucocyte migration to a certain degree, but the molecular mechanisms remain different[133]. The most striking difference is that leukocytes can alter the endothelium only temporary in contrast to tumor cells that induces irreversible changes of structure and function of microvasculature.

The currently reported evidence of tumor cell transmigration suggests different strategies. Malignant cells were shown to cross without destroying the endothelial monolayer similar to the processes of leucocytes

transmigration that includes upregulation of adhesion molecule receptors (e.g. LFA-1, L-selectin) on endothelial cells, VEGF-dependent Src-mediated loosening of VE-cadherin/β-catenin junctions and subsequent increase of vascular permeability[134,135], re-organization of the cytoskeleton via myosin-light chain (MLC) dependent contraction of actin-cytoskeleton[136], or the induction of programmed cell death. For the latter, it was demonstrated that tumor cells were able to induce both apoptosis[137] as well as programmed necrosis[138] of endothelial cells in order to transmigrate through the created gap.

1.5.5. The tumor microenvironment

The tumor is not just a mass of malignant cells, but consists of many other untransformed cells that were recruited (Figure 8). A growing and progressing tumor is a dynamic interplay between cancer cells that communicate and manipulate the neighboring stromal cells as well as cells of the immune system to create an environment that benefits tumor growth. Interestingly, the dynamic processes within a tumor that is created by a variety of cellular interactions has many parallels to the wound-healing process[139,140]. This communication is mediated by a complex and dynamic network of cytokines, chemokines, growth factors, and inflammatory and matrix remodeling enzymes. These interactions between malignant and the variety of non-transformed cells make the tumor microenvironment (TME)[141].

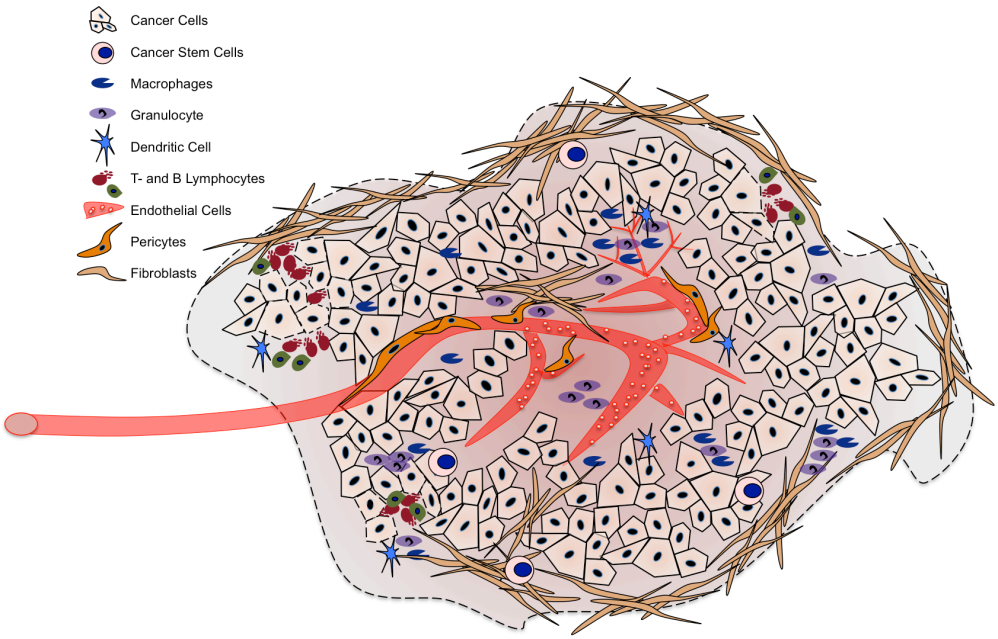

Figure 8: Cells of the tumor microenvironment (TME). Apart from cancer cells and cancer stem cells, the TME of most human tumors consist of stromal cells such as fibroblasts and endothelial cells from both, vascular and lymphatic vessels. Both the stromal and parenchymal cells of tumors contain distinct cell types and subtypes that promote tumor growth and progression. In addition, specific subtypes of inflammatory immune cells such as tumor-associated macrophages (TAMs), tumor-associated neutrophil (TAN) granulocytes, dendritic cells, B cells and T cells are found as well in most tumors. Important to note, these inflammatory immune subtypes can have tumor promoting as well as tumor killing capabilities. Each of these special cell types fulfills a special role by applying specific functional repertoires to create the TME in its entirety, by which these non-transformed cells within a tumor contribute to particular hallmarks (Adapted from Hanahan and Coussens 2012).

1.5.5.1. The role of inflammatory myeloid cells in the tumor microenvironment

During the last decade it became clear that inflammation is an important component in tumorigenesis. It is recognized that immune cell infiltration is fostering certain hallmarks of cancer and It is now accepted that inflammatory TME is essential for most tumors to develop and progress. Furthermore, chronic inflammation is seen to be associated as a major factor of many environmental caused cancers, such as that induced by chronic infection.

Cells of the myeloid lineage make the majority of non-transformed cells in the TME. Depending on the subtype of innate immune cell, tumor promoting as

well as anti-tumor functions have been described in literature. Tumor-associated macrophages (TAMs) have been characterized as mainly tumor-promoting, and high densities of cells expressing macrophage-associated markers are generally associated with a poor clinical outcome[142]. Macrophage expression of TNF and IL-6 induces survival signaling in neoplastic tissue and resistance to chemotherapy. Further, macrophages can enhance angiogenesis by producing factors such as VEGF[143,144] and by enhancement of VEGF-A bioavailability through enhanced matrix metalloproteinase (MMP)-9 activity[145,146].

1.5.5.2. Tumor associated neutrophils

Neutrophils can neutralize pathogens through phagocytosis and intracellular destruction, production of granules containing antimicrobial peptides and proteases, and the formation of neutrophil extracellular traps (NETosis) to deplete large pathogens. Moreover, by producing cytokines, chemokines and ECM remodeling factors neutrophils are also known to be important for their role in orchestrating the innate and adaptive immune responses that take place both during wound healing and infection. Substantial evidence describes neutrophils that are recruited to the tumor to have mainly tumor promoting ability by elevating tumor angiogenesis (MMP9, VEGF-A/VEGFR), promoting EMT/invasion via CXCL5 or enhance tumor development by producing TNF in the TME. In contrast, neutrophils have also been reported to interfere with T cell activation depending on the type of cancer, TANs have conflicting effects. TAN recruitment was either beneficial or disadvantageous for tumor growth, because of differences in TAN subpopulations and their capabilities to directly suppress CD8+ T cell proliferation[147].

1.5.5.3. The role of dendritic cells

Among the cells of the innate immune system dendritic cells (DCs) form a central cellular network that shapes adaptive immune responses according to peripheral signals. Over the past decade it has been demonstrated that tissue DCs consist of developmentally separable subsets with distinct roles

in immunity. When compared to monocyte-derived DCs (moDCs) and plasmacytoid DCs (pDCs), classical DCs (cDCs) are particularly suited to regulating T lymphocyte function[98]. cDCs can be further divided into two subpopulations according to the expression of the transcription factor interferon regulatory factor 4 (IRF4) and IRF8[42]. *Irf4*-dependent cDCs show enhanced MHCII antigen presentation and represents the majority of cDCs throughout the body and are heterogeneous population that preferentially activates $CD4^+$ T cells. In comparison, *Irf8*-dependent cDC display enhanced capability to cross-present soluble and cell-associated exogenous antigen on MHCI and preferentially activate $CD8^+$ T cells. The central role of DCs is to induce the T cell response that is the foundation of the "cancer-immunity cycle" outlined in Chen and Mellman[148]. This requires the uptake of tumor debris/antigens, maturation of the DC (marked by upregulation of co-stimulatory molecules and inflammatory cytokines), and migration to the draining lymph nodes where T cell priming and activation is initiated[149,150]. Both DCs and macrophages within tumors readily uptake cell debris within tumors but only the rare IRF8-dependent $CD103^+$ DC population transports tumor antigen and activates T cells within the lymph nodes[104,151]. In addition to delivering tumor antigen, only the $CD103^+$ cDC have been found to activate naive $CD8^+$ T cells *ex vivo* following separation of the various cDC subsets[104]. Consistent with these findings, these migratory $CD103^+$ DCs are required for rejection of highly immunogenic cancer lines and for responsiveness to checkpoint blockade therapy with antibodies against programmed death 1 (PD-1)[104,106].

1.5.5.4. The role of cytotoxic T lymphocytes

The role of T lymphocytes – The T lymphocyte mediated immunity is the pivotal element of adaptive immune system. T cells cannot only recognize foreign infectious agents such as viral-, bacteria- or parasitic infections, but can also detect abnormal malignant cells. Cytotoxic CD8+ T cells and CD4+ T helper (Th1) provide the type I immune responses against pathogenic sources, and so it is for anti cancer immunity. After initiation of strong type I

immune responses, a variety of T cell-inhibitory functions are activated. Tumor infiltration of CD8+ T cells occurs in many human cancers. In order to allow for antitumor immunity in most model systems the CD8+ T cells occur to be crucial. It has been convincingly demonstrated that the cross-presenting CD8/CD103+ cDC population is required for rejection of highly immunogenic cancer lines and for non-responsiveness to checkpoint blockade therapy using antibodies against programmed death 1 (PD-1)[104,106]. T cell activation is also modulated by the co-stimulatory signals present in the TME. As mentioned earlier in this section, myeloid cells contribute with co-stimulatory signals for an effective induction of T cell immunity. However, the effectiveness of T cell mediated tumor killing is a result of the competing contribution between immune suppressive- and stimulatory signals in the TME. Therefore, the CD8 T cells represent the most abundant T cell subtype among leucocytes found in many tumors. This results in T-cell mediated cytotoxicity against cancer cells, and indeed high densities of CD8+ T cell influx into the tumor correlates with a good prognosis. However, depending on the polarization phenotype and the abundance of CD4+ T regulatory (Treg) cells, the suppressive signals from Tregs such as IL-10, TGF-b and CTLA4 overrule T cell stimulatory signals, and thus allow for tumor growth and progression.

1.5.5.5. The role of vascular endothelial cells

The sprouting of new blood vessel is induced by angiogenic factors such as VEGFs, FGFs, PDGFs and chemokines present in the TME, which are mainly produced by cancer associated fibroblasts (CAFs), malignant cells and myeloid cells. The tumor-associated blood vessels reveal chaotic structure and show leakiness that increases interstitial pressure and alters nutrient and drug delivery in the TME. Therefore, a tumor requires enhanced angiogenesis to fulfill its need for nutrients and oxygenation[152].

1.5.5.6. The role of IAPs and RIPKs in endothelial cells

Genetic deletion of Caspase-8 or FADD results in embryonic lethality. The embryos die during development around E10.5 stage and show heart defects. Embryonic lethality of *Fadd*$^{-/-}$ or *Caspase-8*$^{-/-}$ mice was rescued by simultaneous genetic loss of *Ripk3*[153,154]. Similar to the loss of Caspase-8 and FADD, *Birc2*$^{-/-}$*;Birc3*$^{-/-}$ (cIAP1/cIAP2 knockout) mice also obtained heart failure when embryos died at around E10.5[155]. In addition, tissue specific FADD depletion or Caspase-8 depletion in *Tie2*^{cre} mice, where Tie2 is mainly expressed by endothelial cells and to a small extent in monocyte/macrophage populations, led to embryonic lethality that could be rescued with simultaneous RIPK3 deletion[156-158] [156,157]. Therefore, this suggests a role for RIPKs and IAPs in regulating cell death by apoptosis and necroptosis during embryonic development.

1.5.5.7. Mechanism of VEGF-induced angiogenesis and vascular permeability

For tumor progression, quiescent endothelial cells and their associated pericytes need to undergo the angiogenic switch in order for a tumor to vascularize. Many of soluble factors are present in the TME that enforce neovascularization and. Among the variety of factors secreted by tumor cells or myeloid cells such as PDGFs, HGFs, GM-CSF, chemokines (SDF-1, CCL2/MCP-1, RANTES) and pro-inflammatory cytokines (TNF, IL-1β, IL-6). For transmigration of immune cells, vascular permeability can be a result of either the release of vasoactive signals into the blood or by direct contact of lymphocytes with endothelial cells via adhesive junctions[159] such as intercellular adhesion molecule 1 (ICAM-1) and vascular cell adhesion molecule 1 (VCAM-1). CCL2 ligand signaling through CCR2 receptors on endothelial cells has been implicated to promote vascular permeability and therefore allow for increased metastatic potential[114,160]. However, the majority of processes that regulate angiogenesis and vascular permeability in disease converge through the VEGF signaling axis. The mechanism and signaling

events by which VEGF modulates vascular dynamics are illustrated (Figure 9).

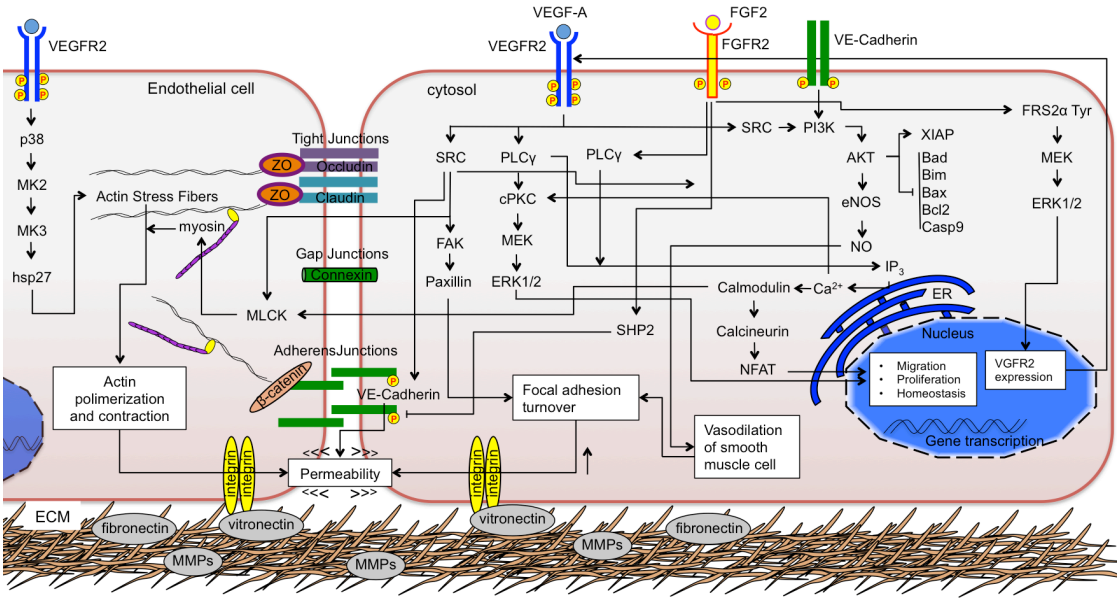

Figure 9: Regulation of vascular permeability by the VEGF- and FGF signaling cascade (adapted from Hoeben et al., 2004; Dudek et al., 2001; Eichmann et al., 2012; Simons et al., 2016)[161-164].

1.5.5.8. VEGFR2 signaling

The Src family of proteins in endothelial cells belongs to the cytoplasmic tyrosine kinases that are activated upon phosphorylation of murine VEGFR2 at tyrosine 949. These Src- dependent signals for permeability go in conjunction with alterations in cell shape by modulating the cytoskeleton and focal adhesion. Src regulates focal adhesion by phosphorylating focal adhesion kinase (FAK). Src/FAK interacts and regulates the turnover of integrins in large complexes formed at sites of focal adhesions by which the actin cytoskeleton is connected with the extracellular matrix (ECM).

Upon binding of VEGF, phosphorylation of VEGFR2 at Tyr1173 (Y1175 in humans) leads to the activation of PLCγ, followed by generation of inositol 1,4,5-triphosphate (IP_3). IP_3 then mediates the release of Ca^{2+} form the endoplasmic reticulum (ER) that leads to the activation of Ca^{2+}-dependent protein kinase C (PKC), which then results in signaling through RAF1-MEK-ERK1/2 cascade[165-168]. The PLCγ-PKC signaling cascade regulates

proliferation, migration and cell fate during development by regulating transcription factors of the E26 transformation-specific (ETS) family. These factors play a pivotal role in regulating endothelial cell function[169-173]. In addition, Ca^{2+} signaling is important for activation of nuclear factor of activated T cell (NFAT) family of transcription factors. Here, Calmodulin (Ca^{2+} sensor) and Calcineurin that is a Ca^{2+} dependent Ser/Thr phosphatase regulate the nuclear translocation of NFAT which then results in an increased signaling by VEGFR2 because of NFAT induced reduction of VEGFR1 transcription levels [174].

VEGFR2 leads to the activation of the canonical survival pathway via Src and PI3K/AKT, that which results in loosening of tight junction molecules (e.g. VE-cadherin, ZO-1 *Occludin*). In addition, VEGFR2 activates PI3K and subsequently protein kinase B (PKB or Akt) indirectly, which can also occur by activated VE-cadherin or AXL[175,176]. Akt has a broad spectrum of substrates and regulates survival, proliferation and apoptosis[177,178] of endothelial cells, and is of importance during pathological angiogenesis, vascular maturation and metabolism by the mTOR complex 2. Activation of eNOS by Akt results in production and diffusion of nitric oxide (NO) from endothelial cells to adjacent smooth muscle cells. The activation of NO-signaling in smooth muscle cells leads to the dilation of the blood vessel.

In addition to the signaling cascades listed, VEGF stimulation via VEGFR2 activated also stress kinases such as STAT and p38 MAPK. The activation of p38 in endothelial cells has been linked to cell migration and lipopolysaccharide (LPS)-induced p38 activation was shown to cause vascular permeability[179-183]. The mechanism by which p38 mediates this is still unclear, however the functional role of p38 upon VEGF stimulation is linked to HSP27, a known substrate of p38 that inhibits actin polymerization tremendously, once activated. Furthermore, the induction of p38 showed to depend on neuropilin-1 (NRP1) and Ca^{2+} influx, but not on PLCγ. Under this condition, Src together with RAFTC/Pyk2 was also shown to act on p38 activation when Ca^{2+} was released[184,185]. In summary, the role of other

signaling pathways activated by VEGFR2 such as p38 MAPK, SHB, STAT3 still remains poorly understood.

1.5.5.9. Crosstalk of FGFR2 and VEGFR2 signaling events

The fibroblast growth factor (FGF) family interacts with FGF receptors (FGFRs) to activate different signaling cascades as illustrated (Figure 9). The role of FGFs during development, regulation of angiogenesis and wound healing has been well described in literature[186]. The FGFRs are phylogenetically close to VEGFRs and platelet-derived growth factor receptors (PDGFRs) and it is therefore not unexpected that there exists crosstalk and synergies e.g between FGF and VEGF signaling[187]. Interestingly, FGF-induced angiogenesis and lymphangiogenesis has not been permitted upon VEGF inhibition and FGF stimulation of endothelial cells resulted in VEGF-A production and release [188-190]. FGF signaling through such as PI3K-AKT and MEK-ERK are dependent on the adaptor protein FRS2α. FGF2 induced FRS2α-dependent activation of ERK1/2 amongst other things promoted transcriptional activation of the *Vegfr2* gene, which resulted in increased sensitivity towards VEGF[170]. In this sense, FRS2α can also bind to VEGFRs and has been shown to be important for angiogenesis, arteriogenesis and lymphangiogenesis by activating VEGFA and VEGFC signal transduction[191].

1.5.6. Transplantable mouse tumor models

The use of transplantable syngeneic cell lines into inbred strains have been used for a long time and proven to uncover many features of cancer disease, such as the intrinsic immunogenicity of dying tumor cells, the existence of shared and tumor-specific antigens, and therapeutic intervention could provide predictive value[192-196].

The cell lines are derived from spontaneously or carcinogen-induced occurring tumors in inbred mouse strains and are then selected for efficient propagation both *in vitro* and *in vivo*. A range of cell lines have been generated that cover a variety of tumor types, such as B16 melanoma, CT26

orMC-38 colon carcinoma, Lewis Lung Carcinoma (LLC), 4T1 breast carcinoma, and methylcholanthrene-induced fibrosarcoma cell lines.

These cells are grown in tissue culture dishes and can be injected into syngeneic mice. In order to study tumor growth subcutaneous and orthotopic inoculation can be used. In addition, tumor dissemination to distant organs such as liver, spleen and lung can be studied by resection of an established tumor that may allow to study spontaneous metastasis, while intravenous injection can be used as an alternative approach that resembles halfway metastasis. The advantage of these transplantable models in comparison to transgenic tumor models, are the short time frame (few weeks) that tumors can be harvested, as well as the reproducibility of tumor growth.

2. Aims and Outline

Our preliminary data suggested, that RIPK1 and RIPK3 have additional functions in orchestrating inflammatory responses by directly regulating cytokines that was independent of cell death to occur[50]. Moreover, evidence suggested that RIPK3 is a tumor suppressor because it was found that RIPK3 is epigenetically silenced in several cancer cell lines as well as patient samples[12,69]. However, it has not been known what the role of necroptosis proteins in the tumor microenvironment is. Due to this, we hypothesized that RIPKs can alter inflammation in the tumor microenvironment, and that this would affect the ability of a tumor to form and grow. Therefore we aimed to:

- Determine the relevance of IAPs and RIPKs in the tumor and the tumor microenvironment

- Understand the function of IAPs and RIPKs *in vivo* and how they affect the malignancy of cancer

- Elucidate in detail how IAPs and RIPKs affect inflammation, and whether RIPKs cause necroptosis related inflammation or directly by modulating cytokines

3. Results I

3.1. Title: RIPK3 promotes vascular permeability via VEGF/p38 axis to allow tumor cell extravasation independent of its necroptotic function

Declaration

I declare that I have contributed the majority of this work. I planned the experimental design, performed experiments, analyzed and interpreted data, created the figures and wrote the manuscript.

RIPK3 promotes vascular permeability to allow tumor cell extravasation independent of its necroptotic function

Kay Hänggi[1], Lazaros Vasilikos[1], Janin Knop[1], Aida Freire Valls[2,3], Kristy Rieck[1], Lisanne Spilgies[1], Tvisha Misra[1], John Bertin[4], Peter J. Gough[4], Thomas Schmidt[3], Carmen Ruiz de Almodovar[2], W. Wei-Lynn Wong[1]

[1]Institute of Experimental Immunology, University of Zurich, Zurich, Switzerland

[2] Heidelberg University, Biochemistry Center, Heidelberg, Germany

[3] Department of General, Visceral and Transplantation Surgery, Heidelberg University, Heidelberg, Germany

[4]Pattern Recognition Receptor Discovery Performance Unit, Immuno-Inflammation Therapeutic Area, GlaxoSmithKline, Collegeville, PA 19426, USA

Running title: RIPK3 promotes vascular permeability

Corresponding author:
W. Wei-Lynn Wong
Institute of Experimental Immunology
University of Zurich
Winterthurerstrasse 190 Y44 J55
8057 Zurich, Switzerland

e: wong@immunology.uzh.ch
p: +41-44 635 3720
f: +41-44 635 6883

Abstract

Receptor interacting protein kinase 3 and its kinase activity are critical proteins in regulating the inflammatory form of cell death called necroptosis. RIPK3 phosphorylates mixed lineage kinase domain-like protein (MLKL) causing MLKL to form a pore-like structure, insert into the cell membrane allowing intracellular contents to release and subsequent necroptosis to occur. Alternatively, RIPK3 has been shown to regulate cytokine production directly influencing inflammatory immune infiltrates. Recent data suggests that RIPK3 may contribute to the malignant transformation of tumor cells *in vivo* and we asked whether RIPK3 may play a role in the tumor microenvironment altering the ability of the tumor to grow or metastasize. To determine if RIPK3 in the tumor microenvironment could promote inflammation alone or by initiating necroptosis and thereby influencing growth or metastasis of tumors, we utilized a syngeneic tumor model of metastasis. Loss of RIPK3 in the tumor microenvironment reduced the number of tumor nodules in the lung by 46% formed. Loss of the kinase activity in RIPK1, a member of the necrosome also reduced tumor nodules in the lung by 38%. However, the loss of kinase activity in RIPK3 or the loss of MLKL only marginally altered the ability of tumor cells to form in the lung. Using bone marrow chimeras, the decrease in tumor nodules could not be explained by RIPK3 deficiency in the immune infiltrates but due to the stromal compartment. Transmigration assays showed decreased ability of tumor cells to transmigrate through the vascular endothelial layer, which correlated with decreased permeability in the *Ripk3*$^{-/-}$ mice after tumor injection. In response to permeability factors such as vascular endothelial growth factor, RIPK3 null endothelial cells showed decreased p38/HSP27 activation and subsequent permeability. Taken

together, our results suggest an alternative function for RIPK1/RIPK3 in vascular permeability leading to decreased number of metastasis.

Keywords: extravasation, endothelial cells, RIPK3, RIPK1, MLKL, necrosome, vascular permeability

Introduction

Cell death is considered to be one of the hallmarks of malignancy – either by up-regulation of anti-apoptotic genes or down-regulation or silencing of pro-apoptotic genes[1]. In doing so, tumor cells become resistant to extracellular cues to commit cell death. Programmed necrosis or necroptosis is a cell death pathway triggered in response to tumor necrosis factor (TNF), Fas, toll like receptor ligands and type I interferon upon loss or inhibition of caspase-8[2-6]. Therefore, necroptosis can serve as an alternative cell death program when caspase dependent apoptosis is inhibited or absent.

RIPK1, a multifunctional protein that contains an N-terminal Ser/Thr kinase domain, is known to be a critical regulator at the decision point of cytokine induced NF-kB activation for survival or cell death by either apoptosis or necroptosis[7]. Necroptosis is triggered by RIPK1 interaction with RIPK3, RIPK3 dimerization, autophosphorylation of RIPK3 and subsequent phosphorylation of mixed lineage kinase domain-like protein (MLKL)[8-10]. Upon phosphorylation, MLKL trimerizes and forms a pore-complex that can compromise cell membrane integrity[11,12] and subsequently lead to the execution of necroptosis. The result is an inflammatory response to the release of danger associated molecular patterns and/or the direct regulation of cytokines by RIPK1/RIPK3 dimerization[13]. Indeed, tissue-specific loss of caspase-8 or FADD in intestinal epithelial cells results in chronic inflammation that is rescued in part by loss of RIPK3[14-16].

Recent evidence suggests RIPK3 is a tumor suppressor. RIPK3 has been found to be epigenetically silenced in breast and pancreatic cancer tissue[17,18] and in melanoma cell line[19]. In tumor models, loss of RIPK3 aided a TAK1-induced inflammation model of hepatocarcinogenesis[20] while loss of RIPK3 in combination with internal tandem duplication mutations of FMS-like tyrosine kinase-3 led to an increase in leukemia *in vivo* which was due to the absence of inflammasome activation[21]. Expression of RIPK3 in patient samples also has been associated with disease outcome. In cervical cancers, low RIPK3 protein expression in patient biopsies correlated to a reduced response to PolyIC-based adjuvant immunotherapeutic approaches[22]. In patients suffering from intestinal bowel disease and presenting with colorectal cancer, loss of RIPK3 expression was detected in neoplastic tissue compared to non-neoplastic and the loss of expression was correlative to a poor prognosis[23]. These findings suggest a role for RIPK3 and potentially necroptosis in tumorigenesis as well as prognosis.

By contrast, the deletion of RIPK1, RIPK3 or MLKL in breast cancer cell lines reduced the tumorigenic potential of the cell to form colonies and subcutaneous tumors in immunocompromised mice[24]. To add to the complexity, increased expression in RIPK3, RIPK1 and MLKL was found in patient pancreatic ductal adenocarcinoma (PDA) compared to normal tissue and the loss of RIPK3 in a V12Kras induced pancreatic ductal adenocarcinoma model increased survival by reducing the expression of CXCL1/Mincle pathway and by altering the presence of tumor suppressive immune cell[25]. In addition, our

work and others show that RIPK1/RIPK3 drive cytokine production either in conjunction with initiating necroptosis or completely independently[26,27]. This makes it difficult to interpret inflammation driven *in vivo* models of tumorigenesis in RIPK3 deficient mice.

We sought to differentiate the role of RIPK3 or necroptosis in tumorigenesis versus the tumor microenvironment by utilizing syngeneic mouse tumor models. In addition, these models can be used to simulate metastasis, what 90% of cancer patients die from rather than the primary tumor. Few compounds are in the clinic targeted against metastasis, mostly due to the ineffective ability of these compounds to reduce primary tumor. Similar to recently published results, we found the role of RIPK3 in the tumor microenvironment was not due to altered immune response but the ability of tumor cells to extravasate into the lung[28]. However, we found the kinase activity of RIPK1 but not RIPK3 was important in the extravasation step of metastasis. Loss of MLKL showed a reduction but not significant number of tumor nodules formed in the lung compared to *Ripk3*$^{-/-}$. Our data shows that in addition to the possibility of activating necroptosis through a death receptor 6 (DR6) mediated manner as previously found, RIPK3 plays a critical role as signaling platform downstream of stimuli promoting permeability through p38/HSP27. These data supports the role of RIPK1/RIPK3 in promoting vascular permeability required for tumor cell extravasation as a signaling platform.

Results

To determine whether tumor cells were able to form a solid tumor, *Ripk3*$^{-/-}$ mice were injected subcutaneously with B16-F10 cells. In agreement with recently published data[25], solid tumors formed at the same rate and volume in both wildtype and *Ripk3*$^{-/-}$ mice (Figure 10a). This suggested the loss of RIPK3 in the tumor microenvironment did not affect established tumor cells from growing. To determine if RIPK3 in the tumor microenvironment could play a role in a tumor metastasis model, B16-F10 tumor cells were injected tail vein into wildtype mice. Lung homogenates were made 2, 6 and 12 hours after tail vein injection and probed on a western blot for levels of RIPK3. After 12 hours, the level of RIPK3 protein was approximately 2 fold higher (Figure 10b), suggesting a potential role for RIPK3 in tumor formation in the lung. Using littermates, mice were injected tail vein with B16-F10 cells without knowledge of the genotype and 14 days post injection (dpi), lungs were counted for tumor nodules. After genotyping, the number of tumor nodules were reduced significantly by approximately 50% (Figure 10c, $p<0.05$) in the Ripk3$^{-/-}$ mice compared to Ripk3$^{+/+}$. Interestingly, *Ripk3*$^{+/-}$ mice showed an intermediate phenotype between wildtype and *Ripk3*$^{-/-}$. Additional wildtype and *Ripk3*$^{-/-}$ mice were then injected tail vein with B16-F10 cells and 14 days post injection (dpi), after blinding, the lungs were counted for tumor nodules. There was a 46% (±7.6%) decrease in tumor nodules in the RIPK3 null lungs compared to wildtype (Figure 10d left panel, $p< 0.01$). The size of the tumor nodules was categorized into large, medium or small based on width of the nodule from pictures of the lungs and though not significant, there was a tendency towards smaller nodules (Figure 10d, right panel). To ensure the phenotype was not restricted to B16-F10 tumor model, MC-38 colon carcinoma cells were injected intravenously and tumor nodules in the lung were counted 20 dpi. Consistent with the B16-F10 tumor model, a decreased number of nodules in the *Ripk3*$^{-/-}$ mice were found compared to wildtype mice (Figure 10e) suggesting the decrease in tumor nodules in the *Ripk3*$^{-/-}$ was not dependent on the tumor cell type.

The necrosome is composed of RIPK1 and RIPK3 and the kinase activity of RIPK1 and RIPK3 is believed to be important and/or essential for activating necroptosis by

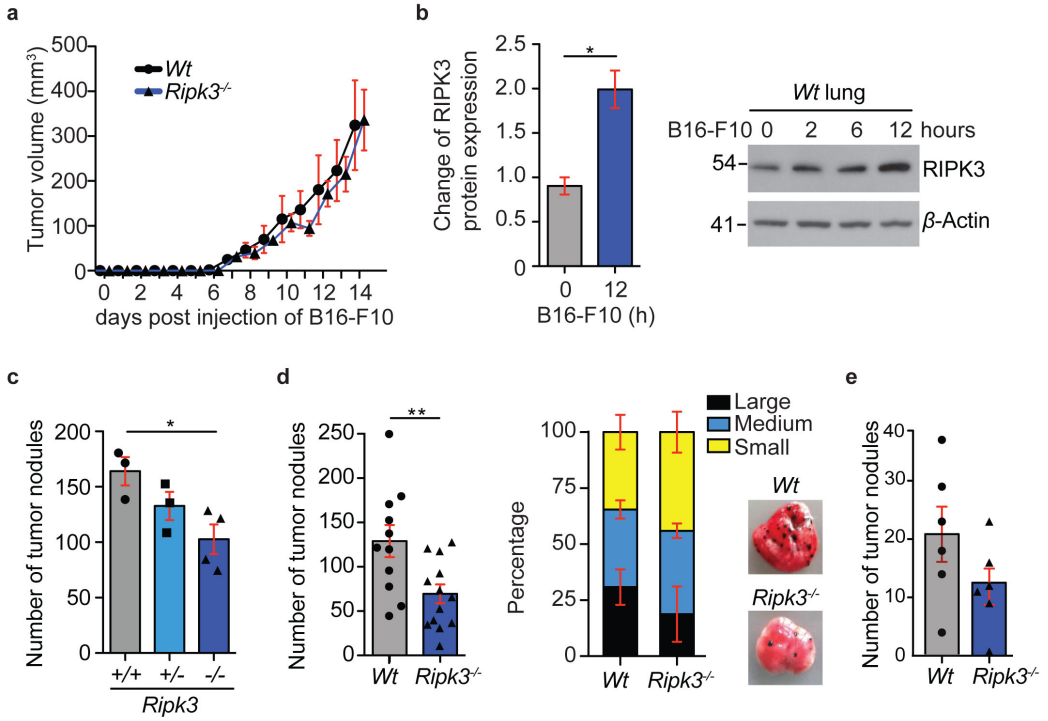

Figure 10: Loss of RIPK3 in the tumor microenvironment reduces tumor nodules in the lung in a tumor model of extravasation. (a) Wildtype (Wt) and Ripk3$^{-/-}$ mice were injected subcutaneously with 1x10^5 B16-F10 tumor cells and tumor size was measured over time (pooled data of n=2 experiments n=2; 5-7 mice used per group in each experiment. **(b)** RIPK3 protein levels were elevated in total lung lysates of wildtype mice 12h after injection of B16-F10 cells shown by representative immunoblot and corresponding quantification of pixel density from 3 mice per timepoint. Fold change relative to untreated Wt control is shown from values normalized to Actin. **(c)** Tumor nodules were counted 14 days post tail vein injection (dpi) of B16-F10 cells (2x10^5) into Ripk3 littermate control mice (left panel, n=1 ; 3-4 mice used per group) and **(d)** tumor nodules were counted 14 dpi of B16-F10 cells (2x10^5) into Wt and Ripk3$^{-/-}$ mice (left panel, SEM and pooled data shown of n=3 experiments ; 3-5 mice used per group in each experiment. Corresponding Size is shown of tumor nodules classified macroscopically into large (>1mm), medium (0.5mm-1mm) and small (<0.5mm) shown (right panel), and corresponding representative macroscopic pictures of the lungs were shown. **(e)** Tumor nodules were counted 20 dpi of MC-38 cells (3x10^5) into Wt and Ripk3$^{-/-}$ mice (n=1, SEM; 6 mice used per group). Each dot represents a mouse except stated otherwise; Statistical analysis by t-test.

phosphorylating MLKL. Currently, MLKL is considered to be the essential and the only known effector protein for necroptosis[10,11]. To determine if proteins composing the necrosome were important in the reduction of tumor nodules in the lung, RIPK1 kinase dead (K45A) mice were injected with B16-F10 cells (tail i.v.) and after 14 dpi, the lungs were harvested, blinded and tumor nodules were counted. Tumor nodules in the *Ripk1*$^{K45A/K45A}$ mice were decreased by 38.3% (±8.5%) decrease compared to wildtype mice (Figure 11a, $p<0.05$). Next, RIPK3 kinase dead mice were injected tail vein with B16-F10 cells and again, after 14 dpi, lungs were blinded and nodules were counted in the lung. No difference in the number of tumor nodules were found (Figure 11b). As protein levels of the kinase dead RIPK3 K51A mutant have been shown to be decreased due to protein instability, we assessed the levels of protein present in lung homogenates and found the expression of the RIPK3 mutant to be significantly decreased (Supplementary Figure 1a)[29]. To control for the decreased change in expression, we compared the *Ripk3*$^{wt/K51A}$ to the *Ripk3*$^{K51A/K51A}$ mice. No difference in the number of tumor nodules formed in the lung (Figure 11c). To verify that loss of RIPK3 kinase activity was able to block necroptosis, isolated endothelial cells from the lungs of *Ripk3*$^{K51A/K51A}$ mice were tested with typical activators of necroptosis, TNF, zVAD and/or Smac mimetics (Supplementary Figure 1b). As expected, compared to wildtype the RIPK3 deficient- and *Ripk3*$^{K51A/K51A}$ expressing cells were resistant to necroptosis caused by the combination of TNF, zVAD and Smac mimetic treatment. Interestingly while the kinase activity of RIPK1 was required, it appeared the loss of kinase activity from RIPK3 was not required in tumor formation in the lung. Finally, to assess if necroptosis was indeed the reason for the decrease in tumor nodules in the lung, we injected B16-F10 cells tail vein into wildtype, *Mlkl*$^{-/-}$ and *Ripk3*$^{-/-}$ mice. After blinding the harvested lungs, nodules were counted. Only a slight decrease in the number of tumor nodules was seen upon loss of MLKL in the tumor microenvironment while the loss of tumor nodules re-capitulated in the complete *Ripk3*$^{-/-}$ mice (Figure 11d). The combined results of the number of tumor nodules found in the kinase dead RIPK3 and MLKL deficient mice suggested an alternative role for RIPK3 involving the kinase activity of RIPK1.

As the loss of RIPK3 in Vucur et al., led to an increase in caspase-8 dependent apoptosis in a TAK1 inflammatory driven hepatocarcinoma[20], we assessed for the presence of cell death in the lung during B16-F10 cell homing and extravasation. TUNEL staining was used to determine cell death as this technique will pick up both apoptosis or necrosis/necroptosis[30]. For this, lung sections of mice injected with B16-F10 at different timepoints (0, 6, 12 hours) were analyzed for TUNEL positive cells. The positive control, intestinal epithelial cells from wildtype mice injected with TNF stained positive for TUNEL while lungs from wildtype or *Ripk3*$^{-/-}$ mice did not stain TUNEL positive (Figure 11e). In addition, little to no caspase-3 activity was measured in lung homogenates of mice injected with B16-F10 at different time points (Supplementary Figure 1c). This suggests the kinase activity of RIPK3 and therefore the ability for necroptosis to occur in the tumor microenvironment did not alter tumor nodule formation and that inhibition of necroptosis was not dependent on levels of protein expression.

To determine the additional role the loss of RIPK3 may play in metastasis, we next assessed whether the B16-F10 cells were able to home to the lung in the *Ripk3*$^{-/-}$ mice. B16-F10 luciferase cells were injected and monitored after injection for movement to the lung over time. Equivalent luminescence was measured between wildtype and *Ripk3*$^{-/-}$ mice

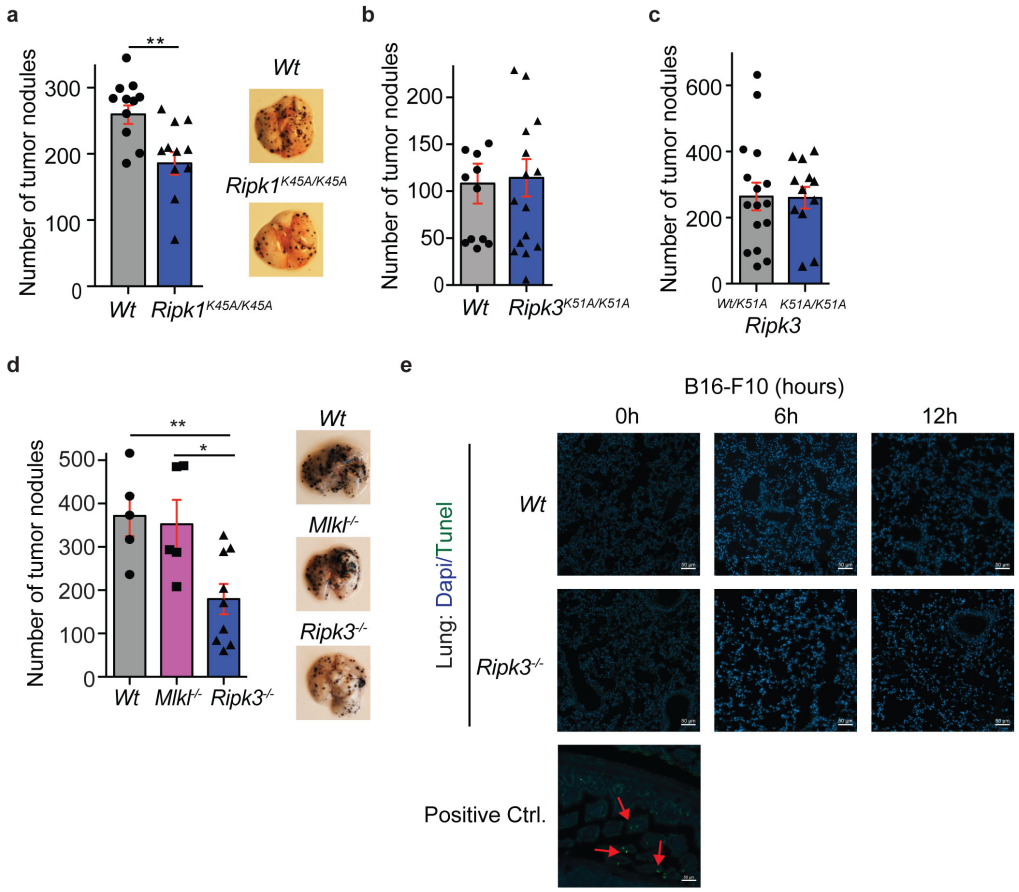

Figure 11: RIPK1 kinase activity but not RIPK3 kinase activity or MLKL in the tumor-microenvironment is needed for tumor nodule formation in the lung. Tumor nodules were counted 14 dpi of B16-F10 cells into **(a)** Wt and Ripk1$^{K45A/K45A}$ mice (pooled data of n=2 experiments; 4-7 mice were used per group in each experiment) and representative pictures of lungs are shown ,**(b)** Wt and Ripk3 $^{K51A/K51A}$ mice (pooled data of n=2 experiments; 5-8 mice were used per group in each experiment) and **(c)** into Ripk1$^{Wt/K45A}$ and Ripk1$^{K45A/K45A}$ mice (pooled data of n=4 experiments; 3-4 mice were used per group in each experiment). **(d)** Tumor nodules were counted 14 dpi of B16-F10 cells into Wt, Mlkl$^{-/-}$ and Ripk3 $^{-/-}$ mice and representative pictures are shown (data from of n=2 experiments; 2-6 mice were used per group in each experiment. **(e)** Paraffin embedded lung sections from mice injected tail vein with B16-F10 at indicated time points were stained for TUNEL (FITC) and DAPI. intestine of cIAP1$^{-/-}$ mice injected with TNF was used as a positive control and red arrows indicate TUNEL positive cells. Each dot represents a mouse; Statistical analysis by t-test.

within the first 24 hours (Figure 12a). This suggested the B16-F10 cells were surviving and homing to the lung the same in the *Ripk3*$^{-/-}$ mice compared to wildtype.

Chemokines such as C-C motif chemokine ligand 2 (CCL2) have been shown to induce signaling to recruit inflammatory monocytes as well as induce endothelial extravasation[31,32]. To determine if RIPK3 was critical in producing cytokines or chemokines required to recruit inflammatory monocytes, myeloid infiltrates and cytokines/chemokines post injection of B16-F10 cells were analyzed in lungs of wildtype and *Ripk3*$^{-/-}$ mice. We examined whether chemokines/cytokines to attract inflammatory monocytes were altered in *Ripk3*$^{-/-}$ mice compared to wildtype mice after B16-F10 injection using lung homogenates. An increase in CCL2, CCL7 and CXCL10 is seen in both wildtype and *Ripk3*$^{-/-}$ mice (Figure 12b). In addition, inflammatory cytokines such as IL-1β were induced in a similar pattern in lung homogenates (Figure 12b) while TNF was below the limit of detection. This suggests the ability to produce cytokines to attract monocytes was functional in the lung of *Ripk3*$^{-/-}$ mice. We then assessed the immune infiltrates in the lung by flow cytometry. After 6 hours post B16-F10 injection, a significant increase in the number of inflammatory monocytes (Ly6C^{hi}CCR2^{+}) were seen in *Ripk3*$^{-/-}$ mice compared to wildtype (Figure 12c). Similarly, CD11b^{high} dendritic cells increased while the CD103^{+} dendritic cell population decreased in wildtype and *Ripk3*$^{-/-}$ lungs after B16-F10 injection (Supplementary Figure 2). Natural killer T cells also responded in a similar manner in both wildtype and *Ripk3*$^{-/-}$ lungs after B16-F10 injection (Supplementary Figure 2b).

To determine the potential for the hematopoietic or stromal compartment to play a role in the reduction in tumor nodules found in *Ripk3*$^{-/-}$ lungs, we performed bone marrow chimeric experiments. CD45.1 recipient mice were irradiated and reconstituted with either wildtype or RIPK3 deficient bone marrow. Only mice with reconstitution efficiency greater than 95% were used for B16-F10 injection (data not shown). After 14 days post injection, tumor nodules in the mice with RIPK3 deficient hematopoietic compartment were similar in number compared to mice with wildtype hematopoietic compartment (Figure 12d). This suggests that the hematopoietic compartment does not influence the total number of tumor nodules in the lung. We then irradiated *Ripk3*$^{-/-}$ and CD45.2 mice and reconstituted the bone marrow with wildtype or RIPK3 deficient bone marrow. After 14 dpi, tumor nodules were counted. In comparison to wildtype mice reconstituted with *Ripk3*$^{-/-}$ bone marrow, there was a decreasing amount of tumor nodules in the *Ripk3*$^{-/-}$ mice reconstituted with wildtype (17.6%±23) or *Ripk3*$^{-/-}$ bone marrow (38.6%±22.6), respectively (Figure 12d, right graph). Taken together, the data suggested that the reduction in tumor nodules in the *Ripk3*$^{-/-}$ mice was due to the stromal compartment and not due to the hematopoietic compartment.

The first barrier to the tumor cells to form tumors in the lung is the vascular endothelial barrier. To determine if there was a tumor cell transmigration defect, we isolated CD31^{+} cells from the lungs of wildtype, *Ripk3*$^{-/-}$ or *Ripk3*$^{K51A/K51A}$ mice and performed transmigration assays. A decreased number of B16-F10 cells transmigrated through *Ripk3*$^{-/-}$ endothelial cells compared to wildtype or *Ripk3*$^{K51A/K51A}$ endothelial cells (Figure 13a). We also determined if wildtype monocytes could facilitate increased tumor cell transmigration. Two fold more B16-F10 cells transmigrated through wildtype endothelial monolayer in the presence of monocytes (Figure 13a). Strikingly, the addition of *wildtype* monocytes did not increase the ability of B16-F10 cells to transmigrate through a RIPK3 null endothelial monolayer. By contrast, the addition of RIPK3 null monocytes did enhance B16-F10

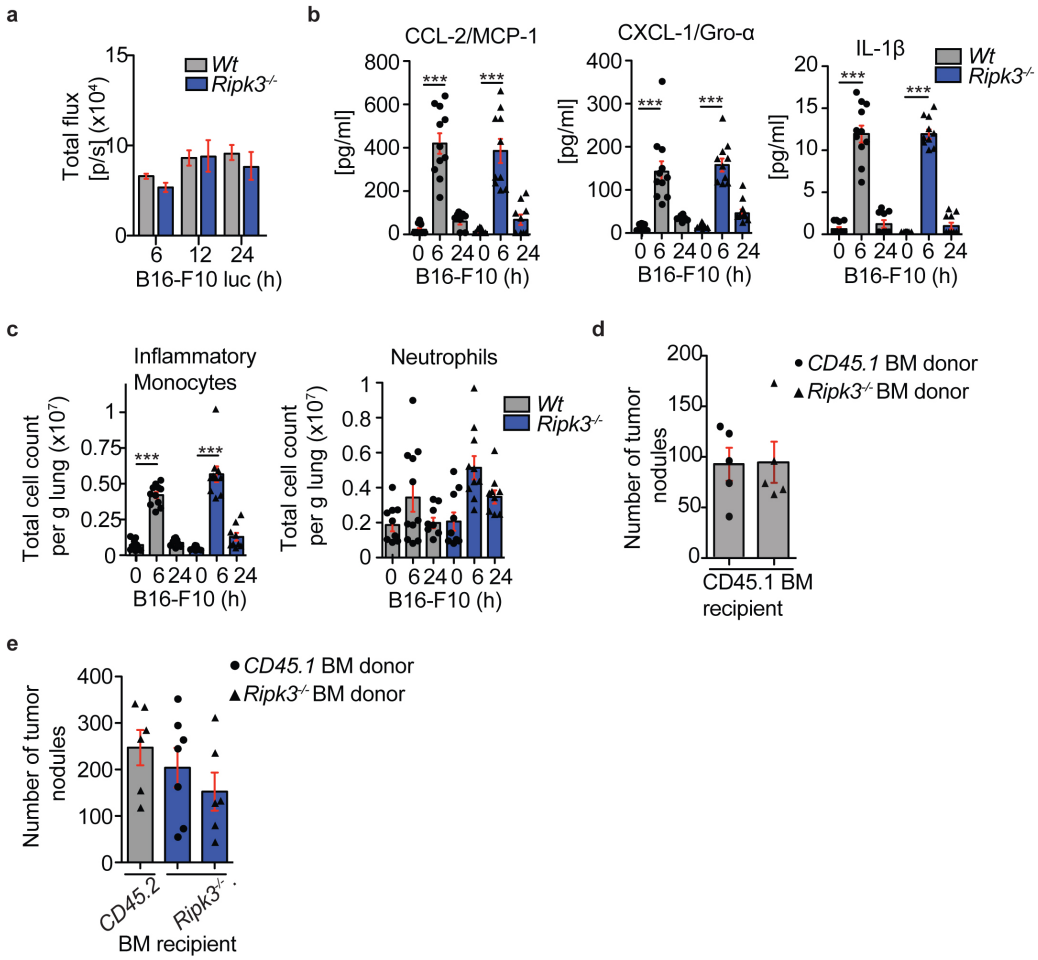

Figure 12: Loss of RIPK3 in the microenvironment does not alter early immune and cytokine response upon B16-F10 injection, and bone marrow reconstitution shows RIPK3 in the stromal compartment to be important for tumor formation. (a) B16-F10 luciferase cells home to the lung in both Wt and Ripk3$^{-/-}$ mice measured by IVIS luminescent imaging (representative shown from n=2 experiments, 4-5 mice per group in each experiment). **(b)** Cytokine levels in total lung lysates were measured by multiplex bead assay and levels of CCL-2, CXCL-1 and IL-1β are shown (data pooled of n=2 experiments, 4-6 mice were used per group in each experiment) and **(c)** corresponding immune cell infiltration analysis by flow cytometry shows inflammatory monocytes (SiglecF- Ly6G- Ly6Chi CCR2+) and neutrophil granulocyte (SiglecF- CD11b+ Ly6G+) populations. Populations were pre-gated on singlets, live cells, Ter119- and CD45+ cells. **(d)** Tumor nodules were counted 14 dpi of B16-F10 into CD45.1 recipient mice reconstituted with CD45.2 Wt and CD45.2 Ripk3$^{-/-}$ bone marrow cells (data pooled of n=3 experiments, 2-4 mice were used per group) and **(e)** CD45.2 or Ripk3$^{-/-}$ recipient mice reconstituted with CD45.1 or Ripk3$^{-/-}$ bone marrow cells (data pooled of n=2 experiments, 2-3 mice were used per group). Each dot represents a mouse; Statistical analysis done by one-way ANOVA and Bonferroni post-test.

transmigration through wildtype endothelial monolayer but not through the RIPK3 null endothelial monolayer. Moreover, the *Ripk3*$^{K51A/K51A}$ endothelial cells allowed B16-F10 cells to transmigrate through similar to wildtype with either wildtype or *Ripk3*$^{-/-}$ monocytes. These results support the idea that the hematopoietic compartment does not play a role in the loss of tumor formation in the *Ripk3*$^{-/-}$ mice similar to findings in Figure 12d and further supports observation that the kinase activity of RIPK3 in the endothelial cells is not required for the ability of tumor cells transmigrate and tumor nodules to form in the lung (Figure 11b and c).

To determine if necroptosis occurred to allow for transmigration, we isolated CD31^{+} cells from the lungs of wildtype, *Ripk3*$^{-/-}$ and *Mlkl*$^{-/-}$ mice. Primary lung endothelial cell (EC) monolayers were incubated with either $3x10^4$ or $9x10^4$ B16-F10 cells. Cell death was assessed 8 hours later by flow cytometry as our *in vivo* imaging suggested the tumor cells homed to the lung within 6 hours (Figure 12a). B16-F10 cells were stained for identification with the membrane dye PKH26 and were removed from the population for cell death assessment of endothelial cells. Cells were then stained using Annexin-V FITC and propidium iodide to discriminate live, early apoptotic, or late apoptotic or necrotic cells. The overall percentage of dead wildtype ECs (either early apoptotic or late apoptotic/necrotic cells) increased by 1-3 % with the increasing amount of tumor cells whereas *Ripk3*$^{-/-}$ or *Mlkl*$^{-/-}$ ECs only showed an increase of 1-2% dead cells upon $9x10^4$ tumor cell addition. However, the percentage of late apoptotic or necrotic ECs increased upon tumor cell addition was independent of the genotype of the ECs. This suggested RIPK3 may play an additional role to that of the proposed tumor cell induced necroptosis as proposed[28].

Vascular permeability has been proposed as a hypothesis for tumor metastasis with a number of factors, such as vascular endothelial growth factor (VEGF), fibroblast growth factor (FGF), and CCL2 mediated by the tumor cell interaction with the endothelial cells[33-35]. Recent data shows that activation of VEGF leading to c-Src activation and subsequent adherens junction change in VE-cadherin increases vascular permeability and aids in tumor metastasis[36]. To determine if factors involved in vascular permeability was affected, we assayed for VEGF, FGF-b or TWEAK in lung homogenates of widltype and *Ripk3*$^{-/-}$ mice injected with B16-F10 cells. Interestingly the loss of RIPK3 showed no increase in VEGF at 6 hours after B16-F10 cell injection compared to wildtype (Figure 14a). A decrease in metalloproteinase 9 (MMP-9) was detected at 24 hours after B16-F10 cell injection in the lungs of *Ripk3*$^{-/-}$ compared to wildtype (Figure 14a). VEGF and FGF was also detected in supernatant of transmigration assays of either wildtype or *Ripk3*$^{-/-}$ ECs with monocytes and tumor cells after 20 hours. There was also a decrease in MMP-9 in the supernatant of transmigration assays where RIPK3 deficient monocytes were added independent of the genotype of the endothelial cells (Supplementary Figure 3a). These data suggested that factors involved in vascular permeability were present with the exception of VEGF which was reduced at 6 hours in the lung of *Ripk3*$^{-/-}$ after B16-F10 cell injection. We therefore assessed if pulmonary vascular permeability after tumor injection was affected in the *Ripk3*$^{-/-}$ mice using the Evans blue permeability assay was assessed. Evans blue dye binds to albumin and uptake of the dye in organs is a measure of tissue permeability. Evans blue dye was injected into wildtype and *Ripk3*$^{-/-}$ mice 20 hours post injection of B16-F10 cells. The amount of Evans blue dye in wildtype lung homogenate increased slightly when B16-F10 cells were injected, but no increase in Evans blue dye was observed in RIPK3 deficient mice (Figure 14b).

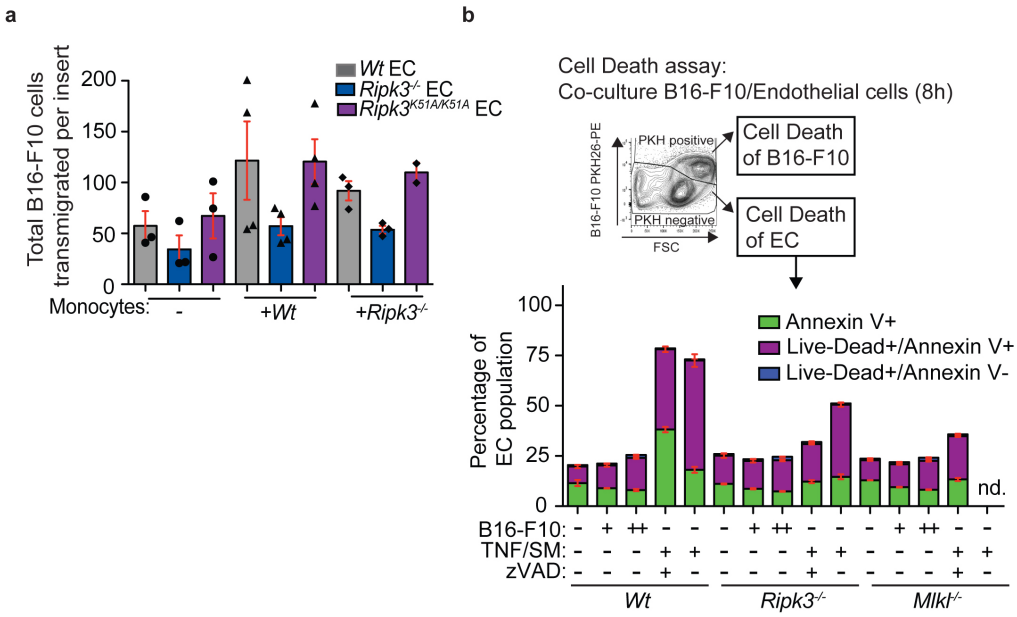

Figure 13: Ripk3 promotes tumor cell transendothelial migration independent of its ability to block necroptosis. (a) Boyden chamber transendothelial migration assay using B16-F10 cells and primary CD31+ endothelial cells (EC) isolated from lungs of Wt, Ripk3$^{-/-}$ or Ripk3$^{K51A/K51A}$ mice. Primary monocytes were isolated on the day of seeding B16-F10 cells and 20 hours later, transwells were fixed, stained, and imaged. Images analysis was blinded and tumor cells were counted per field of view. The data is pooled from n=2 experiments; 1-3 transwell inserts were assayed per group in each experiment and 10-17 fields per view were analyzed per transwell insert. Total number of B16-F10 transmigrated cells per transwell insert is shown. Each dot represents an insert. Statistical analysis by one-way ANOVA and Bonferroni post-test. **(b)** EC monolayers from Wt, Ripk3$^{-/-}$ and Mlkl$^{-/-}$ mice were co-incubated with PKH26 stained B16-F10 (+=3x10^4; ++=9x10^4) cells and assayed for cell death 8 hours later by flow cytometry (n=3; nd.= not determined). Cells were stained for annexin V and propidium iodide (live/dead) to identify early apoptotic cells (annexin V+ Live-Dead-) and dead cells (Live-Dead+ annexin V+ or Live-Dead+ annexin V-). Statistical analysis done by one-way ANOVA and Bonferroni post-test.

To further assess the issue of vascular permeability, we treated primary endothelial cells for 4h with VEGF-A_{164} and assayed for endothelial leakiness using dextran-FITC. While there was a significant increase of 15.7% ±3.9% in levels of dextran-FITC detected from VEGF-A_{164} treated wildtype endothelial cells there was no increase of permeability seen in treated *Ripk3*$^{-/-}$ endothelial cells (Figure 14c). Furthermore we asked if RIPK3 in the endothelium could limit VEGF-A_{164} induced increase in B16-F10 transmigration. A trend to an increase of 26.8% B16-F10 cells migrated past Wildtype endothelial cells upon VEGF-A_{164} pre-stimulation. However, VEGF-A_{164} pre-stimulated *Ripk3*$^{-/-}$ endothelial cells did not show a similar increase of transmigrated B16-F10 cells compared to VEGF-A_{164} pre-stimulated wildtype (Figure 14d). Similar, when RIPK3 was downregulated in human umbilical vein endothelial cells (HUVECs), these cells showed a two-fold increase in basal vessel sprouting. More important, the addition of VEGF-A induced the outgrowth of sprouts in this angiogenesis assay as expected in the cells transfected with control siRNA. Interestingly, the RIPK3 silenced HUVECs were not capable to respond to VEGF-A and enhance vascular sprouting and vessel growth (Figure 14e). Taken together these results show that RIPK3 deficient endothelial cells fail to respond towards tumor induced vascular permeability and towards VEGF-A induced permeability and angiogenesis, resulting in a defect in B16-F10 transendothelial migration.

To determine the potential mechanism of how RIPK3 may affect vascular permeability, we examined downstream signaling in response to VEGF-A, VEGF-B or FGF-b. In response to VEGF-A, VEGF-B and FGF-b, wildtype endothelial cells showed an increase in phospho-p38 followed by the downstream phosphorylation of HSP27 protein, while phospho-ERK1/2 decreased in signal (Figure 15a and b and Supplementary Figure 3a). The inverse status of phospho-p38 and phospho-ERK1/2 in response to VEGF-A has been previously shown in HUVECs where activation of p38 leads to decreased levels of ERK1/2 activation[37]. By contrast, RIPK3 null endothelial cells stimulated with either VEGF-A, VEGF-B or FGF-b resulted in reduced phospho-p38 activation compared to wildtype. More strikingly, the downstream phosphorylated protein, HSP27 was also reduced (Figure 15a and b and Supplementary Figure 3a). Put in a different perspective, the increased levels of phosphorylated ERK1/2 at 5min after VEGF-A_{164} in the *Ripk3*$^{-/-}$ endothelial cells compared to wildtype reflected the dampened p38 activation in the RIPK3 knockouts. Interestingly, *Ripk3*$^{-/-}$ endothelial cells without stimulation, had an increased basal level of phospho-p38 present compared to wildtype cells. This slight basal increase of phospho-p38 was observed throughout experiments that had been performed with endothelial cells from different mice as a source. No major differences in the activation of p38/HSP27 between wildtype and *Ripk3*$^{-/-}$ endothelial cells was seen when treated with TNF (Supplementary Figure 3b). To determine if the signaling differences occurred *in vivo* after tumor cell injection, we injected mice with tumor cells and homogenized lung at 2, 6 and 12 hours. Interestingly, basal levels of phospho-p38 occurred in the *Ripk3*$^{-/-}$ lungs compared wildtype. At 2 hours, phospho-p38 was up-regulated in wildtype mice but not in *Ripk3*$^{-/-}$ mice. Taken together, our data shows that RIPK3 positively regulates the activation of p38 and HSP27 upon permeability factor treatment (VEGF-A, VEGF-B, FGF-b) and therefore promoting permeability in the tumor microenvironment and enhancing the ability of tumor cells to metastasize (Figure 15c).

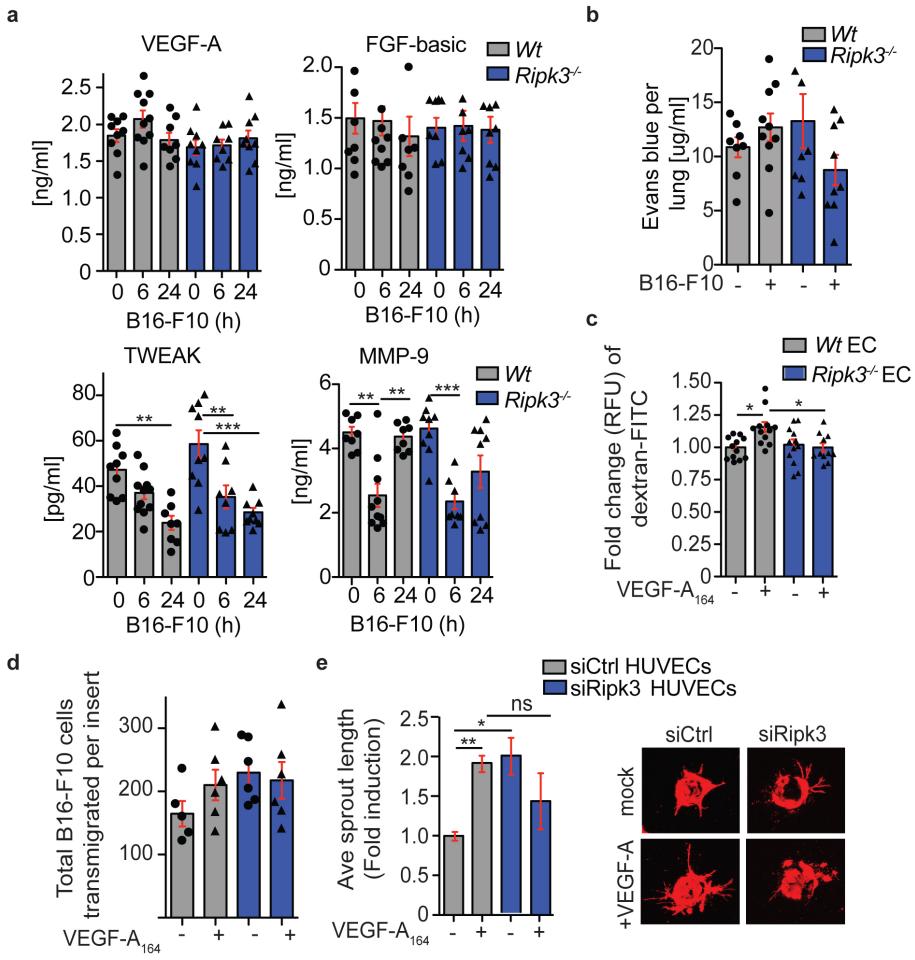

Figure 14: Ripk3 promotes VEGF-A dependent vascular permeability and sprouting. (a) Levels of angiogenic- and remodeling factors in total lung lysates of were measured by multiplex bead assay and levels of VEGF-A, FGF-basic, TWEAK and MMP-9 are shown (data pooled of n=2 experiment; SEM; 4-6 mice were used per group; each dot represents a mouse). **(b)** Evans blue blood vessel permeability assay of Wt and Ripk3$^{-/-}$ lungs 20h after B16-F10 tumor cell injection i.v. (pooled data of n=2 experiments, 4-5 mice were used per group in each experiment; Each dot represents a mouse). **(c)** Primary lung endothelial monolayer on transwell inserts were treated with VEGF-A164 (100ng/ml) for 4 hours and dextran-FITC permeability assay was performed. Data shows relative fluorescence unit (RFU) of dextran-FITC that passed EC barrier (pooled data of n=5 experiments; SEM; 2-3 transwell inserts were used per group in each experiment; Each dot represents a transwell insert).**(d)** Subsequent B16-F10 transendothelial migration assay was performed after dextran-FITC permeability assay and 20h after B16-F10 (PKH26+) cells were seeded into inserts, transwells were fixed, stained, and imaged. Image analysis was blinded and tumor cells were counted per field of view. The data is pooled from n=2 experiments; 2-3 transwell inserts were assayed per group in each experiment and 10-17 fields per view were analyzed per transwell insert. SEM and total number of B16-F10 transmigrated cells per transwell insert is shown . Each dot represents an insert. Statistical analysis by one-way ANOVA and Bonferroni post-test. **(e)** HUVECs were transfected with indicated siRNAs and fibrin-gel angiogenesis assay was performed. HUVECs were coated on microcarrier beads and cultured in fibrin-gels at indicated conditions and after six days sprout length was determined. Representative fluorescnece microscopy images are shown. Data from n=3 experiments; SEM; statistical analysis by t-test.

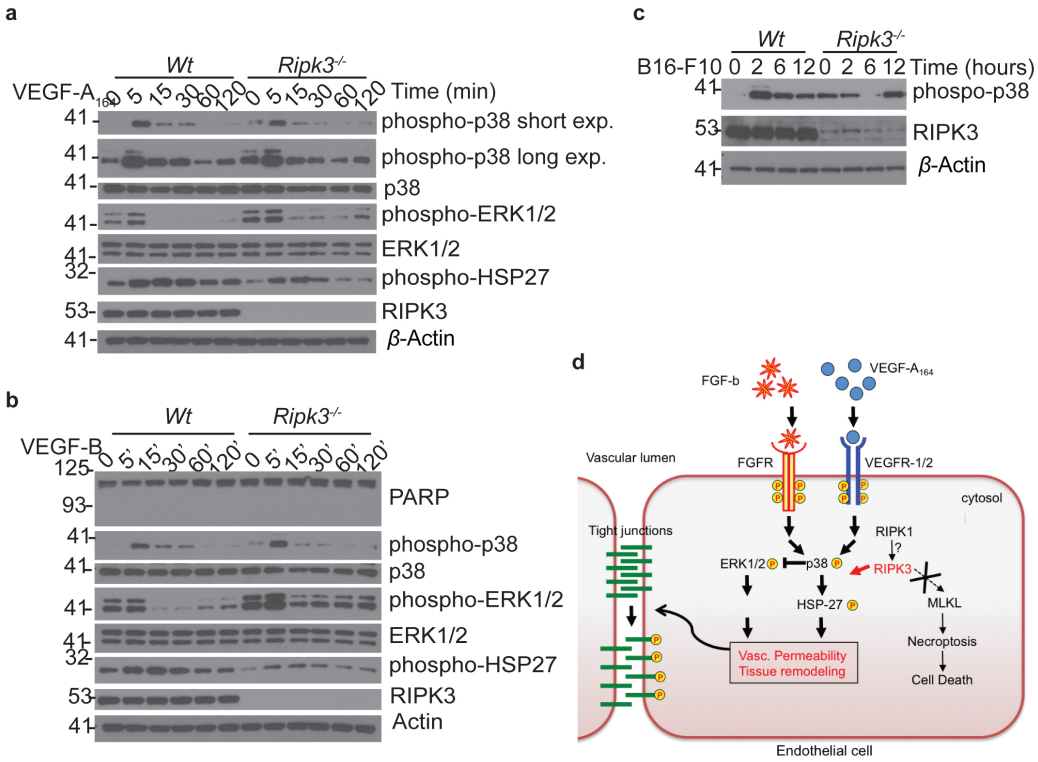

Figure 15: Ripk3 promotes VEGF-A dependent activation of HSP27 MAP kinase signaling axis. (a+b) SV40 large T immortalized endothelial cells isolated from Wt or Ripk3$^{-/-}$ mice were treated with VEGF-A or VEGF-B (10ng/ml) and assayed for signaling by immunoblot analysis as indicated. Representative immunoblot is shown of n=3 experiments; SEM shown. **(c)** Tumor cells were injected into mice at indicated timepoints and lungs were lysated and assayed by immunoblot analysis for phosphorylated p38, RIPK3 and loading control. **(d)** Proposed model: The data suggests that upon VEGF-A or FGF but not TNF stimulation RIPK3 promotes the phosphorylation of HSP27 in endothelial cells. We hypothesize that the dampened activation of the p38/HSP27 axis upon loss of RIPK3 could explain the reduced responsiveness towards angiogenic factors such as VEGF-A or FGF-b and therefore RIPK3 promotes VEGF-A dependent vascular permeability and angiogenesis. Summarizing, our study reveals a physiological example that RIPK3 has and novel separable roles besides altering cell death modalities.

Discussion

The current dogma is that RIPK3 causes inflammation due to the induction of necroptosis. However, our previous results suggest that RIPK3 may alter cytokine release, particularly TNF in response to loss of IAPs[27]. We therefore set out to determine if RIPK3 may play a role in the tumor microenvironment by promoting cytokine production or causing necroptosis leading to tumor progression. Our results show RIPK3 did not alter tumor growth of established tumors. Changes in cytokine production in *Ripk3*$^{-/-}$ mice compared to wildtype after tumor injection were minimal. Activation of cell death *in vivo* was not detected and when we assessed the involvement of different proteins involved in the necrosome, we found the kinase activity of RIPK1 was important in the ability of tumor cells to form lung nodules. Bone marrow chimeras showed the involvement of the stromal but not the hematopoietic compartment was critical for the loss of tumor nodules in the lung in RIPK3 deficient mice. Finally, we found the loss of RIPK3 in the endothelial compartment in the lung decreased the ability of tumor cells to transmigrate due to the inability of the RIPK3 deficient endothelial cells to respond to permeability factors. These results suggest the role of the necrosome is minimal in the process of tumor cells extravasating and presents a novel role for RIPK3 as a signaling platform downstream of angiogenic factors such as VEGF and FGF.

The current difficulty in assessing the role of necroptosis in related pathologies of human inflammatory disease is the absence of identifying markers. The use of RIPK3 genetic deletion, pharmacological inhibition of RIPK1 and/or correlative evidence of RIPK3 protein or RNA up-regulation has been used to associate the disease state with necroptosis[38,39]. However, as RIPK1 has been shown to have alternative function in regulating apoptosis and necroptosis[40-42] and also directly influencing inflammation[27,43,44], further downstream effectors of necroptosis such as the use of *Mlkl*$^{-/-}$ mice are required to prove the role of necroptosis[45]. In our experiments, the number of pulmonary tumor nodules in the *Mlkl*$^{-/-}$ mice were slightly reduced compared to wildtype mice but did not reduce the number of tumor nodules similar to the loss of *Ripk3*$^{-/-}$. It is unclear what may be the reason for the difference in the tumor nodule numbers in the MLKL knock-out mice we obtained compared to Strilic et al., except for the source of the MLKL null mice[28]. Our data also shows that the kinase activity of RIPK1 plays a role in the ability of tumor nodules to form in the lung. Activation of VEGFR2 by VEGF-A or VEGF-B causes phosphorylation of c-Src and has been linked to increased permeability by altering adherens junction formation, VE-cadherin [36,46]. c-Src has been shown to inhibit Fas induced caspase-8 activation by phosphorylation at Tyr380[47]. Further studies are required to determine if RIPK1 and RIPK3 alter tumor cell extravasation as a complex with or without caspase-8 involvement or if these proteins regulate different pathways to result in vascular permeability.

Vascular permeability requires tissue remodeling similar to wound healing. Impaired wound healing was found in *Ripk3*$^{-/-}$ mice compared to wildtype, characterized by a decreased MMP-9 protein expression and delayed CD31^{+} staining and VEGF production[48]. Of the cytokines and growth factors we assayed, only MMP-9 was reduced at 24 hours in the *Ripk3*$^{-/-}$ mice compared to wildtype upon tumor cell injection. The decrease in MMP-9 protein levels correspond to an increase in neutrophil infiltration of the lung at 24 hours in the *Ripk3*$^{-/-}$, suggesting an attempt of the immune system to compensate for the lack of response in the endothelial compartment. The ability of *Ripk3*$^{-/-}$ monocytes to enhance transmigration of tumor cells through a wildtype endothelial layer further suggests a defect in

the *Ripk3*$^{-/-}$ endothelial cells to respond to extracellular cues. Indeed, the absence of RIPK3 reduced signaling in response to VEGF-A, VEGF-B and FGF-b but not TNF in the p38/HSP27 pathway, a key pathway in permeability. Our results show that the reduced tumor nodule formation in RIPK3 deficient mice cannot be attributed to the failure to respond to one stimuli alone. Interestingly, in Seifert et al., the loss of Mincle combined with the V12K-Ras pancreatic ductal adenocarcinoma did not protect as well as the loss of RIPK3, suggesting additional factors might play a role in the ability of RIPK3 to form pancreatic ductal adenocarcinoma in a V12Kras model[25]. Further investigation of other permeability factors *in vivo* and whether these ligands can form complexes of RIPK1/RIPK3 will be of interest to determine if these intracellular proteins can be targeted to block several pathways involved in tumor metastasis.

The effect of RIPK3 on calcium signaling as well as the production of reactive oxygen species (ROS) has been reported for necroptosis to occur in a model of ischemia/reperfusion[49,50]. Calcium release and ROS have also been reported to play a role in vascular permeability but at much lower levels than that measured for cell death[51]. Whether the loss of RIPK3 in endothelial cells may lead to the combined dampened effect on these signaling pathways may also play a role in the ability of endothelial cells to respond to vascular dilation. Given another effector molecule such as Ca2+ /calmodulin-dependent protein kinase II has been reported to play a role in cardiac ischemia/reperfusion downstream of RIPK3[50], these processes will need to be explored. Moreover, It will be important to determine whether cell death in endothelial cells *in vivo* may play role for a subset of endothelial cells and/or if altering tight junctions dynamics in endothelial barriers results in the loss of critical survival signals that then leads to cell death.

Ripk3$^{-/-}$ mice have not been reported to have any vascular defects during normal development. Interestingly, we repeatedly detect increased basal phospho-p38 levels in untreated primary endothelial cells and lung homogenates suggesting the loss of RIPK3 is compensated during development and regular homeostasis. It appears only during stress such as wound healing or tumor challenge, does RIPK3 become required for the response to the additional stimuli. Changes at the basal level in structure of the vessels or lung vessel structure have not been assessed and may provide insight to why the *Ripk3*$^{-/-}$ mice develop with little to no overt phenotype.

In summary, our study shows RIPK3 has a physiological role in the tumor microenvironment, in particular tumor cell extravasation and re-modeling by altering the downstream signaling pathways of permeability factors. This is a novel role for RIPK3 in addition to its role in regulating necroptosis. In the context of inflammation and cell death, this supports previous reports suggesting RIPK3 cannot be used as an indicator of necroptosis and the potential of RIPK3 to be a signaling platform will need to be assessed in each disease model individually.

Materials and Methods

Animal work. Animals were maintained under optimized hygiene conditions (OHB), and experiments were approved by Zürich Cantonal Veterinary Committee in accordance to the guidelines of the Swiss Animal Protection Law (License 119/2012 and 186/2015). C57BL/6 mice were purchased from Janvier Labs, *Ripk3*$^{-/-}$ mice were a kind gift from V. Dixit[52], SNP analyzed at N=7, *Ripk1*$^{K45A/K45A}$, *Ripk3*$^{K51A/K51A}$ *mice* were a kind gift from John Bertin and

Peter J. Gough from GlaxoSmithKline[29,43], *Mlkl*$^{-/-}$ mice were obtained from J.Murphy[10] (WEHI) . Mice were injected with B16-F10 (2x10^5 cells) or MC-38 (3x10^5 cells) intravenously in 200ul PBS or subcutaneous in 100ul PBS (1x10^5). Mice were euthanized at indicated timepoints by overdose (Ketamin/Xylazin cocktail), lungs perfused and blinded before further processing (nodule counting, flow cytometric analysis). For bone marrow chimeric experiments Wt CD45.1 or *Ripk3*$^{-/-}$ mice were irradiated two times at 550 rads, 6 hours apart, injected with donor bone marrow and assessed for reconstitution efficiency at 6 weeks. Only mice with reconstitution efficiency greater than 95% were used for further experiments.

Cell culture. MC-38 and B16-F10 cells were cultured at max. 50% confluence in Dulbecco's modified Eagle medium (DMEM; GIBCO) with high glucose (4.5g/L) supplemented with 10% fetal bovine serum (FBS; GIBCO) and Penicillin/Streptomycin/Glutamine (GIBCO). Primary- and SV40 immortalized lung endothelial cells were cultured in EBM-2 media supplemented with EGM according to manufacturers recommendation (LONZA).

Primary lung endothelial cell isolation. Lungs were perfused with PBS and HBSS(+Collagenase 1mg/ml; Sigma) and minced before incubated with HBSS(+Collagenase) for 45min and further processed for antibody incubation. Mouse lung cell suspension was incubated with anti-CD31(eBioscience, clone 390) antibody for 30min in PBS (0.5% BSA) at 1:20 dilution in order to isolate lung endothelial cells. To isolate monocytes from bone marrow cell suspension the anti-CD115-biotin (eBioscience, clone AFS98) antibody was used at dilution of 1:50 in HBSS+2% FBS. Cell suspensions were incubated in primary antibody for 30min at 4°C followed by incubation with anti-rat IgG or streptavidin magnetic particels and sorted on LS columns according to the manufacturers recommendations (Miltenyi).

Transendothelial migration assay. Endothelial cell populations greater than 85% purity for CD31$^+$ cells were used. 3x10^4 primary endothelial cells were seeded 5-8 days after isolation on a gelatin coated insert (Corning, 8 um pore size) in EBM2 (Lonza). Two days after seeding cell culture media was changed RPMI (GIBCO) in bottom well (3%FBS) and insert (1% FBS) with or without pre-treatement of VEGF(100ug/ml) for 4h or 1h before addition of 2x10^4 PKH26 (Sigma Aldrich) membrane stained B16-F10 tumor cells and/or 1x10^5 primary isolated monocytes (CD115$^+$). After 20h, the remaining cells inside the insert were removed, membrane fixed in 2% PFA and mounted using slow fade gold with dapi (Thermoscience). Microscopic fluorescence picture were taken at 10x magnification using AXIO Scan (Zeiss). PKH26$^+$ cells were counted per field of view. A minimum of 10-17 field of views were counted per transwell.

Dextran-FITC permeability assay. 3x10^4 primary endothelial cells were seeded 5-8 days after isolation on a gelatin coated insert (Corning, 8 um pore size) in EBM2 (Lonza) and grown to confluent monolayer for 3 days. Cells were then pre-treated with VEGF-A$_{164}$ for 4h before dextran-FITC was added into insert at final concentration of 1mg/ml. Supernatant from bottom well was collected 1h after addition of dextran-FITC and fluorescence intensity was measured by TECAN Infinite 200 Pro multireader using λ_{Ex}=485nm and λ_{Em}=525nm. Relative fluorescence unit was quantified.

Cytokine measurement. Cell culture supernatant and lung lysates were prepared according to manufacturers instructions. Multiplex cytokine kits from eBioscience/Affymetrix and BioTechne were used. The measurements were performed on Bio-Plex 200 system (BioRad) and data was analyzed by Bio-Plex software 6.0.

Immunohistochemistry. Organs were fixed in 4% paraformaldehyde, paraffin embedded, and 4um sections were stained for TUNEL according to manufacturer recommendation (Biotool). Heat-induced epitope retrieval with citrate buffer, blocked in 3% goat serum, permeabilized with 0.3% Triton X-100, and stained with cleaved caspase-3 (Cell Signaling Technology) or TUNEL. Images were taken using a Widefield Mirax Midi BF slide scanner (Zeiss) and analysed with PanoramicViewer software (3DHistech). Microscopic fluorescence picture were taken at indicated magnification using AXIO Scan (Zeiss) microscope.

Antibodies. Flow cytometry analysis was performed according to standard procedure and the following antibodies were purchased from eBioscience unless noted otherwise. The following antibodies were used: CD45.1-eFluor 450, CD45.2-APC-Cy7, CD45-brilliant violet 605, CD11b-PE-Cy7, Ly6C-brilliant violet 711, CD11c-brilliant violet 510, Ly6G-PerCP-Cy5.5, MHC-II-alexa fluor 700, CD103-FITC, Siglec-F-brilliant violet 421, CD86-brilliant violet 650, Ter119-brilliant violet 421, CCR-2-APC (RnD systems), fixable live/dead eFluor 780 or propidium iodide (PI) for live/dead assays. For immunoblotting antibodies were diluted at recommended dilution in 5% skim milk in PBS (0.1% tween). The following antibodies were used: RIPK3 (Immgenex), phospho p38, total p38, phospho-ERK1/2, total ERK1/2, phospho-HSP27 (clone D1H2) from Cell Signaling, beta-Actin (clone AC-15, Sigma), HSP70 (clone 3A3, SantaCruz), secondary anti-rat IgG and anti-mouse IgG (Southern Biotec).

Statistics. N refers to the number of independent experiments performed. For each experiment 3-8 mice were used per group. Every dot shown in the graphs represents an individual mouse. GraphPad Prism (GraphPad Software) was used for statistical analyses. All *p* values were calculated by either t-test or one-way ANOVA as indicated in the corresponding figure legend and indicated as asterisks (* $p \leq 0.05$, ** $p \leq 0.01$, *** $p \leq 0.001$).

Acknowledgements
We thank LASC animal technicians for animal husbandry, D Haefali, O Klimes. We also thank our research funding agencies for supporting this study: Peter Müller Fellowship (KH), Forschungskredit "CanDoc" Universität Zürich Fellowship (KH, LV, LSM) and SNSF project grant (310030-138085), Krebsliga Schweiz (KFS-3386-02-2014) and Julius Müller Stiftung to WWLW.

Conflict of Interest
The authors declare no conflict of interest with the exception of PJG and JB are employees of GlaxoSmithKline.

Supplementary Figures

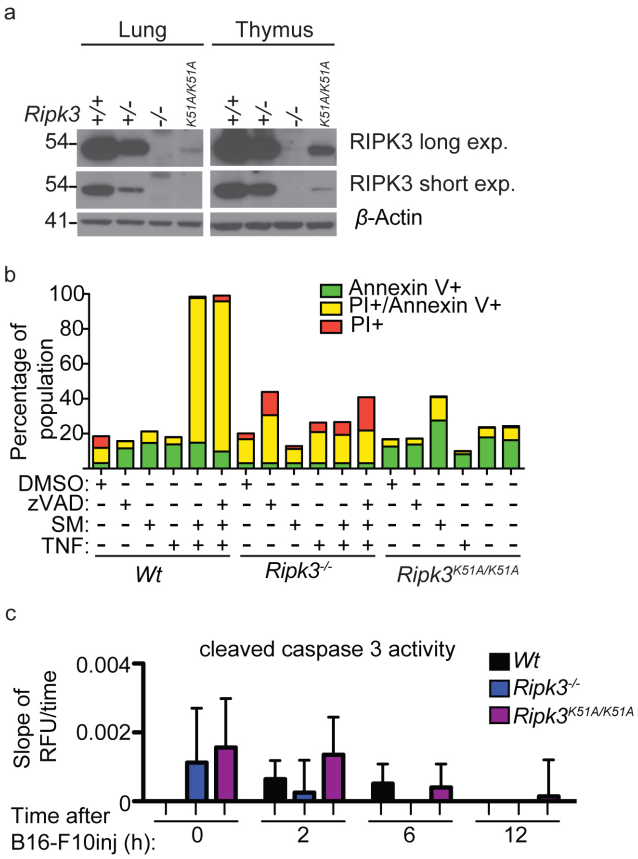

Supplementary Figure 1: (a) RIPK3 protein expression in lung and thymus from Wt, Ripk3$^{+/-}$, Ripk3$^{-/-}$, Ripk3$^{K51A/K51A}$ mice. **(b)** Cell death was measured using flow cytometry analysis by staining live/dead cells with propidium iodide (PI) and apoptotic cells by (Annexin-V FITC) after treatment of endothelial cells of Wt, Ripk3$^{-/-}$ and Ripk3$^{K51A/K51A}$ mice for 24h with indicated combinations of TNF (100ng/ml), Smac-mimetic compound A (SM, 500nM) or zVAD-FMK (5ug/ml). Quantification of one representative experiment shown (n=3). **(c)** Cleaved caspase 3 activity assay from lung lysates of mice injected with B16-F10 (3-4 mice per condition).

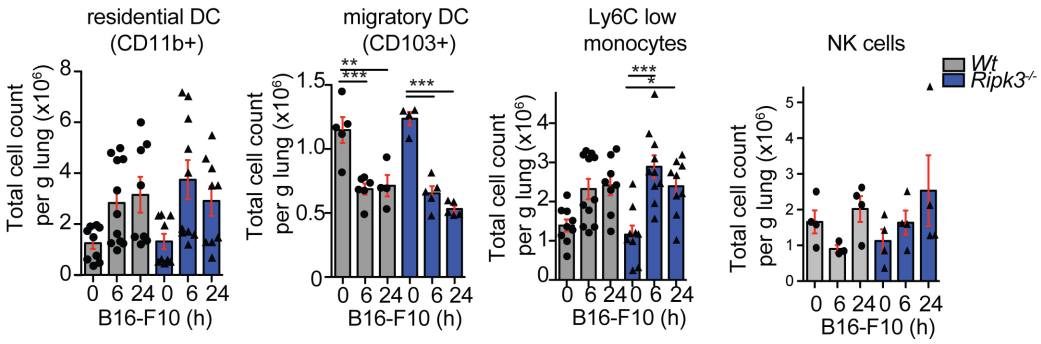

Supplementary Figure 2: Immune cell infiltration analysis of the lung by flow cytometry shows CD11b+ dendritic cells (DC; CD11c+, MHCII+, CD11b+ CD103-), CD103 DC (CD11c+, MHCII+, CD11b- CD103+) and L6C- Monocytes/Macrophages (CD11c-, CD11b+, Ly6C-) and natural killer (NK; NK1.1+ NKp46+) cells at indicated timepoints after B16F10 injection. Populations were pre-gated on singlets, live cells, Ter119- , CD45+ , SiglecF-, Ly6G-). Data pooled of n=2 experiments except NK cells. Each dot represents a mouse; SEM displayed and statistical analysis done by one-way ANOVA and Bonferroni post-test.

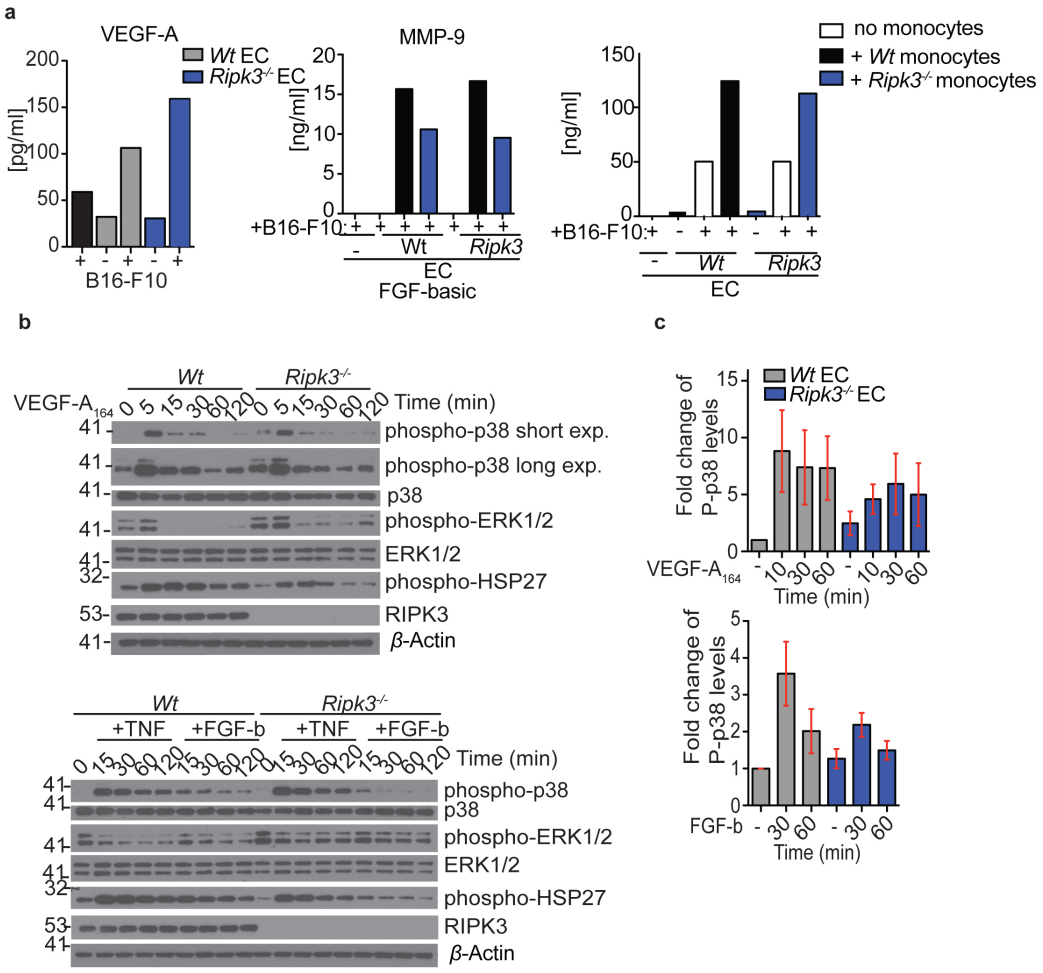

Supplementary Figure 3: (a) Protein levels of VEGF-A, FGF basic and MMP-9 were measured from supernatants of transwell migration assays 20h after addition of tumor cells and or monocytes as indicated. **(b)** SV40 large T immortalized endothelial cells isolated from

Wt or Ripk3$^{-/-}$ mice were treated with TNF (10ng/ml) or FGF-b (10ng/ml) and assayed for signaling by immunoblot analysis as indicated. Representative immunoblot is shown of n=3 experiments. Statistical analysis by one-way ANOVA and Bonferroni post-test. **(c)** Immunoblot quantification of pixel density normalized to total p38 from VEGF-A164 or FGF-b treated endothelial cells. Values shown as relative change to untreated Wt control. SEM shown and statistical analysis by one-way ANOVA and Bonferroni post-test.

References

1 Hanahan D, Weinberg RA. Hallmarks of cancer: the next generation. *Cell* 2011; **144**: 646–674.

2 Cho YS, Challa S, Moquin D, Genga R, Ray TD, Guildford M *et al.* Phosphorylation-driven assembly of the RIP1-RIP3 complex regulates programmed necrosis and virus-induced inflammation. *Cell* 2009; **137**: 1112–1123.

3 Zhang D-W, Shao J, Lin J, Zhang N, Lu B-J, Lin S-C *et al.* RIP3, an energy metabolism regulator that switches TNF-induced cell death from apoptosis to necrosis. *Science* 2009; **325**: 332–336.

4 Kaiser WJ, Sridharan H, Huang C, Mandal P, Upton JW, Gough PJ *et al.* Toll-like receptor 3-mediated necrosis via TRIF, RIP3, and MLKL. *Journal of Biological Chemistry* 2013; **288**: 31268–31279.

5 He S, Wang L, Miao L, Wang T, Du F, Zhao L *et al.* Receptor interacting protein kinase-3 determines cellular necrotic response to TNF-alpha. *Cell* 2009; **137**: 1100–1111.

6 Holler N, Zaru R, Micheau O, Thome M, Attinger A, Valitutti S *et al.* Fas triggers an alternative, caspase-8-independent cell death pathway using the kinase RIP as effector molecule. *Nat Immunol* 2000; **1**: 489–495.

7 Ofengeim D, Yuan J. NatureReview_RIPK1-nrm3683. *Nat Rev Mol Cell Biol* 2013; **14**: 727–736.

8 Sun L, Wang H, Wang Z, He S, Chen S, Liao D *et al.* Mixed lineage kinase domain-like protein mediates necrosis signaling downstream of RIP3 kinase. *Cell* 2012; **148**: 213–227.

9 Newton K, Dugger DL, Wickliffe KE, Kapoor N, de Almagro MC, Vucic D *et al.* Activity of protein kinase RIPK3 determines whether cells die by necroptosis or apoptosis. *Science* 2014; **343**: 1357–1360.

10 Murphy JM, Czabotar PE, Hildebrand JM, Lucet IS, Zhang J-G, Alvarez-Diaz S *et al.* The pseudokinase MLKL mediates necroptosis via a molecular switch mechanism. *Immunity* 2013; **39**: 443–453.

11 Hildebrand JM, Tanzer MC, Lucet IS, Young SN, Spall SK, Sharma P *et al.* Activation of the pseudokinase MLKL unleashes the four-helix bundle domain to induce membrane localization and necroptotic cell death. *Proc Natl Acad Sci USA* 2014; **111**: 15072–15077.

12 Dondelinger Y, Declercq W, Montessuit S, Roelandt R, Goncalves A, Bruggeman I *et al.* MLKL Compromises Plasma Membrane Integrity by Binding to Phosphatidylinositol Phosphates. *CellReports* 2014; **7**: 1–11.

13 Yatim N, Jusforgues-Saklani H, Orozco S, Schulz O, Barreira da Silva R, Reis e Sousa C *et al.* RIPK1 and NF-κB signaling in dying cells determines cross-priming of $CD8^+$ T cells. *Science* 2015; **350**: 328–334.

14 Günther C, Martini E, Wittkopf N, Amann K, Weigmann B, Neumann H *et al.* Caspase-8 regulates TNF-α-induced epithelial necroptosis and terminal ileitis. *Nature* 2011; **477**: 335–339.

15 Wittkopf N, Günther C, Martini E, He G, Amann K, He Y-W *et al.* Cellular FLICE-like inhibitory protein secures intestinal epithelial cell survival and immune homeostasis by regulating caspase-8. *Gastroenterology* 2013; **145**: 1369–1379.

16 Bonnet MC, Preukschat D, Welz P-S, van Loo G, Ermolaeva MA, Bloch W *et al.* The adaptor protein FADD protects epidermal keratinocytes from necroptosis in vivo and prevents skin inflammation. *Immunity* 2011; **35**: 572–582.

17 Koo G-B, Morgan MJ, Lee D-G, Kim W-J, Yoon J-H, Koo JS *et al.* Methylation-dependent loss of RIP3 expression in cancer represses programmed necrosis in response to chemotherapeutics. *Nature Publishing Group* 2015; : 1–19.

18 Tan AC, Jimeno A, Lin SH, Wheelhouse J, Chan F, Solomon A *et al.* Characterizing DNA methylation patterns in pancreatic cancer genome. *Molecular Oncology* 2009; **3**: 425–438.

19 Geserick P, Wang J, Schilling R, Horn S, Harris PA, Bertin J *et al.* Absence of RIPK3 predicts necroptosis resistance in malignant melanoma. *Cell Death Dis* 2015; **6**: e1884–12.

20 Vucur M, Reisinger F, Gautheron J, Janssen J, Roderburg C, Cardenas DV *et al.* RIP3 Inhibits Inflammatory Hepatocarcinogenesis but Promotes Cholestasis by Controlling Caspase-8- and JNK-Dependent Compensatory Cell Proliferation. *CellReports* 2013; **4**: 776–790.

21 Höckendorf U, Yabal M, Herold T, Munkhbaatar E, Rott S, Jilg S *et al.* RIPK3 Restricts Myeloid Leukemogenesis by Promoting Cell Death and Differentiation of Leukemia Initiating Cells. *Cancer Cell* 2016; **30**: 75–91.

22 Schmidt SV, Seibert S, Walch-Rückheim B, Vicinus B, Kamionka E-M, Pahne-Zeppenfeld J *et al.* RIPK3 expression in cervical cancer cells is required for PolyIC-induced necroptosis, IL-1α release, and efficient paracrine dendritic cell activation. *Oncotarget* 2015; **6**: 8635–8647.

23 Bozec D, Iuga AC, Roda G, Dahan S, Yeretssian G. Critical function of the necroptosis adaptor RIPK3 in protecting from intestinal tumorigenesis. *Oncotarget* 2016. doi:10.18632/oncotarget.10135.

24 Liu X, Zhou M, Mei L, Ruan J, Hu Q, Peng J *et al.* Key roles of necroptotic factors in promoting tumor growth. *Oncotarget* 2016; **7**: 22219–22233.

25 Seifert L, Werba G, Tiwari S, Ly NNG, Alothman S, Alqunaibit D *et al.* The necrosome promotes pancreatic oncogenesis via CXCL1 and Mincle-induced immune suppression. *Nature* 2016; : 1–17.

26 Moriwaki K, Balaji S, Mcquade T, Malhotra N, Kang J, Chan FK-M. The Necroptosis Adaptor RIPK3 Promotes Injury-Induced Cytokine Expression and Tissue Repair. *Immunity* 2014; **41**: 567–578.

27 Wong WW-L, Vince JE, Lalaoui N, Lawlor KE, Chau D, Bankovacki A *et al.* cIAPs and XIAP regulate myelopoiesis through cytokine production in an RIPK1- and RIPK3-dependent manner. *Blood* 2014; **123**: 2562–2572.

28 Strilic B, Yang L, Albarrán-Juárez J, Wachsmuth L, Han K, Müller UC *et al.* Tumour-cell-induced endothelial cell necroptosis via death receptor 6 promotes metastasis.

Nature 2016; **536**: 215–218.

29 Mandal P, Berger SB, Pillay S, Moriwaki K, Huang C, Guo H *et al.* RIP3 Induces Apoptosis Independent of Pronecrotic Kinase Activity. *Molecular Cell* 2014; **56**: 481–495.

30 GRASLKRAUPP B, RUTTKAYNEDECKY B, KOUDELKA H, BUKOWSKA K, BURSCH W, SCHULTEHERMANN R. In-Situ Detection of Fragmented Dna (Tunel Assay) Fails to Discriminate Among Apoptosis, Necrosis, and Autolytic Cell-Death - a Cautionary Note. *Hepatology* 1995; **21**: 1465–1468.

31 Qian B-Z, Li J, Zhang H, Kitamura T, Zhang J, Campion LR *et al.* CCL2 recruits inflammatory monocytes to facilitate breast-tumour metastasis. *Nature* 2011; **475**: 222–225.

32 Wolf MJ, Hoos A, Bauer J, Boettcher S, Knust M, Weber A *et al.* Endothelial CCR2 signaling induced by colon carcinoma cells enables extravasation via the JAK2-Stat5 and p38MAPK pathway. *Cancer Cell* 2012; **22**: 91–105.

33 García-Román J, Zentella-Dehesa A. Vascular permeability changes involved in tumor metastasis. *Cancer Lett* 2013; **335**: 259–269.

34 Carmeliet P, Lampugnani MG, Moons L, Breviario F, Compernolle V, Bono F *et al.* Targeted deficiency or cytosolic truncation of the VE-cadherin gene in mice impairs VEGF-mediated endothelial survival and angiogenesis. *Cell* 1999; **98**: 147–157.

35 Murakami M, Nguyen LT, Zhuang ZW, Zhang ZW, Moodie KL, Carmeliet P *et al.* The FGF system has a key role in regulating vascular integrity. *J Clin Invest* 2008; **118**: 3355–3366.

36 Li X, Padhan N, Sjöström EO, Roche FP, Testini C, Honkura N *et al.* VEGFR2 pY949 signalling regulates adherens junction integrity and metastatic spread. *Nature Communications* 2016; **7**: 11017.

37 McMullen ME, Bryant PW, Glembotski CC, Vincent PA, Pumiglia KM. Activation of p38 has opposing effects on the proliferation and migration of endothelial cells. *J Biol Chem* 2005; **280**: 20995–21003.

38 Luedde M, Lutz M, Carter N, Sosna J, Jacoby C, Vucur M *et al.* RIP3, a kinase promoting necroptotic cell death, mediates adverse remodelling after myocardial infarction. *Cardiovascular Research* 2014; **103**: 206–216.

39 Pierdomenico M, Negroni A, Stronati L, Vitali R, Prete E, Bertin J *et al.* Necroptosis Is Active in Children With Inflammatory Bowel Disease and Contributes to Heighten Intestinal Inflammation. *Am J Gastroenterol* 2013; **109**: 279–287.

40 Rickard JA, O'Donnell JA, Evans JM, Lalaoui N, Poh AR, Rogers T *et al.* RIPK1 regulates RIPK3-MLKL-driven systemic inflammation and emergency hematopoiesis. *Cell* 2014; **157**: 1175–1188.

41 Dillon CP, Weinlich R, Rodriguez DA, Cripps JG, Quarato G, Gurung P *et al.* RIPK1 blocks early postnatal lethality mediated by caspase-8 and RIPK3. *Cell* 2014; **157**: 1189–1202.

42 Kaiser WJ, Daley-Bauer LP, Thapa RJ, Mandal P, Berger SB, Huang C *et al.* RIP1

suppresses innate immune necrotic as well as apoptotic cell death during mammalian parturition. *Proc Natl Acad Sci USA* 2014; **111**: 7753–7758.

43 Berger SB, Kasparcova V, Hoffman S, Swift B, Dare L, Schaeffer M *et al.* Cutting Edge: RIP1 Kinase Activity Is Dispensable for Normal Development but Is a Key Regulator of Inflammation in SHARPIN-Deficient Mice. *The Journal of Immunology* 2014; **192**: 5476–5480.

44 Shutinoski B, Alturki NA, Rijal D, Bertin J, Gough PJ, Schlossmacher MG *et al.* K45A mutation of RIPK1 results in poor necroptosis and cytokine signaling in macrophages, which impacts inflammatory responses in vivo. 2016; : 1–10.

45 Newton K, Dugger DL, Maltzman A, Greve JM, Hedehus M, Martin-McNulty B *et al.* RIPK3 deficiency or catalytically inactive RIPK1 provides greater benefit than MLKL deficiency in mouse models of inflammation and tissue injury. 2016; : 1–12.

46 Sun Z, Li X, Massena S, Kutschera S, Padhan N, Gualandi L *et al.* VEGFR2 induces c-Src signaling and vascular permeability in vivo via the adaptor protein TSAd. *J Exp Med* 2012; **209**: 1363–1377.

47 Cursi S, Rufini A, Stagni V, Condò I, Matafora V, Bachi A *et al.* Src kinase phosphorylates Caspase-8 on Tyr380: a novel mechanism of apoptosis suppression. *EMBO J* 2006; **25**: 1895–1905.

48 Godwin A, Sharma A, Yang W-L, Wang Z, Nicastro J, Coppa GF *et al.* Receptor-Interacting Protein Kinase 3 Deficiency Delays Cutaneous Wound Healing. *PLoS ONE* 2015; **10**: e0140514.

49 Liu S, Wang X, Li Y, Xu L, Yu X, Ge L *et al.* Necroptosis mediates TNF-induced toxicity of hippocampal neurons. *BioMed Research International* 2014; **2014**: 290182–11.

50 Zhang T, Zhang Y, Cui M, Jin L, Wang Y, Lv F *et al.* CaMKII is a RIP3 substrate mediating ischemia- and oxidative stress–induced myocardial necroptosis. *Nature Medicine* 2016; **22**: 175–182.

51 Görlach A, Bertram K, Hudecova S, Krizanova O. Calcium and ROS_ A mutual interplay. *Redox Biology* 2015; **6**: 260–271.

52 Newton K, Sun X, Dixit VM. Kinase RIP3 is dispensable for normal NF-kappa Bs, signaling by the B-cell and T-cell receptors, tumor necrosis factor receptor 1, and Toll-like receptors 2 and 4. *Molecular and Cellular Biology* 2004; **24**: 1464–1469.

4. Results II

Declaration

I declare that I have contributed to this by planning and designing experimental layout, performing experiments, analyzing and interpreting the data.

4.1. Title: Targeting p38 or MK2 Enhances the Anti-Leukemic Activity of Smac-Mimetics

Article

Cancer Cell

Targeting p38 or MK2 Enhances the Anti-Leukemic Activity of Smac-Mimetics

Highlights

- Genetic loss or chemical inhibition of p38 or MK2 increases SM-induced TNF
- p38 and MK2 inhibit SM-induced phosphorylation of JNK and ERK
- The combination of SM and p38 inhibitor is well tolerated in vivo
- p38 and MK2 inhibitors potentiate SM killing of AML in vivo

Authors

Najoua Lalaoui, Kay Hänggi, Gabriela Brumatti, ..., David L. Vaux, W. Wei-Lynn Wong, John Silke

Correspondence

silke@wehi.edu.au

In Brief

Lalaoui et al. show that inhibition of p38 or its downstream kinase MK2, in contrast to reducing Toll-like receptor-mediated tumor necrosis factor (TNF) production, increases TNF production upon smac-mimetic (SM) treatment and enhances the anti-tumor efficacy of SM.

Lalaoui et al., 2016, Cancer Cell *29*, 145–158
February 8, 2016
http://dx.doi.org/10.1016/j.ccell.2016.01.006

CellPress

Cancer Cell
Article

Targeting p38 or MK2 Enhances the Anti-Leukemic Activity of Smac-Mimetics

Najoua Lalaoui,[1,2] Kay Hänggi,[3] Gabriela Brumatti,[1,2] Diep Chau,[1,2] Nhu-Y.N. Nguyen,[4,5] Lazaros Vasilikos,[3] Lisanne M. Spilgies,[3] Denise A. Heckmann,[1,2] Chunyan Ma,[1,2] Margherita Ghisi,[6,7] Jessica M. Salmon,[6,7] Geoffrey M. Matthews,[6,7] Elisha de Valle,[8,9] Donia M. Moujalled,[4,5] Manoj B. Menon,[10] Sukhdeep Kaur Spall,[1,2] Stefan P. Glaser,[1,2] Jennifer Richmond,[11] Richard B. Lock,[11] Stephen M. Condon,[12] Raffi Gugasyan,[8,9] Matthias Gaestel,[10] Mark Guthridge,[4,5] Ricky W. Johnstone,[6,7] Lenka Munoz,[13] Andrew Wei,[4,5] Paul G. Ekert,[1,14,15] David L. Vaux,[1,2] W. Wei-Lynn Wong,[3] and John Silke[1,2,*]

[1]Cell Signaling & Cell Death and Cancer & Hematology Divisions, The Walter and Eliza Hall Institute of Medical Research, Parkville, VIC 3052, Australia
[2]Department of Medical Biology, University of Melbourne, Parkville, VIC 3050, Australia
[3]Institute of Experimental Immunology, University of Zürich, Zürich 8057, Switzerland
[4]Department of Clinical Hematology, The Alfred Hospital and Monash University, Melbourne, VIC 3004, Australia
[5]Australian Centre for Blood Diseases, Monash University, Melbourne, VIC 3004, Australia
[6]Gene Regulation Laboratory, Cancer Therapeutics Program, Peter MacCallum Cancer Centre, East Melbourne, VIC 3002, Australia
[7]The Sir Peter MacCallum Department of Oncology, University of Melbourne, Parkville, VIC 3050, Australia
[8]Immunomonitoring Facility and Centre for Biomedical Research, The Burnet Institute, Melbourne, VIC 3004, Australia
[9]Department of Immunology, Central Clinical School, Monash University, Melbourne, VIC 3181, Australia
[10]Institute of Physiological Chemistry, Hannover Medical School, Carl-Neuberg-Street 1, 30625 Hannover, Germany
[11]Children's Cancer Institute Australia, Lowy Cancer Research Centre, UNSW, Randwick, NSW 2031, Australia
[12]TetraLogic Pharmaceuticals Corporation, 343 Phoenixville Pike, Malvern, PA 19355, USA
[13]Department of Pathology, School of Medical Sciences, University of Sydney, Sydney, NSW 2006, Australia
[14]Department of Pediatrics, University of Melbourne, Parkville, VIC 3050, Australia
[15]Murdoch Children's Research Institute, Royal Children's Hospital, Parkville, VIC 3052, Australia
*Correspondence: silke@wehi.edu.au
http://dx.doi.org/10.1016/j.ccell.2016.01.006

SUMMARY

Birinapant is a smac-mimetic (SM) in clinical trials for treating cancer. SM antagonize inhibitor of apoptosis (IAP) proteins and simultaneously induce tumor necrosis factor (TNF) secretion to render cancers sensitive to TNF-induced killing. To enhance SM efficacy, we screened kinase inhibitors for their ability to increase TNF production of SM-treated cells. We showed that p38 inhibitors increased TNF induced by SM. Unexpectedly, even though p38 is required for Toll-like receptors to induce TNF, loss of p38 or its downstream kinase MK2 increased induction of TNF by SM. Hence, we show that the p38/MK2 axis can inhibit or promote TNF production, depending on the stimulus. Importantly, clinical p38 inhibitors overcame resistance of primary acute myeloid leukemia to birinapant.

INTRODUCTION

Inhibitor of apoptosis (IAP) proteins control a broad range of cellular processes by regulating canonical and non-canonical nuclear factor κB (NF-κB) activation, mitogen-activate protein kinase (MAPK) signaling pathways, and programmed cell death (Silke and Meier, 2013; Silke and Vucic, 2014). The presence of baculoviral IAP repeat (BIR) domains allows IAPs to bind to proteins, such as TRAFs, caspases, and IAP antagonists including Smac/Diablo and HtrA2/Omi. Cellular IAPs (cIAPs)

Significance

Smac-mimetics (SM) are currently in early-phase clinical trials as anti-cancer agents. A better understanding of their mode of action would improve the design of future clinical trials. The p38/MK2 pathway is known to be required for production of the inflammatory cytokine tumor necrosis factor (TNF), which led to the development of p38 inhibitors that were evaluated as anti-inflammatory drugs in the clinic. Unexpectedly, p38 inhibitors promoted production of TNF by SM and increased SM killing. The combination of birinapant and p38 inhibitors was well tolerated in vivo and an effective treatment for primary acute myeloid leukemia compared with either drug alone. Our preclinical study provides a rationale for clinical trials of SM combined with p38 or MK2 inhibitors.

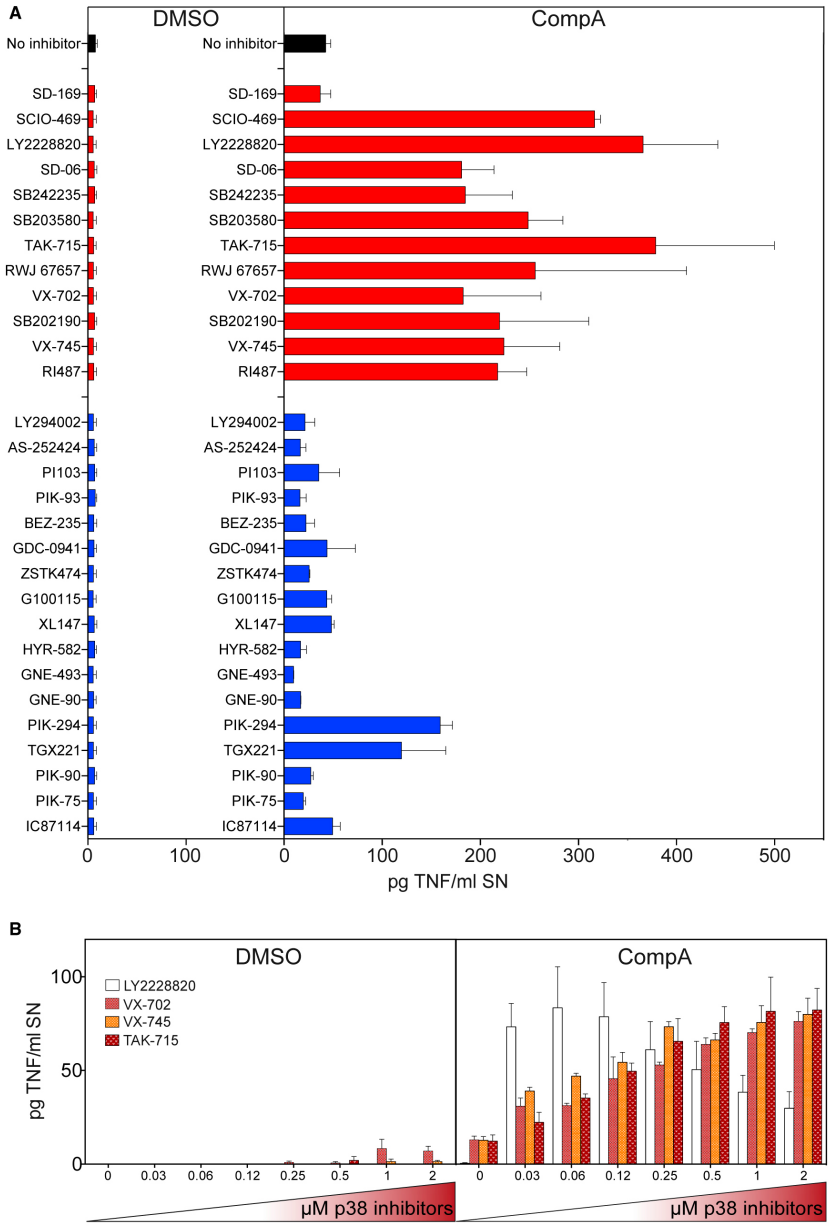

(legend on next page)

and XIAP bear a RING domain that provides an E3 ubiquitin ligase activity. XIAP directly inhibits the proteolytic activity of caspase-3, -7, and -9 (Deveraux et al., 1997, 1998). Unlike XIAP, 1 and cIAP2 are poor caspase inhibitors and instead use their E3 ligase activity to regulate RIP kinases, NF-κB, and MAPK pathways (Silke and Meier, 2013).

Aberrations in IAP gene expression have been associated with cancer onset and development (Fulda and Vucic, 2012). Given the role of these proteins in inhibiting cell death and potentially promoting oncogenesis, several pharmaceutical companies have designed small molecules that target IAPs for cancer therapy. These compounds, called smac-mimetics (SM), bind to the BIR domains of the IAPs (Silke and Meier, 2013). SM binding typically triggers rapid auto-ubiquitylation and proteasomal degradation of cIAPs and prevents XIAP from binding to and inhibiting caspases (Silke and Vucic, 2014).

In the absence of IAPs, tumor necrosis factor (TNF) does not fully activate canonical NF-κB and triggers formation of multiprotein complexes that signal cell death (Silke and Vucic, 2014). In response to TNFR1 activation, cIAPs normally ubiquitylate RIPK1, which provides docking sites for different kinases to activate the transcription of downstream genes such as the caspase-8 inhibitor cFLIP (Bertrand et al., 2008; Micheau et al., 2001). Ubiquitylated RIPK1 also prevents formation and activation of RIPK1-dependent apoptotic and necroptotic complexes. Therefore, loss of RIPK1 ubiquitylation due to SM-induced IAP depletion can simultaneously promote the formation of the so-called Ripoptosome complex containing RIPK1, FADD, and caspase-8, and reduce expression of cFLIP leading to caspase-8 activation and apoptosis (Feoktistova et al., 2011; Tenev et al., 2011). In some cell types or conditions where caspase-8 function is absent or low, RIPK1 can promote RIPK3 phosphorylation, which in turn phosphorylates MLKL to trigger necroptosis (Cho et al., 2009; He et al., 2009; Murphy et al., 2013; Sun et al., 2012).

The cytotoxicity of SM as single agents usually involves simultaneous promotion of autocrine TNF secretion and formation of cell death-inducing complexes (Bertrand et al., 2008; Gaither et al., 2007; Petersen et al., 2007; Varfolomeev et al., 2007; Vince et al., 2007). Consistent with this, cells that secrete TNF upon SM treatment are usually efficiently killed by it, and some cancer cell lines that are not killed by SM alone do die when SM is combined with exogenous TNF. The exact mechanisms underlying SM-induced TNF production are, however, largely unknown. cIAPs inhibit the non-canonical NF-κB pathway by constitutive K48-linked ubiquitylation and ensuing proteasomal degradation of the NF-κB interacting kinase, NIK (Vallabhapurapu et al., 2008; Varfolomeev et al., 2007; Vince et al., 2007; Zarnegar et al., 2008). When cIAPs are depleted after SM treatment, NIK levels increase, thereby activating expression of downstream targets of NF-κB such as TNF. Consistent with a role for NF-κB in SM-induced TNF production dominant negative IκBα prevented SM-induced TNF (Vince et al., 2007). RIPK1 and RIPK3, kinases involved in the necroptotic cell death pathway, are also required for an optimal SM-induced TNF secretion and killing (Christofferson et al., 2012; Wong et al., 2014), suggesting that there is a complex interplay between different signaling pathways to control TNF production when IAPs are antagonized.

Production of TNF is induced by a large number of stimuli, including Toll-like receptor (TLR) ligands such as lipopolysaccharide (LPS). There is strong genetic evidence showing that Tpl2, p38α, and MK2 play important roles in TLR-induced TNF secretion (Dumitru et al., 2000; Kotlyarov et al., 1999). Because of the key role of TNF in inflammatory diseases such as rheumatoid arthritis and Crohn's disease, small-molecule inhibitors of these kinases have been developed to inhibit TNF production. However, p38 inhibitors (p38i) have not been as clinically effective as hoped (Genovese, 2009). In fact the role of p38α in regulating transcription of both pro- and anti-inflammatory cytokines, as well as its participation in a feedback control loop to suppress inflammation, have perhaps contributed to dose-limiting toxicities of this class of inhibitors (Cohen and Alessi, 2013). The p38 downstream kinase MK2 is not believed to display such a pleiotropic role, and has therefore been proposed to be a better drug target than p38α to prevent inflammation (Cohen, 2009; Gaestel et al., 2009; Genovese, 2009; Gurgis et al., 2014).

SM are in phase 1/2 clinical trials for a number of types of cancer, including acute myeloid leukemia (AML) (https://clinicaltrials.gov). Understanding how SM promote TNF production could extend their application and increase their efficacy. Here, we investigated the kinases that inhibit production of TNF in the context of SM treatment.

RESULTS

p38 Inhibition Increases TNF Production Induced by SM

CompA is a pan-IAP antagonist that induces TNF production in bone marrow-derived macrophages (BMDM) in an RIPK1- and RIPK3-dependent manner (Wong et al., 2014). To identify other kinases that alter TNF expression in response to SM, we screened a library of 134 compounds that inhibit kinases involved in MAPK, AKT/PI3K, JAK, EGFR, or VEGFR signaling pathways (Figure S1A). Treatment of BMDM generated from wild-type (WT) C57BL/6 mice with CompA alone induced TNF production after 24 hr (Figures 1A and S1A). Interestingly, of the 12 p38i present in the library, 11 increased TNF production induced by CompA (Figures 1A and S1A). In contrast, only 2 of 17 PI3K inhibitors increased CompA-induced TNF (Figure 1A). p38i inhibit p38 activity in vitro at nanomolar concentrations (Table S1), and consistent with the increase in TNF being the result of an on-target effect, the p38i LY2228820, VX-702, VX-745, and TAK-715 increased CompA-induced TNF secretion at

Figure 1. p38 Inhibitors Increase TNF Production Induced by Smac-Mimetic

(A) Levels of TNF in the supernatant (SN) of wild-type (WT) BMDM pre-treated for 20 min with 1 μM of the indicated p38 (red) or PI3K (blue) inhibitors and then treated with or without 500 nM CompA for 24 hr.

(B) Levels of TNF in the SN of WT BMDM pre-treated for 20 min with increasing concentrations of the indicated p38i and then treated with or without 250 nM CompA for 24 hr.

Graphs show mean ± SEM, n = 3 independent biological repeats. See also Figure S1 and Table S1.

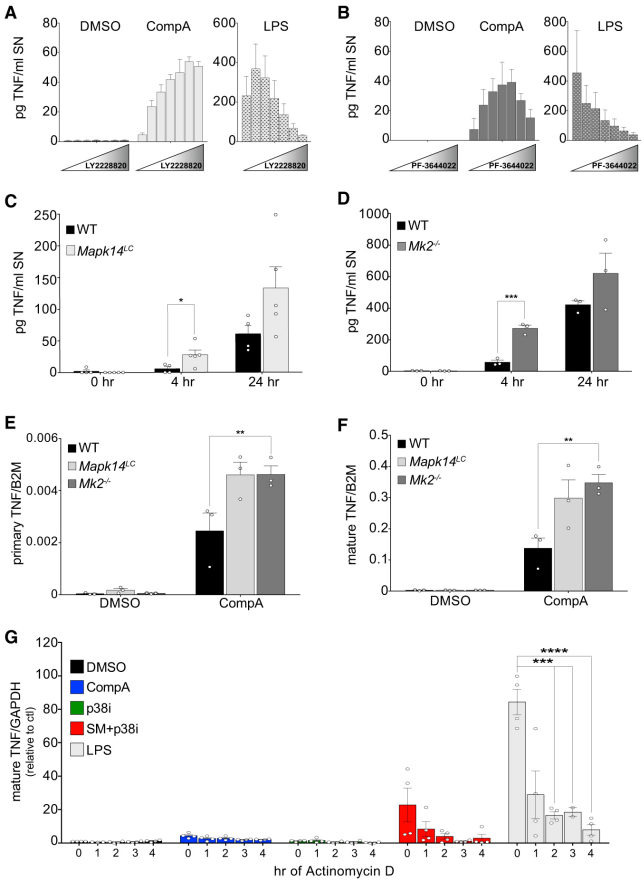

Figure 2. p38 and MK2 Deficiency or Inhibition Increases TNF Transcription in Response to Smac-Mimetic

(A and B) Levels of TNF in the SN of WT BMDM treated with increasing concentrations (0; 0.03; 0.06; 0.125; 0.25; 0.5; 1 μM) of the p38i LY2228820 (A) or the MK2i PF-3644022 (B) ± 250 nM CompA or ± 25 ng/ml LPS for 24 hr.

(C and D) Levels of TNF in the SN of WT, *Mapk14*^{LC} (C), or *Mk2*$^{-/-}$ (D) BMDM treated with 500 nM CompA for 4 hr or 24 hr.

(E and F) Levels of primary (E) and mature (F) TNF transcripts relative to B2M transcripts in WT, *Mapk14*^{LC} and *Mk2*$^{-/-}$ BMDM treated 4 hr with CompA (500 nM).

(G) Levels of mature TNF transcripts relative to GAPDH transcripts in WT BMDM treated for 4 hr with CompA (500 nM) ± p38i LY2228820 (1 μM). Actinomycin D (100 nM) was added for the indicated period of the 4 hr incubation.

Graphs show mean ± SEM throughout, n = 3–5 independent biological repeats. *p ≤ 0.05; **p ≤ 0.01; ***p ≤ 0.005; ****p ≤ 0.001. See also Figure S2.

low-nanomolar concentrations, while none induced TNF on their own (Figure 1B). Of the 12 p38i tested, only SD-169 did not increase CompA-induced TNF secretion (Figure 1A). SD-169 reportedly inhibits p38 kinases at nanomolar concentrations (Table S1). However, our preparation of SD-169 was unable to either prevent or reduce TNF-induced phosphorylation of the main p38α target, MK2, while three other p38i, with similar IC_{50} values, were able to do so (Figure S1B), indicating that this preparation of SD-169 was not an active p38i.

The p38/MK2 Pathway Negatively Regulates TNF Synthesis Induced by SM

A role for p38α in inhibiting CompA-induced TNF secretion was unexpected, because p38α is required to increase TNF expression in response to TLR ligation. Upon TLR activation, p38α is phosphorylated and in turn phosphorylates the kinase MK2, which then phosphorylates downstream factors required for full TNF transcription and translation (Gaestel et al., 2009). To explore whether the p38/MK2 pathway inhibited SM-induced TNF production, we selected the p38i LY2228820 from our original screen and compared it with the MK2 inhibitor (MK2i) PF-3644022. As reported previously (Campbell et al., 2014; Mourey et al., 2010), both inhibitors decreased LPS-induced TNF production in a dose-dependent manner (Figures 2A and 2B). However, both inhibitors significantly increased the production of TNF in response to CompA at low-nanomolar concentrations (Figures 2A and 2B).

To confirm the inhibitory role of the p38/MK2 pathway in CompA-induced TNF production, and to exclude an off-target effect of the inhibitors, we challenged BMDM from *Mapk14*^{LC} and *Mk2*$^{-/-}$ mice with CompA. The *Mapk14*^{LC} mice bear myeloid cells in which the p38α gene has been deleted. We found that BMDM treated with CompA produced greater amounts of TNF when either p38α or MK2 were absent (Figures 2C and 2D). In agreement with our in vitro studies, we found that injection of a similar SM, GT13702, induced higher levels of TNF in the sera of *Mapk14*^{LC} mice than in control mice (Figure S2). In response to CompA treatment, *Mk2*$^{-/-}$ or *Mapk14*^{LC} BMDM increased TNF production more so than in WT cells, not only at the protein level but also at the RNA level (Figures 2E and 2F). There was no difference in the relative levels of either primary or mature TNF mRNA (Figures 2E and 2F), and actinomycin D rapidly prevented upregulation of TNF mRNA following combined p38i and SM treatment (Figure 2G). These results indicate that the increase in TNF production caused by inhibition of p38 or MK2 is the result

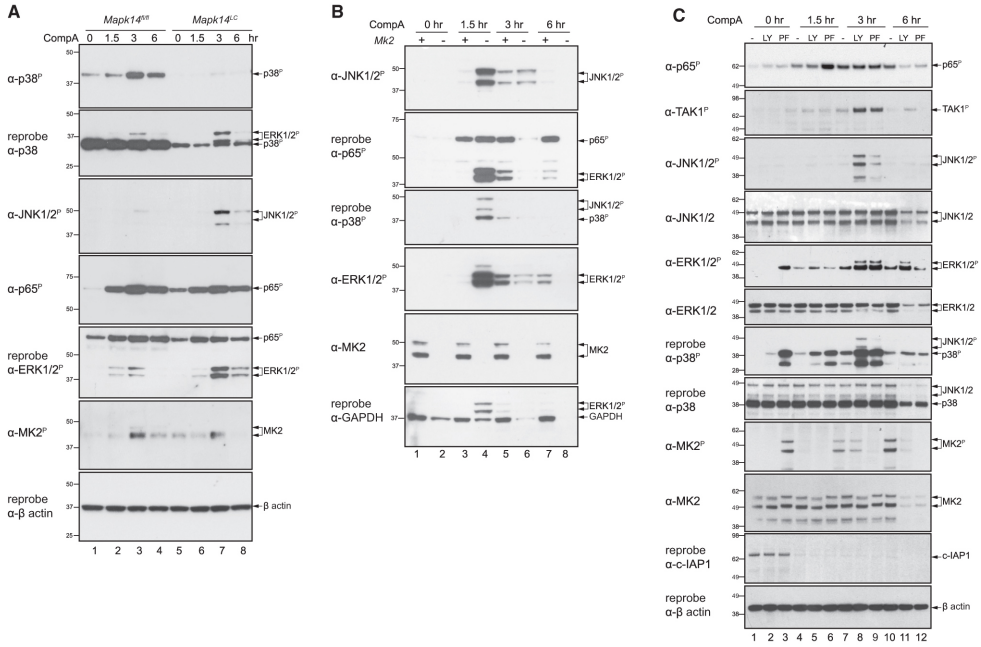

Figure 3. p38/MK2 Inhibits Smac-Mimetic-Induced JNK1/2 and ERK1/2 Phosphorylation

(A and B) Western blot (WB) analysis of lysates generated from *Mapk14*$^{fl/fl}$ and *Mapk14*^{LC} (A) or from WT and *Mk2*$^{-/-}$ (B) BMDM treated with 500 nM CompA for the indicated times.

(C) WB analysis of lysates from WT BMDM pre-treated for 20 min with LY2228820 (1 μM) or PF-3644022 (1 μM) and then treated for the indicated times with 500 nM CompA.

Blots are representative of three independent experiments. See also Figure S3.

of an on-target effect leading to an increase of TNF mRNA transcription.

The p38/MK2 Pathway Inhibits JNK and ERK Phosphorylation in Response to SM

To determine the molecular mechanism by which the p38/MK2 pathway controls SM-induced TNF production, we investigated other signaling molecules that are directly involved in TNF expression, such as NF-κB, ERK, and JNK (Das et al., 2009; Dumitru et al., 2000; Shakhov et al., 1990), in the presence or absence of p38 or MK2. Although the deletion of p38α was incomplete, BMDM deficient in p38α showed greatly enhanced ERK1/2 and JNK1/2 phosphorylation in response to CompA when compared with *Mapk14*$^{fl/fl}$ BMDM (Figure 3A cf. lanes 3 and 7 and Figure S3A). Similarly, MK2 deficiency resulted in an increase of phospho-ERK1/2 and phospho-JNK1/2 compared with WT cells (Figure 3B, cf. lanes 3 and 4 and Figure S3B). It has been shown that loss of MK2 can result in reduced p38α levels in some cell types (Kotlyarov et al., 1999; Ronkina et al., 2007). Although the level of p38α was slightly reduced in *Mk2*$^{-/-}$ BMDM, if β-actin loading controls are taken into account, it was phosphorylated upon TNF treatment at levels comparable with that observed in WT BMDM (Figure S3C). A reduction of phospho-p38α could potentially explain the increase in phospho-ERK1/2 and phospho-JNK1/2 in *Mk2*$^{-/-}$ cells (Figures 3B and S3C), however, inhibition of MK2 activity using PF-3644022 did not decrease p38α levels or p38α phosphorylation yet consistently increased ERK1/2 and JNK1/2 phosphorylation in response to CompA (Figures 3C and S3D). Similarly to PF-3644022, LY2228820 also strongly increased ERK1/2 and JNK1/2 phosphorylation in response to CompA (Figures 3C and S3D). These results were internally controlled because only the p38i, and not the MK2i, blocked MK2 phosphorylation (lanes 7–9, Figures 3C and S3D).

To test whether JNK1/2 phosphorylation, and presumable activation, contributed to increased induction of TNF, we challenged WT, p38α-deficient, and MK2-deficient BMDM with SM and the specific JNK1/2 inhibitor JNK-IN-8 (Knapp et al., 2013; Zhang et al., 2012). At a concentration where phosphorylation of JNK1/2 targets was significantly inhibited (Figure S4A), JNK-IN-8 was able to reduce TNF production of SM-treated *Mapk14*^{LC} and *Mk2*$^{-/-}$ cells (Figure 4A). Both JNK-IN-8 and a less specific JNK1/2 inhibitor, SP600125, blocked CompA + p38i-induced increase of TNF (Figures 4B and S4A). To test

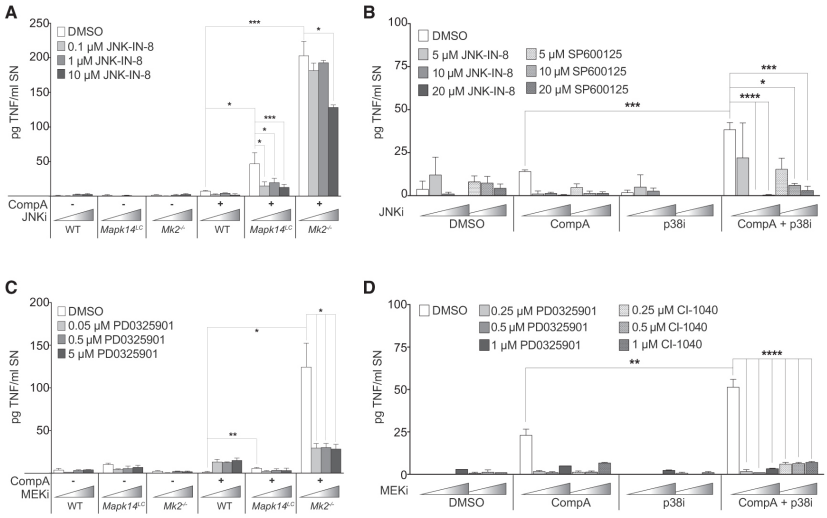

Figure 4. Inhibition of JNK1/2 and ERK1/2 Decrease TNF Production Induced by SM + p38i

(A and C) Levels of TNF in the SN of WT, *Mapk14*^{LC}, or *Mk2*$^{-/-}$ BMDM treated with 100 nM CompA ± indicated concentrations of JNK-IN-8 (A) or PD0325901 (C) for 6 hr.

(B and D) Levels of TNF in the SN of WT BMDM treated with 250 nM CompA ± p38i LY2228820 (1 μM) ± indicated concentrations of JNK-IN-8 or SP600125 (B) or PD0325901 or CI-1040 (D) for 6 hr.

Graphs show mean ± SEM, n = 3–6 independent biological repeats. *p ≤ 0.05; **p ≤ 0.01; ***p ≤ 0.005; ****p ≤ 0.001. See also Figure S4.

whether ERK1/2 phosphorylation, and presumable activation, contributed to increased SM induction of TNF, we performed identical experiments with the MEK inhibitors CI-1040, from our original screen, and PD0325901 (Barrett et al., 2008), and these also blocked the increase in TNF in either *Mapk14*^{LC} and *Mk2*$^{-/-}$ (Figure 4C) or in WT cells treated with CompA + p38i (Figures 4D and S4B).

p38 and MK2 Inhibition Enhances SM-Mediated Killing

We next investigated whether inhibition of the p38/MK2 pathway was associated with increased cell death in response to SM. When added alone, the p38i LY2228820, VX-702, VX-745, and TAK-715, and the MK2i PF-3644022 did not reduce the viability of BMDM (Figure S5A). However, they dramatically decreased cell viability when combined with CompA. Moreover, this was dose dependent, and occurred at nanomolar concentrations, indicating an on-target effect (Figure 5A).

Treatment with SM can lead to caspase-dependent apoptosis or RIPK1-/RIPK3-dependent necroptosis. However, we have shown that besides their role in executing necroptosis, RIPK1 and RIPK3 are also required for SM-induced TNF secretion (Wong et al., 2014). We therefore tested whether these kinases also play a role in SM-induced TNF secretion when p38 or MK2 are deleted or inhibited. As before, inactivation of the p38/MK2 pathway increased TNF production in response to CompA (Figures 5B, 5C, S5B, and S5C). The RIPK1 inhibitor nec-1 completely abolished TNF production and cell death in response to either CompA alone or when p38 and MK2 were deleted or inactivated in cells treated with CompA (Figures 5B–5D, S5B, and S5C). Deletion of *Tnfr1* also prevented CompA plus p38i-induced TNF production and cell death (Figures 5E and 5F). As described by Wong et al. (2014), deletion of *Ripk3* but not *Mlkl* reduced CompA-induced TNF production and death of BMDM (Figures 5E and 5F). However, the absence of either RIPK3 or MLKL did not prevent TNF production or killing in response to the combination of CompA and p38i (Figures 5E and 5F). These observations show that RIPK1, but neither RIPK3 nor MLKL, is required for TNF production in response to CompA plus p38i treatment, and imply that the combination of CompA and p38i induces cell death by an apoptotic and not a necroptotic pathway. Consistent with this idea, cells without *Casp8* were resistant to the combination of CompA and p38i (Figure 5F). Surprisingly, these *Casp8*$^{-/-}$*Ripk3*$^{-/-}$ macrophages also failed to secrete high levels of TNF in response to either CompA alone or the CompA plus p38i combination (Figure 5E). Because TNF was not secreted into the supernatant in either *Tnfr1*$^{-/-}$ or *Casp8*$^{-/-}$*Ripk3*$^{-/-}$ macrophages, this suggests that caspase activity contributes to TNF secretion when IAPs and p38 are inhibited.

Consistent with an apoptotic mechanism for cell death, we observed higher caspase-8, caspase-3, and poly(ADP-ribose) polymerase (PARP) cleavage after 3 hr of CompA treatment in *Mapk14*^{LC} and *Mk2*$^{-/-}$ cells compared with WT cells (Figures 6A and S6A). Similarly, in the presence of the p38i LY2228820 or the MK2i PF-3644022, CompA caused caspase and PARP cleavage and cell death within 3 hr (Figures 6B, 6C, and S6B).

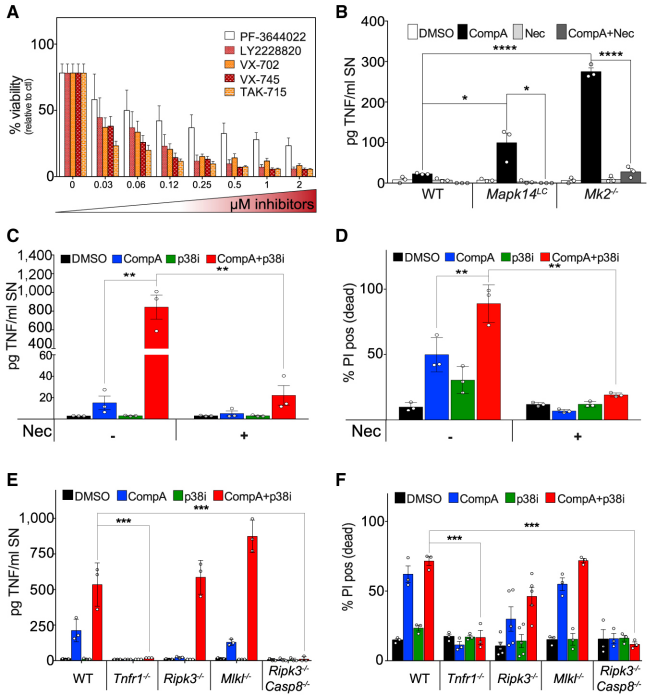

Figure 5. p38i Plus SM Induces TNF-Dependent Apoptosis that Requires RIPK1 Kinase Activity, but Not RIPK3 or MLKL

(A) Cell viability of WT BMDM treated for 20 min with increasing concentrations of indicated p38 and MK2 inhibitors (0–2 μM) and then treated for 24 hr with 500 nM CompA.

(B) Levels of TNF in the SN of WT, *Mapk14*^{LC} or *Mk2*$^{-/-}$ BMDM treated for 4 hr with 100 nM CompA ± 50 μM necrostatin (Nec).

(C and D) Levels of TNF in the SN (C) or cell death (D) of WT BMDM treated with CompA (500 nM), p38i LY2228820 (1 μM), or both ± Nec (50 μM) for 24 hr.

(E and F) Levels of TNF in the SN (E) or cell death (F) of WT, *Tnfr1*$^{-/-}$, *Ripk3*$^{-/-}$, *Mlkl*$^{-/-}$, or *Casp8*$^{-/-}$ *Ripk3*$^{-/-}$ BMDM treated ± CompA (500 nM) ± p38i LY2228820 (1 μM) for 24 hr.

Graphs show mean ± SEM, n = 3–5 independent biological repeats. *p ≤ 0.05; **p ≤ 0.01; ***p ≤ 0.005; ****p ≤ 0.001. See also Figure S5.

Collectively, these results indicate that p38/MK2 inactivation enhances CompA-induced apoptosis.

The Combination of Clinical IAP and p38 Inhibitors Is Therapeutically Effective in AML

SM that strongly inhibit cIAP1, cIAP2, and XIAP, such as CompA, induce inflammatory cytokines in vitro and induce inflammation in vivo that is reminiscent of the inflammatory phenotype seen in *Birc2*^{LC}*Birc3*$^{-/-}$*Xiap*$^{-/-}$ triple knockout mice (Condon et al., 2014; Lawlor et al., 2015; Vince et al., 2012; Wong et al., 2014). Birinapant is an SM that is less effective at inhibiting cIAP2 and XIAP, and thus may be more tolerable (Condon et al., 2014). Despite this reduction in IAP-antagonizing potential, loss of p38 or MK2 increased birinapant-induced TNF secretion in an RIPK1-dependent manner (Figure 7A). Furthermore, while SM that strongly inhibit all IAPs (e.g. CompA and GT13072) induced a higher secretion of TNF upon p38 inhibition compared with birinapant (Figure S7A), the p38i LY2228820 increased birinapant-induced TNF secretion and cell killing in a dose-dependent manner (Figures 7B and 7C).

We next tested whether the p38i/birinapant combination would be useful in treating leukemia. Murine AML models have been used to predict the behavior of chemotherapy in the clinic (Zuber et al., 2009), so we generated MLL-ENL ± NRas^{G12D}, MLL-AF9 ± Nras^{G12D}, AML1-ETO9a + Nras^{G12D}, CBFβ-MYH11 + Nras^{G12D}, NUP98-HoxA9, and HoxA9/Meis1 AML mouse models and examined their viability when treated with birinapant combined with the p38i LY2228820 or SCIO-469 or with the MK2i PF-3644022. Consistent with our studies using BMDM, inhibition of the p38/MK2 pathway dramatically increased cell death induced by birinapant in all primary AML models, except for AML1-ETO9a + Nras^{G12D} and CBFβ-MYH11 + Nras^{G12D} (Figures 7D and S7B). Addition of exogenous TNF did not sensitize AML1-ETO9a + Nras^{G12D} and CBFβ-MYH11 + Nras^{G12D} to birinapant, even at high concentrations of birinapant, suggesting that the mechanism of resistance is upstream of the p38/MK2 pathway (Figure S7C). On the other hand, at a clinically relevant dose of 1 μM LY2228820, MLL-ENL leukemic cells were sensitized to low doses of birinapant, and nanomolar concentrations of LY2228820 potentiated birinapant killing (Figures S7D and S7E). Moreover, blockade of either RIPK1 kinase activity with nec-1 or TNFR1 activity by deletion of *Tnfr1* or with a neutralizing antibody abrogated cell killing by birinapant plus p38i in MLL-ENL and HoxA9/Meis1 leukemias (Figures 7E and S7F). Consistent with our studies using BMDM, we found that p38 inhibition increased TNF transcript levels upon birinapant treatment in MLL-ENL cells (Figure 7F).

We tested the activity of LY2228820 with birinapant in vitro in AMLs from eight patients. The samples had FLT3-internal tandem duplication (ITD) mutation (patients #1, #2, #4, #6, and #7), FLT3 D835 missense mutation (patient #4), nucleophosmin exon-12 mutation (patients #2 and #4), MLL translocation (patient #3), inv(3) (patient #1), and inv(16) (patient #8). LY2228820 alone was not toxic to any of the tested human samples (Figure 7G). In contrast, eight of eight human AMLs were sensitive to birinapant alone to varying degrees, and four of these showed evidence of increased cell death with LY2228820 (Figure 7G).

Peripheral blood mononuclear cells from healthy donors were more resistant to 10 μM p38i and 500 nM birinapant combination

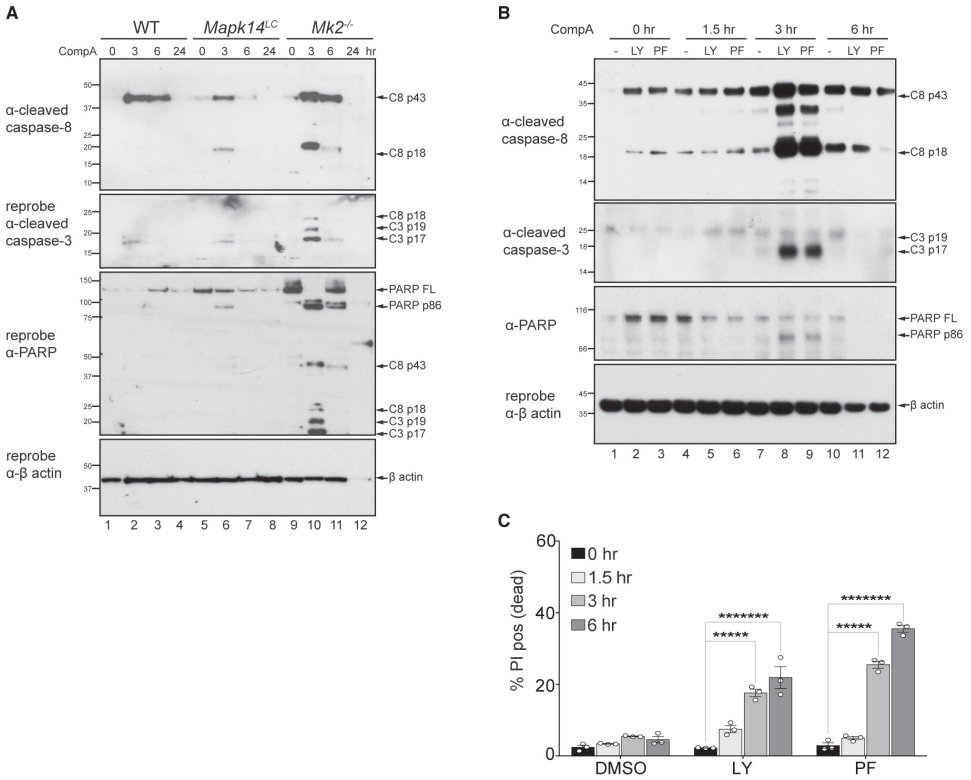

Figure 6. p38 or MK2 Inhibition Increases Smac-Mimetic-Induced Apoptosis

(A) WB analysis of lysates from WT, *Mapk14*^{LC} or *Mk2*$^{-/-}$ BMDM treated with 500 nM CompA for the indicated times.

(B) WB analysis of lysates from WT BMDM pre-treated for 20 min with LY2228820 (1 μM) or PF-3644022 (1 μM) and then treated with 500 nM CompA for indicated times. Blots in (A) and (B) are representative of three independent experiments.

(C) WT BMDM treated with 250 nM CompA ± LY2228820 (1 μM) or PF-3644022 (1 μM) at indicated times. Graphs show mean ± SEM, n = 3 independent biological repeats. *****p ≤ 0.0005; *******p ≤ 0.00005.

See also Figure S6.

than low doses of the standard chemotherapies cytarabine, daunorubicin, or idarubicin (Figure S8A). Monocytes (CD14$^+$), T (CD3$^+$CD4$^+$, CD3$^+$CD8$^+$), and natural killer (CD16$^+$) cells were mostly resistant, and only B cells were less than 20% viable after 48 hr of the combination treatment (Figure S8A). Most importantly, at concentrations that were toxic to AML CD34$^+$ cells, birinapant combined with LY2228820 was far less toxic to normal CD34$^+$ cells than the conventional therapies cytarabine, daunorubicin, and idarubicin (Figures 7G and S8B). Together, these results demonstrate that the combination of birinapant and p38i has therapeutic potential and that the combination is likely to be tolerated in vivo.

To explore this therapeutic potential, we determined the anti-leukemic activity of birinapant plus LY2228820 in vivo. Birinapant and LY2228820 are well tolerated in animals and humans as single agents (Condon et al., 2014; Tate et al., 2013). Because the safety of the combination treatment has not been reported, we evaluated the combination in non-tumor-bearing mice. After 4 weeks of co-administration of LY2228820 with two different doses of birinapant, no overt acute or chronic toxicity was observed as determined by organ or body weight or blood cell populations (Figure S8C). Most encouragingly, administration of LY2228820 did not exacerbate the splenomegaly induced by the more inflammatory SM GT13072 or affect the populations of white blood cells as determined (Figure S8D).

To assess the therapeutic efficacy of this combination, we transplanted multiple primary MLL-ENL and MLL-AF9

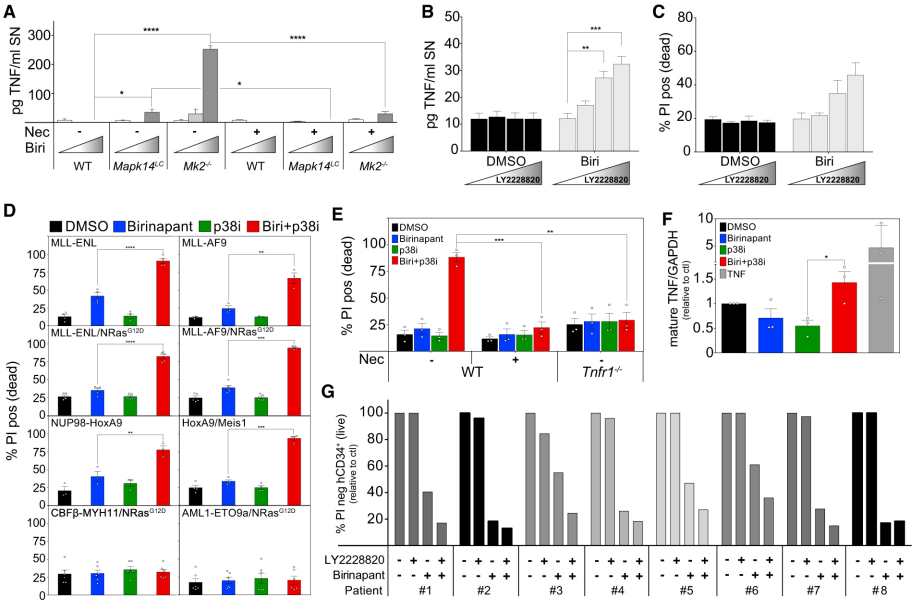

Figure 7. p38 and MK2 Inhibitors Sensitize Primary AML Cells to the Clinical SM Birinapant in a TNFR1- and RIPK1-Dependent Manner

(A) Levels of TNF in the SN of WT, *Mapk14*^{LC}, or *Mk2*$^{-/-}$ BMDM treated for 6 hr with 500 nM birinapant ± Nec (50 μM).

(B and C) Levels of TNF in the SN (B) or cell death (C) of WT BMDM treated with increasing concentrations (0; 0.05; 0.5; 1 μM) of LY2228820 ± 250 nM birinapant (Biri).

Graphs in (A)–(C) show mean ± SEM of three independent biological repeats.

(D) Cell death of indicated AMLs treated with birinapant (100 nM for MLL-ENL, 250 nM for MLL-AF9 and NUP98-HoxA9, 500 nM for MLL-ENL/NRas^{G12D}, MLL-AF9/NRas^{G12D}, HoxA9/Meis1, CBFβ-MYH11/NRas^{G12D}, and AML1-ETO9a/NRas^{G12D}) ± 1 μM LY2228820 for 24 hr.

(E) Cell death of WT and *Tnfr1*$^{-/-}$ MLL-ENL cells treated with either 50 nM birinapant, LY2228820 (1 μM), or both ± Nec (50 μM).

(F) Levels of mature TNF transcripts relative to GAPDH transcripts in MLL-ENL treated for 2 hr with 50 nM birinapant ± LY2228820 (1 μM) or with TNF (100 ng/ml).

Graphs in (D)–(F) show mean ± SEM of n = 3–6 independent leukemias.

(G) Cell death of CD34^{+} mononuclear cells isolated from AML patients and treated for 48 hr with 250 nM birinapant ±1 μM LY2228820. For each patient sample, graphs show mean of at least n = 2 technical replicates across n = 2–3 independent experiments.

*p ≤ 0.05; **p ≤ 0.01; ***p ≤ 0.005; ****p ≤ 0.001. See also Figure S7.

leukemias and treated the secondary recipient mice with the different drugs. Congenic albino mice were injected with MLL-ENL cells co-expressing luciferase. Engraftment and trafficking were evaluated by in vivo bioluminescent imaging. Treatment started when the photon-emission average of the cohorts was one log above the background level, typically 8 days after injection of leukemic cells (Figure 8A). After 1 week of treatment with the drug combination whole-body bioluminescence activity, reflecting the number of circulating leukemic cells, dramatically decreased and reached levels equal to the background levels observed in control mice without leukemia (Figure 8A). Even though the whole-body bioluminescence activity of most of the mice was above background level at the start of the treatment, it appeared that 25% of the vehicle-treated mice rejected the tumor, possibly due to immunogenicity of the luciferase transgene (Limberis et al., 2009). Birinapant treatment prolonged survival, although the co-therapy with p38i was more potent (Figure 8B). Remarkably, ~82% of mice treated with the co-therapy remained in remission 70 days after the treatment was stopped (Figure 8B). Histologically the liver and spleen of vehicle- and LY2228820-treated mice revealed massive infiltration of myeloid cells and spleens with few follicles (Figure 8C). Treatment with birinapant decreased myeloid cell infiltration in the liver and improved the splenic architecture, even in mice that had to be euthanized due to the leukemia (Figure 8C). Consistent with the bioluminescent imaging in the combination-treated mice, the organs appeared phenotypically normal (Figure 8C).

These results prompted us to test additional AML leukemias. In line with the MLL-ENL results, co-therapy improved the survival of mice bearing MLL-AF9 AMLs compared with mice that received single agents or no treatment (Figure 8D). Finally, we utilized the highly aggressive oncogenic NRas^{G12D} mutant/MLL-AF9/Luc model. Consistent with our in vitro data, co-

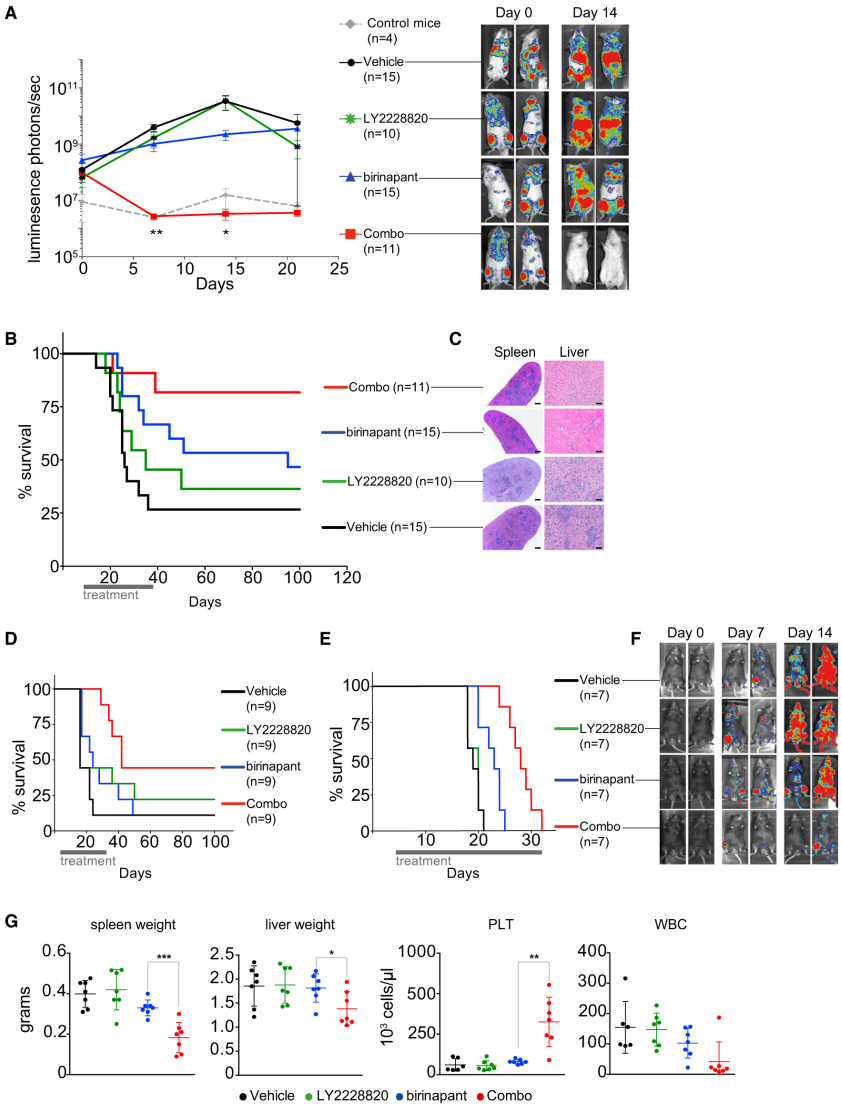

Figure 8. Combination of Clinical Inhibitors of IAPs and p38 Demonstrate Therapeutic Efficacy in AML

(A) Representative picture and quantification of in vivo imaging of leukemia progression from mice bearing MLL-ENL/Luc and treated with indicated regimen. Day 0 is the day the treatments start. Data represent mean ± SEM. For the statistical analysis, comparisons were performed between the birinapant-treated group and birinapant + p38i (Combo).

(B) Kaplan-Meier survival curve of C57BL/6 albino mice harboring MLL-ENL/Luc and treated with indicated regimen.

(C) H&E staining of liver and spleen sections from MLL-ENL/Luc-bearing mice treated with indicated regimen. Mice were euthanized due to adverse effects of leukemia on the indicated days except for combination, in which case the mouse was euthanized at the end of the experiment: vehicle (day 25), birinapant (day 25), LY2228820 (day 29), combination (day 100). Scale bars represent 50 μm for the spleen and 200 μm for the liver sections.

(legend continued on next page)

expression of NRas^{G12D} did not limit the efficacy of the combination in vivo (Figures 7D and 8E–8G). Unlike the MLL-ENL and MLL-AF9 models, the drug combination was unable to cure mice of their leukemia; however, 2 weeks of treatment dramatically decreased luciferase activity in the group that received the combined drugs and prolonged survival compared with birinapant alone (Figures 8E and 8F). Although all mice harboring MLL-AF9/NRas^{G12D} eventually developed a leukemia-induced hind-leg paralysis that necessitated their euthanasia, the co-administration nevertheless profoundly decreased leukemic symptoms, and the white blood cell and platelet counts and spleen and liver weights of these mice were significantly decreased compared with the untreated mice or those treated with single agents (Figure 8G).

DISCUSSION

Befitting its major inflammatory role, pathways leading to TNF production have been well characterized. For example, TLR pathways produce TNF in response to a range of pathogen-related products, via a coordinated set of ubiquitylation reactions catalyzed by TRAF6 and phosphorylation by IRAKs, leading to activation of IKKs (Akira and Takeda, 2004). Downstream of these events, NF-κB, p38, ERK, and JNK are activated, leading to the transcription, mRNA stabilization, and increased translation of TNF and other cytokines necessary for a coordinated inflammatory response. TNF production is also a key event in SM-induced killing (Gaither et al., 2007; Varfolomeev et al., 2007; Vince et al., 2007). Surprisingly, however, when IAPs are depleted by treatment with SM, rather than promoting TNF production the p38/MK2 signaling pathway acts to limit TNF production.

This role reversal of p38 function correlates with an increase in JNK and ERK phosphorylation and, presumably, activation. One explanation for the increased JNK phosphorylation might be the participation of p38 in a negative feedback loop whereby p38 suppresses TAK1 activity through direct phosphorylation of TAB1 (Cheung et al., 2003; Gaestel et al., 2009). However, in this regard it is surprising that MK2 inhibition also causes the same increase in JNK phosphorylation because it is not clear how MK2 might affect a direct p38-TAB1 phosphorylation event, and a role for MK2 in JNK phosphorylation has not been described. Consistent with a feedback effect, however, we observed that both p38α and MK2 inhibition resulted in increased TAK1 phosphorylation. The inhibitory effect of p38 on TAK1 activation is a suspected reason for the failure of p38i in clinical trials to treat inflammatory diseases (Gaestel et al., 2009). If this is correct, our results suggest that MK2 inhibitors might be similarly compromised as a treatment for chronic inflammatory diseases. However, this would not limit their use in anti-cancer combinations.

Inhibition of p38 or MK2 greatly sensitized MLL-ENL-, MLL-AF9-, NUP98-HoxA9-, and HoxA9/Meis1-expressing leukemic cells to killing by birinapant in a TNFR1-dependent manner. Kadia et al. (2012) found that phospho-p38 was higher in Ras-mutated AML than in Ras WT AML. However, we found that overexpression of oncogenic Ras did not limit the efficacy of birinapant plus p38 or MK2 inhibitors of MLL-ENL- or MLL-AF9-expressing cells. This suggests that the increase of p38 activity due to hyperactivity of Ras will not limit the efficacy of the combination of birinapant plus p38i in clinical settings.

Murine AML harboring CBFβ-MYH11 and AML1-ETO9a translocation oncogenes did not respond to birinapant plus p38i treatment. A recent gene expression analysis revealed that leukemias of CBF AML patients that were sensitive to the SM BV6 had a distinct gene expression signature to those leukemias that were resistant (Luck et al., 2011). Although the level of p38/MK2 expression or activation was not assessed in these samples, Luck et al. (2011) found that the p38 MAPK pathway was one of 43 BioCarta pathways that were differentially regulated. Thus it is possible that disruption of the p38 pathway in this leukemia affects its response to birinapant/p38i-induced death. However, addition of exogenous TNF did not sensitize CBFβ-MYH11 and AML1-ETO9a leukemic cells to birinapant killing, suggesting that the mechanism of resistance is potentially independent of a disruption of the p38/MK2 pathway. Despite the fact that AMLs with CBFβ-MYH11 and AML1-ETO9a translocations express TNFR1 (Volk et al., 2014), one explanation for resistance could be a lack of TNFR1 expression in our AML models. Irrespective of the reason, our results indicate that the p38i plus birinapant co-therapy is likely to be less suitable for inv(16;16) or t(8;21) AML patients.

The "7 + 3" combination of daunorubicin and cytarabine is routinely used as chemotherapy for adult patients with AML (Burnett, 2012). While high-dose chemotherapy can be effective against AML, these drugs induce substantial toxicity and relapses frequently occur. After four decades of clinical investigation, approximately 50% of adults with AML achieve durable remissions with anthracyclines when dosed in combination with cytarabine (Burnett et al., 2013; Fernandez et al., 2009). The management of elderly patients with AML, however, remains an area of highly unmet need, and the combination of two clinical drugs that have greatly reduced toxicity against normal CD34$^+$ human cells at concentrations that were toxic to AML CD34$^+$ human cells is encouraging.

The consistent responses that we observed with birinapant plus p38i in models of MLL-fusion gene AML and in primary samples with FLT3-ITD are of particular relevance to poor-risk AML patients with these mutations, who have a high relapse rate despite intensive chemotherapy (Gale et al., 2008). An important cause of on-target resistance to FLT3 inhibitors has been the emergence of FLT3-TKD mutant clones (Smith et al., 2012). Interestingly, the birinapant plus p38i combination was active in a primary AML sample with this mutation, suggesting this combination as a rational option for FLT3 inhibitor resistance. It has also been suggested that birinapant could be combined

(D and E) Kaplan-Meier survival curve of C57BL/6 mice harboring MLL-AF9 (D) or MLL-AF9/Ras^{G12D}/Luc (E) and treated with indicated regimen.
(F) Representative picture of mice at the start of treatment (day 0), then 1 week (day 7) and 2 weeks (day 14) after treatment.
(G) Spleen and liver weights and platelets (PLT) and white blood cell (WBC) counts at the time of euthanasia of mice harboring MLL-AF9/Ras^{G12D}/Luc and treated with indicated drugs. Graphs show mean ± SEM, n = 7 mice per group.
*p ≤ 0.05; **p ≤ 0.01; ***p ≤ 0.005. See also Figure S8.

with demethylating agents to treat AML (Carter et al., 2014). In that study, however, the association of birinapant with azacitidine had an additive effect on the survival of one AML xenograft model, whereas our clinical p38i plus birinapant combination provided synergistic effects in two MLL-fusion AML models with complete responses, beyond 100 days. In addition, we show a therapeutic efficacy of the combination in a setting of well-established and aggressive disease, the scenario most often encountered in clinical practice. Taken together, our in vivo data provide strong evidence of therapeutic potential and suggest that disease eradication is possible using the proposed co-therapy.

In summary, we have shown that p38/MK2 inhibition specifically increased SM killing of certain types of AML. The combination of the clinical SM birinapant and a clinical p38i was well tolerated in vivo, and therefore has clear advantages over the systemic toxicity of standard-of-care chemotherapy. Validation of the efficacy of birinapant/p38i against AML in clinical trials could lead to the repurposing of the extensive pharmaceutical efforts to develop specific and highly active p38i and rescue them from the therapeutic graveyard. Another attractive feature of using p38i is that rapid reductions in the level of C-reactive protein were frequently observed after initiation of treatment with a diverse range of p38i, affording a simple serum marker of pharmacodynamic activity in clinical studies (Genovese, 2009). Birinapant has entered clinical trials as monotherapy for patients with myelodysplastic syndrome and AML and in combination with azacitidine (https://www.clinicaltrials.gov/). Altogether, this study provides a strong rationale for early-phase clinical studies of birinapant combined with p38i or MK2i for leukemias and, potentially, other types of cancer.

EXPERIMENTAL PROCEDURES

Reagents

CompA, birinapant, GT13072, and necrostatin-1 were synthesized by TetraLogic Pharmaceuticals following published procedures (Condon et al., 2014; Vince et al., 2007). The kinase inhibitor library was from SYNthesis Med Chem. LY2228820, JNK-IN-8, SP600125, PD0335901, and CI-1040 were from Selleckchem. SCIO-469 and PF-3644022 were from Tocris Bioscience.

Generation of BMDM, Treatment, and TNF Measurement

See Supplemental Experimental Procedures for the generation of BMDM. For the kinase inhibitor screen, 1×10^5 BMDM (per well in 96-well plates) were pre-treated for 30 min with the kinase inhibitor library and then treated with ± 500 nM CompA for 24 hr. Supernatants were harvested to measure TNF levels by ELISA following the manufacturer's instructions (eBioscience). Cell viability was measured using CellTiter-Glo (Promega). For TNF measurements, and cell death assays 2×10^5 BMDM per well were seeded in 48-well plates. The following day BMDM were treated with CompA ± kinase inhibitors at indicated times and concentrations. Cell death was analyzed by flow cytometry quantification of PI (2 μg/ml) uptake using a FACSCalibur (BD Biosciences).

Generation of Murine AML and In Vitro Treatment

The Walter and Eliza Hall Institute Animal Ethics Committee approved all mouse experiments. See Supplemental Experimental Procedures for generation of primary leukemias. For cell death assays 1×10^5 leukemic cells were treated with birinapant ± kinase inhibitors. Cell death was analyzed by flow cytometry quantification of PI as described above.

qPCR and Actinomycin D Treatment

Relative levels of primary and mature TNF transcripts were determined using a relative standard curve to assess TNF transcript level with β-microglobulin (B2M) and GAPDH as housekeeping genes using SYBR Green (Life Technologies). WT BMDM were treated for 4 hr with 500 nM CompA ± 1 μM LY2228820. During the incubation actinomycin D (Sigma, 100 nM) was added for 1, 2, 3, or 4 hr. Primer sequences are listed in Supplemental Experimental Procedures.

In Vitro Human AML Survival Assays

The use of AML human samples in this study was approved by the Alfred Health Human Research Ethics Committee. Apheresis product, bone marrow, or peripheral blood was collected from patients diagnosed with AML following informed consent. Mononuclear cells were isolated by Ficoll-Paque Plus (GE Healthcare), sedimented, and enumerated using Trypan-blue exclusion. Cells were seeded at 0.2–1 × 10^6 cells/ml in Stemspan SFEM II medium (Stem Cell Technologies) supplemented with 100 ng/ml rhFlt-3L, 100 ng/ml rhSCF, 20 ng/ml rhIL-3, 20 ng/ml rhIL-6, 100 IU/ml DNase I, and penicillin/streptomycin; then treated with 250 nM birinapant ± 1 μM LY2228820 for 48 hr at 37°C in 5% CO_2. Following incubation, cell death was determined using flow cytometry via hCD34.PE and PI staining. All samples were tested in at least two to three independent experiments.

In Vivo Treatment and Imaging

5×10^5 leukemic cells were injected intravenously into C57BL/6 mice. In the MLL-ENL/Luc model, luciferase activity was measured every 4–5 days to monitor engraftment. Once the average luciferase activity was above 5×10^7 photons/s/cm^2, mice were randomized into treatment arms. For MLL-AF9 and MLL-AF9/Ras^{G12D}/Luc, treatment started at day 3. For all models mice were treated intraperitoneally twice a week for 4 weeks with either vehicle (6% Captisol) or 5 mg/kg birinapant for MLL-ENL/Luc and MLL-AF9, or 10 mg/kg birinapant for MLL-AF9/Ras^{G12D}/Luc, or 10 mg/kg LY2228820, or combination, by an animal technician blinded to the treatment. Mice bearing MLL-ENL/Luc and MLL-AF9/Ras^{G12D}/Luc were monitored for leukemia progression once a week using in vivo bioluminescent imaging as previously described (Zuber et al., 2009). Animal technicians blinded to treatment conditions euthanized the mice on ethical grounds, without any input from the experimental investigator, at the terminal disease stage, and tissue specimens were fixed in 10% formalin and stained with H&E. Parameters used to determine terminal disease were weight loss, enlarged spleen, anemia, lethargy, hunched posture, and leg paralysis.

Statistics

Unless otherwise specified, data are presented as mean ± SEM. Comparisons were performed with a Student's t test whose values are denoted in the figures as *$p \leq 0.05$, **$p \leq 0.01$, ***$p \leq 0.005$, ****$p \leq 0.001$, and *****$p \leq 0.0005$.

SUPPLEMENTAL INFORMATION

Supplemental Information includes Supplemental Experimental Procedures, eight figures, and one table and can be found with this article online at http://dx.doi.org/10.1016/j.ccell.2016.01.006.

AUTHOR CONTRIBUTIONS

N.L., K.H., D.C., W.W.L.W., L.V., L.S., D.H., S.S., E.d.V., and J.R. performed experiments. G.B., C.M., and S.P.G. generated murine AML models. M.B.M. and M. Gaestel provided *Mk2*$^{-/-}$ bones. M. Ghisi, J.M.S., and G.M. generated murine AML models and performed experiments. G.B., N.N.N., D.M., and J.R. performed experiments with AML patient samples. S.M.C. generated SM and nec-1. W.W.L.W., D.V., P.G.E., R.J., M. Guthridge, A.W., L.M., R.B.L, and M. Gaestel provided expertise, ideas, and critical comments. N.L. and J.S. designed research, analyzed and interpreted data, and co-wrote the paper. J.S. supervised the research.

ACKNOWLEDGMENTS

We thank V. Dixit for *Ripk3*$^{-/-}$, H. Korner for *Tnfr1*$^{-/-}$, W. Alexander for *Mlkl*$^{-/-}$, S. Hedrick for *Casp8*$^{fl/fl}$, M. Pasparakis for *Mapk14*$^{fl/fl}$ mice, and the Burnet

Institute ImmunoMonitoring Facility for technical assistance. This work was supported by NHMRC grants (1016647, 461221, 1016701, 1025594, 1046984, 1046010, 1025239, 637367, 1008131, 1081221, 1051235 and 1057905), Cancer Council Victoria grant-in-aid to S.P.G., NHMRC fellowships to J.S. (541901, 1058190) and D.V. (1020136), Association pour la Recherche sur le Cancer (ARC) fellowship to N.L., Peter Müller fellowship to K.H. with additional support from the Australian Cancer Research Fund, Victorian State Government Operational Infrastructure Support, NHMRC IRIISS grant (361646), grant SFB566 from Deutsche Forschungsgemeinschaft (M. Gaestel), and SNSF project grant (310030-138085). S.C. is an employee, and J.S. and D.V. are on the SAB of TetraLogic Pharmaceuticals. A.W. is performing a clinical trial for Tetralogic with birinapant. J.S, D.V., and N.L. are inventors of a patent describing the combination of smac-mimetic plus p38 inhibitor to treat cancer.

Received: April 8, 2015
Revised: September 17, 2015
Accepted: January 11, 2016
Published: February 8, 2016

REFERENCES

Akira, S., and Takeda, K. (2004). Toll-like receptor signalling. Nat. Rev. Immunol. *4*, 499–511.

Barrett, S.D., Bridges, A.J., Dudley, D.T., Saltiel, A.R., Fergus, J.H., Flamme, C.M., Delaney, A.M., Kaufman, M., LePage, S., Leopold, W.R., et al. (2008). The discovery of the benzhydroxamate MEK inhibitors CI-1040 and PD 0325901. Bioorg. Med. Chem. Lett. *18*, 6501–6504.

Bertrand, M.J.M., Milutinovic, S., Dickson, K.M., Ho, W.C., Boudreault, A., Durkin, J., Gillard, J.W., Jaquith, J.B., Morris, S.J., and Barker, P.A. (2008). cIAP1 and cIAP2 facilitate cancer cell survival by functioning as E3 ligases that promote RIP1 ubiquitination. Mol. Cell *30*, 689–700.

Burnett, A.K. (2012). New induction and postinduction strategies in acute myeloid leukemia. Curr. Opin. Hematol. *19*, 76–81.

Burnett, A.K., Russell, N.H., Hills, R.K., Hunter, A.E., Kjeldsen, L., Yin, J., Gibson, B.E., Wheatley, K., and Milligan, D. (2013). Optimization of chemotherapy for younger patients with acute myeloid leukemia: results of the medical research council AML15 trial. J. Clin. Oncol. *31*, 3360–3368.

Campbell, R.M., Anderson, B.D., Brooks, N.A., Brooks, H.B., Chan, E.M., De Dios, A., Gilmour, R., Graff, J.R., Jambrina, E., Mader, M., et al. (2014). Characterization of LY2228820 dimesylate, a potent and selective inhibitor of p38 MAPK with antitumor activity. Mol. Cancer Ther. *13*, 364–374.

Carter, B.Z., Mak, P.Y., Mak, D.H., Shi, Y., Qiu, Y., Bogenberger, J.M., Mu, H., Tibes, R., Yao, H., Coombes, K.R., et al. (2014). Synergistic targeting of AML stem/progenitor cells with IAP antagonist birinapant and demethylating agents. J. Natl. Cancer Inst. *106*, djt440.

Cheung, P.C., Campbell, D.G., Nebreda, A.R., and Cohen, P. (2003). Feedback control of the protein kinase TAK1 by SAPK2a/p38alpha. EMBO J. *22*, 5793–5805.

Cho, Y.S., Challa, S., Moquin, D., Genga, R., Ray, T.D., Guildford, M., and Chan, F.K. (2009). Phosphorylation-driven assembly of the RIP1-RIP3 complex regulates programmed necrosis and virus-induced inflammation. Cell *137*, 1112–1123.

Christofferson, D.E., Li, Y., Hitomi, J., Zhou, W., Upperman, C., Zhu, H., Gerber, S.A., Gygi, S., and Yuan, J. (2012). A novel role for RIP1 kinase in mediating TNFalpha production. Cell Death Dis. *3*, e320.

Cohen, P. (2009). Targeting protein kinases for the development of anti-inflammatory drugs. Curr. Opin. Cell Biol. *21*, 317–324.

Cohen, P., and Alessi, D.R. (2013). Kinase drug discovery—what's next in the field? ACS Chem. Biol. *8*, 96–104.

Condon, S.M., Mitsuuchi, Y., Deng, Y., LaPorte, M.G., Rippin, S.R., Haimowitz, T., Alexander, M.D., Kumar, P.T., Hendi, M.S., Lee, Y.H., et al. (2014). Birinapant, a smac-mimetic with improved tolerability for the treatment of solid tumors and hematological malignancies. J. Med. Chem. *57*, 3666–3677.

Das, M., Sabio, G., Jiang, F., Rincon, M., Flavell, R.A., and Davis, R.J. (2009). Induction of hepatitis by JNK-mediated expression of TNF-alpha. Cell *136*, 249–260.

Deveraux, Q.L., Takahashi, R., Salvesen, G.S., and Reed, J.C. (1997). X-linked IAP is a direct inhibitor of cell-death proteases. Nature *388*, 300–304.

Deveraux, Q.L., Roy, N., Stennicke, H.R., Van Arsdale, T., Zhou, Q., Srinivasula, S.M., Alnemri, E.S., Salvesen, G.S., and Reed, J.C. (1998). IAPs block apoptotic events induced by caspase-8 and cytochrome c by direct inhibition of distinct caspases. EMBO J. *17*, 2215–2223.

Dumitru, C.D., Ceci, J.D., Tsatsanis, C., Kontoyiannis, D., Stamatakis, K., Lin, J.H., Patriotis, C., Jenkins, N.A., Copeland, N.G., Kollias, G., and Tsichlis, P.N. (2000). TNF-alpha induction by LPS is regulated posttranscriptionally via a Tpl2/ERK-dependent pathway. Cell *103*, 1071–1083.

Feoktistova, M., Geserick, P., Kellert, B., Dimitrova, D.P., Langlais, C., Hupe, M., Cain, K., MacFarlane, M., Hacker, G., and Leverkus, M. (2011). cIAPs block Ripoptosome formation, a RIP1/caspase-8 containing intracellular cell death complex differentially regulated by cFLIP isoforms. Mol. Cell *43*, 449–463.

Fernandez, H.F., Sun, Z., Yao, X., Litzow, M.R., Luger, S.M., Paietta, E.M., Racevskis, J., Dewald, G.W., Ketterling, R.P., Bennett, J.M., et al. (2009). Anthracycline dose intensification in acute myeloid leukemia. New Eng. J. Med. *361*, 1249–1259.

Fulda, S., and Vucic, D. (2012). Targeting IAP proteins for therapeutic intervention in cancer. Nat. Rev. Drug Discov. *11*, 109–124.

Gaestel, M., Kotlyarov, A., and Kracht, M. (2009). Targeting innate immunity protein kinase signalling in inflammation. Nat. Rev. Drug Discov. *8*, 480–499.

Gaither, A., Porter, D., Yao, Y., Borawski, J., Yang, G., Donovan, J., Sage, D., Slisz, J., Tran, M., Straub, C., et al. (2007). A Smac mimetic rescue screen reveals roles for inhibitor of apoptosis proteins in tumor necrosis factor-alpha signaling. Cancer Res. *67*, 11493–11498.

Gale, R.E., Green, C., Allen, C., Mead, A.J., Burnett, A.K., Hills, R.K., Linch, D.C., and Medical Research Council Adult Leukaemia Working Party. (2008). The impact of FLT3 internal tandem duplication mutant level, number, size, and interaction with NPM1 mutations in a large cohort of young adult patients with acute myeloid leukemia. Blood *111*, 2776–2784.

Genovese, M.C. (2009). Inhibition of p38: has the fat lady sung? Arthritis Rheum. *60*, 317–320.

Gurgis, F.M., Ziaziaris, W., and Munoz, L. (2014). Mitogen-activated protein kinase-activated protein kinase 2 in neuroinflammation, heat shock protein 27 phosphorylation, and cell cycle: role and targeting. Mol. Pharmacol. *85*, 345–356.

He, S., Wang, L., Miao, L., Wang, T., Du, F., Zhao, L., and Wang, X. (2009). Receptor interacting protein kinase-3 determines cellular necrotic response to TNF-alpha. Cell *137*, 1100–1111.

Kadia, T.M., Kantarjian, H., Kornblau, S., Borthakur, G., Faderl, S., Freireich, E.J., Luthra, R., Garcia-Manero, G., Pierce, S., Cortes, J., and Ravandi, F. (2012). Clinical and proteomic characterization of acute myeloid leukemia with mutated RAS. Cancer *118*, 5550–5559.

Knapp, S., Arruda, P., Blagg, J., Burley, S., Drewry, D.H., Edwards, A., Fabbro, D., Gillespie, P., Gray, N.S., Kuster, B., et al. (2013). A public-private partnership to unlock the untargeted kinome. Nat. Chem. Biol. *9*, 3–6.

Kotlyarov, A., Neininger, A., Schubert, C., Eckert, R., Birchmeier, C., Volk, H.D., and Gaestel, M. (1999). MAPKAP kinase 2 is essential for LPS-induced TNF-alpha biosynthesis. Nat. Cell Biol. *1*, 94–97.

Lawlor, K.E., Khan, N., Mildenhall, A., Gerlic, M., Croker, B.A., D'Cruz, A.A., Hall, C., Kaur Spall, S., Anderton, H., Masters, S.L., et al. (2015). RIPK3 promotes cell death and NLRP3 inflammasome activation in the absence of MLKL. Nat. Commun. *6*, 6282.

Limberis, M.P., Bell, C.L., and Wilson, J.M. (2009). Identification of the murine firefly luciferase-specific CD8 T-cell epitopes. Gene Ther. *16*, 441–447.

Luck, S.C., Russ, A.C., Botzenhardt, U., Paschka, P., Schlenk, R.F., Dohner, H., Fulda, S., Dohner, K., and Bullinger, L. (2011). Deregulated apoptosis signaling in core-binding factor leukemia differentiates clinically relevant, molecular marker-independent subgroups. Leukemia *25*, 1728–1738.

Micheau, O., Lens, S., Gaide, O., Alevizopoulos, K., and Tschopp, J. (2001). NF-kappaB signals induce the expression of c-FLIP. Mol. Cell. Biol. *21*, 5299–5305.

Mourey, R.J., Burnette, B.L., Brustkern, S.J., Daniels, J.S., Hirsch, J.L., Hood, W.F., Meyers, M.J., Mnich, S.J., Pierce, B.S., Saabye, M.J., et al. (2010). A benzothiophene inhibitor of mitogen-activated protein kinase-activated protein kinase 2 inhibits tumor necrosis factor alpha production and has oral anti-inflammatory efficacy in acute and chronic models of inflammation. J. Pharmacol. Exp. Ther. *333*, 797–807.

Murphy, J.M., Czabotar, P.E., Hildebrand, J.M., Lucet, I.S., Zhang, J.G., Alvarez-Diaz, S., Lewis, R., Lalaoui, N., Metcalf, D., Webb, A.I., et al. (2013). The pseudokinase MLKL mediates necroptosis via a molecular switch mechanism. Immunity *39*, 443–453.

Petersen, S.L., Wang, L., Yalcin-Chin, A., Li, L., Peyton, M., Minna, J., Harran, P., and Wang, X. (2007). Autocrine TNFalpha signaling renders human cancer cells susceptible to Smac-mimetic-induced apoptosis. Cancer Cell *12*, 445–456.

Ronkina, N., Kotlyarov, A., Dittrich-Breiholz, O., Kracht, M., Hitti, E., Milarski, K., Askew, R., Marusic, S., Lin, L.L., Gaestel, M., and Telliez, J.B. (2007). The mitogen-activated protein kinase (MAPK)-activated protein kinases MK2 and MK3 cooperate in stimulation of tumor necrosis factor biosynthesis and stabilization of p38 MAPK. Mol. Cell. Biol. *27*, 170–181.

Shakhov, A.N., Collart, M.A., Vassalli, P., Nedospasov, S.A., and Jongeneel, C.V. (1990). Kappa B-type enhancers are involved in lipopolysaccharide-mediated transcriptional activation of the tumor necrosis factor alpha gene in primary macrophages. J. Exp. Med. *171*, 35–47.

Silke, J., and Meier, P. (2013). Inhibitor of apoptosis (IAP) proteins-modulators of cell death and inflammation. Cold Spring Harb. Perspect. Biol. *5*, http://dx.doi.org/10.1101/cshperspect.a008730.

Silke, J., and Vucic, D. (2014). IAP family of cell death and signaling regulators. Methods Enzymol. *545*, 35–65.

Smith, C.C., Wang, Q., Chin, C.S., Salerno, S., Damon, L.E., Levis, M.J., Perl, A.E., Travers, K.J., Wang, S., Hunt, J.P., et al. (2012). Validation of ITD mutations in FLT3 as a therapeutic target in human acute myeloid leukaemia. Nature *485*, 260–263.

Sun, L., Wang, H., Wang, Z., He, S., Chen, S., Liao, D., Wang, L., Yan, J., Liu, W., Lei, X., and Wang, X. (2012). Mixed lineage kinase domain-like protein mediates necrosis signaling downstream of RIP3 kinase. Cell *148*, 213–227.

Tate, C.M., Blosser, W., Wyss, L., Evans, G., Xue, Q., Pan, Y., and Stancato, L. (2013). LY2228820 dimesylate, a selective inhibitor of p38 mitogen-activated protein kinase, reduces angiogenic endothelial cord formation in vitro and in vivo. J. Biol. Chem. *288*, 6743–6753.

Tenev, T., Bianchi, K., Darding, M., Broemer, M., Langlais, C., Wallberg, F., Zachariou, A., Lopez, J., Macfarlane, M., Cain, K., and Meier, P. (2011). The ripoptosome, a signaling platform that assembles in response to genotoxic stress and loss of IAPs. Mol. Cell *43*, 1–18.

Vallabhapurapu, S., Matsuzawa, A., Zhang, W., Tseng, P.H., Keats, J.J., Wang, H., Vignali, D.A., Bergsagel, P.L., and Karin, M. (2008). Nonredundant and complementary functions of TRAF2 and TRAF3 in a ubiquitination cascade that activates NIK-dependent alternative NF-kappaB signaling. Nat. Immunol. *9*, 1364–1370.

Varfolomeev, E., Blankenship, J.W., Wayson, S.M., Fedorova, A.V., Kayagaki, N., Garg, P., Zobel, K., Dynek, J.N., Elliott, L.O., Wallweber, H.J.A., et al. (2007). IAP antagonists induce autoubiquitination of c-IAPs, NF-kappaB activation, and TNF alpha-dependent apoptosis. Cell *131*, 669–681.

Vince, J.E., Wong, W.W.-L., Khan, N., Feltham, R., Chau, D., Ahmed, A.U., Benetatos, C.A., Chunduru, S.K., Condon, S.M., McKinlay, M., et al. (2007). IAP antagonists target cIAP1 to induce TNF alpha-dependent apoptosis. Cell *131*, 682–693.

Vince, J.E., Wong, W.W., Gentle, I., Lawlor, K.E., Allam, R., O'Reilly, L., Mason, K., Gross, O., Ma, S., Guarda, G., et al. (2012). Inhibitor of apoptosis proteins limit RIP3 kinase-dependent interleukin-1 activation. Immunity *36*, 215–227.

Volk, A., Li, J., Xin, J., You, D., Zhang, J., Liu, X., Xiao, Y., Breslin, P., Li, Z., Wei, W., et al. (2014). Co-inhibition of NF-kappaB and JNK is synergistic in TNF-expressing human AML. J. Exp. Med. *211*, 1093–1108.

Wong, W.W., Vince, J.E., Lalaoui, N., Lawlor, K.E., Chau, D., Bankovacki, A., Anderton, H., Metcalf, D., O'Reilly, L., Jost, P.J., et al. (2014). cIAPs and XIAP regulate myelopoiesis through cytokine production in a RIPK1 and RIPK3 dependent manner. Blood *123*, 2562–2572.

Zarnegar, B.J., Wang, Y., Mahoney, D.J., Dempsey, P.W., Cheung, H.H., He, J., Shiba, T., Yang, X., Yeh, W.C., Mak, T.W., et al. (2008). Noncanonical NF-kappaB activation requires coordinated assembly of a regulatory complex of the adaptors cIAP1, cIAP2, TRAF2 and TRAF3 and the kinase NIK. Nat. Immunol. *9*, 1371–1378.

Zhang, T., Inesta-Vaquera, F., Niepel, M., Zhang, J., Ficarro, S.B., Machleidt, T., Xie, T., Marto, J.A., Kim, N., Sim, T., et al. (2012). Discovery of potent and selective covalent inhibitors of JNK. Chem. Biol. *19*, 140–154.

Zuber, J., Radtke, I., Pardee, T.S., Zhao, Z., Rappaport, A.R., Luo, W., McCurrach, M.E., Yang, M.M., Dolan, M.E., Kogan, S.C., et al. (2009). Mouse models of human AML accurately predict chemotherapy response. Genes Dev. *23*, 877–889.

5. Discussion

Our results show RIPK3 did not alter tumor growth of established tumors. In a metastasis model, changes in cytokine production in *Ripk3*$^{-/-}$ mice compared to wildtype after tumor injection were minimal. Activation of cell death *in vivo* was not detected and when we assessed the involvement of different proteins involved in the necrosome, we found the kinase activity of RIPK1 was important in the ability of tumor cells to form lung nodules but not MLKL. Bone marrow chimeras showed the involvement of the stromal but not the hematopoietic compartment was critical for the loss of tumor nodules in the lung in RIPK3 deficient mice. Finally, we found the loss of RIPK3 in the endothelial compartment in the lung decreased the ability of tumor cells to transmigrate due to the inability of the RIPK3 deficient endothelial cells to respond to permeability factors. These results suggest the role of the necrosome is minimal in tumor cell extravasation and presents a novel role for RIPK3 as a signaling platform downstream of angiogenic factors such as VEGF and FGF. Therefore, my work reveals an example in which non-cell death functions of RIPK3 have a strong impact on the disease outcome, and that this was solely mediated by RIPK3 without additional manipulation to bring RIPK3 into action such as inhibition of Caspase-8 or cIAPs.

In future studies, it needs to be assessed in pre-clinical models whether the deficiency of RIPK3, MLKL or kinase inhibition of RIPK1 provides beneficial effects in certain diseases. Most important, because RIPK1 and RIPK3 have shown to have necroptosis-independent functions in regulating inflammation this adds further complexity that needs to be clarified by which mechanism RIPK1 and RIPK3 regulate the inflammatory arm versus the necroptotic function and how this affects the disease state. Therefore, remaining issues and open questions in order to clarify the role of RIPK1 and RIPK3 are pointed out and discussed in detail in this section.

5.1. The role of RIPK3 in tumor malignancy

The loss of ability of tumor cells to undergo necroptosis is associated with resistance to traditional chemotherapeutic agents and poor prognosis[12,69,70]. In response to typical necroptotic stimuli, the loss of RIPK3 due to epigenetic silencing prevented MLKL activation and execution of necroptosis[71,72].

Insight about the role of RIPK3 in cancer development was confirmed when the loss of RIPK3 in myeloid cells accelerated FLT3-internal tandem duplication (FLT3-ITD) induced myeloproliferation and the development into a leukemia[197]. Here, RIPK3 promoted the differentiation of leukemia-initiating cells (LIC) and identified RIPK3 to regulate inflammasome activation by regulating the release of IL-1β. This was also observed when RIPK3 expression was tested in primary human AML samples and revealed that RIPK3 was downregulated. This data identified RIPK3 and the inflammasome as key regulators to suppress AML development. Interestingly, the loss of MLKL did accelerate leukemogenesis, but it only partially phenocopied the loss of RIPK3, which suggest that RIPK3 has additional functions that mediate leukemogenesis. Another recent study reported that the depletion of RIPK3 in *Kras^{G12D}* pancreatic ductal epithelial cells (PDEC) enhanced proliferation and aggressiveness *in vitro* due to increased expression of Bcl-xL and c-Myc, and loss of CDK4. However, this was in contrast to the finding that *p48^{cre};Kras^{G12D};Ripk3$^{-/-}$ mice blocked against pancreatic oncogenesis compared to p48^{cre};Kras^{G12D};Ripk3$^{+/+}$* mice, as well as orthotopic injection of *Kras^{G12D};Rip3$^{-/-}$* and *Kras^{G12D};Ripk3$^{+/+}$* tumor cells into pancreas of wildtype mice showed decreased tumor growth upon loss of RIPK3 ([198]. The findings from Höckendorf et al., suggest RIPK3 as a tumor suppressor, while Seifert et al., would suggest the opposite, which in turn suggests that the pancreas may have a unique milieu and that the RIPK3 functions are dependent on the cellular and inflammatory context. From that we can conclude that RIPK3 most likely has tumor suppressor function[69-72,197], but the role of RIPK3 in tumors may depend on the tumor type and the surrounding milieu forming the tumor microenvironment.

5.2. The role of RIPK3 in the tumor microenvironment

My work shows an important role for RIPK3 in stromal cells of the TME but not in the hematopoietic compartment (Figure 12). In addition upon intravenous injection, the loss of RIPK3 in the TME resulted in decreased formation of tumor nodules with slightly reduced tumor size, and that this was independent of MLKL-dependent necroptosis(Figure 10c+d+e and Figure 11d). We then tested whether subcutaneous tumor growth was affected in the RIPK3 deficient mice and we found no change in size of B16-F10 tumors compared to wildtype (Figure 10a), which was supported by the same finding of Seifert and colleagues[198]. Yet, we found that the loss of MLKL only slightly reduced pulmonary tumor nodules compared to wildtype mice (Figure 11d). In summary, the study from Höckendorf et al., and ours provide an example in which the alternative functions of RIPK3 come into play without inhibition of cIAPs[197].

Further supportive, we have found that RIPK3 protein levels increased in lungs (Figure 9b), which was similar to the observation that RIPK3 levels were increased in tumor harboring pancreases[198]. In addition, orthotopic injection of *Kras*^{G12D} PDEC or *Pdx1*^{cre}*;Kras*^{G12D}*;TP53*^{R172H} cells into wildtype and Ripk3$^{-/-}$, showed smaller tumors upon loss of RIPK3 in the TME[198]. This could be explained by the function of RIPK3 in the TME that caused immune suppression, by which RIPK3- and Mincle-dependent expression of CXCL1 promoted recruitment of highly immunogenic myeloid and T cell infiltrates. Indeed, blocking CXCL1 protected against pancreatic adenocarcinoma progression. This suggests that RIPK1 and RIPK3 in the TME can significantly contribute to tumorigenesis and tumor progression. Further, it is unclear what process causes the upregulation of RIPK3 protein levels in lungs after B16 injection or in pancreatic tumors and how this affects levels of necroptosis in such cells and due to its proinflammatory nature enhances immunogenicity. Another alternative that needs to be assessed is, whether increased RIPK3 levels are required for cytokine production of CXCL1[198] similar to the observation in Wong et al., [50].

5.3. Defining necroptosis in experimental studies

In order to study RIPK1 and RIPK3 alternative functions it is crucial to detect MLKL, which is a substrate of RIPK3 and considered the crucial effector molecule in necroptosis. So far, MLKL has not been reported yet to have other functions such as the RIPKs, besides its requirement for necroptosis execution by forming pores in the membrane once phosphorylated by RIPK3. Other downstream substrates that have necroptosis execution capabilities are likely to exist but need to be identified.

In order to detect necroptosis, a monoclonal antibody against human phosphorylated MLKL was generated that was suitable for labeling tissue sections[48] and a monoclonal antibody against phosphorylated mouse MLKL was developed but works only to detect by immunoblotting[199]. Alternatively, to conclude for the presence of necroptosis in tissues the absence of apoptotic markers and the presence of necrotic lesions in comparison to $MLKL^{-/-}$ animals, by which necroptosis is blocked, needs to be assessed. It is therefore of great importance to develop robust tools to detect necroptotic cells in tissues in order to study the function of necroptosis *in vivo*.

5.4. The contribution of necroptosis-independent RIPK3-mediated inflammation to tumor malignancy

It is still not entirely clear whether the loss of RIPKs blocked the severity of inflammatory disease models or cancer disease due to regulating inflammation, or cell death or both. So far, very little is known how RIPK3 or RIPK1 control inflammation independent of cell death. In our study, the loss of RIPK3, but not the loss of MLKL in the TME decreased the number of tumor nodules in lungs of mice injected with B16F10 melanoma or MC-38 colon carcinoma cells (Figure 10c-e). This suggested necroptosis independent function of RIPK3 is important for the tumor formation. Due to the ability of RIPKs to drive cytokines we tested whether this is the case in our phenotype. Therefore we tested whether cytokine and chemokines levels in lungs were altered in a RIPK3 dependent manner, but mostly the levels of cytokines have not been altered (Figure 12b, Figure 14a and Supplementary

Figure 3a). This is supported in part by the bone marrow chimera experiments, in which the loss of RIPK3 in stromal cells showed reduced tumor nodules compared to wildtype mice reconstituted with RIPK3 deficient bone marrow cells(Figure 12d+e). However, RIPK3 deficient mice that were reconstituted with wildtype bone marrow showed a slight increase in tumor nodule formation compared to those with RIPK3 deficient bone marrow (Figure 12e). This indicates that RIPK3 in myeloid cells may partially be contributing to promote tumor nodule formation that could be due to regulating the secretion or production of certain inflammatory signals such as cytokines *in vivo*.

The discrepancy that no major changes were observed when looking at total lung lysates may be explained by the fact that cytokines are secreted remain different to what a cell has produced/stored within the cell. Another explanation may be that the inflammatory signals released from macrophages in the process tumor cell extravasation may be disrupted by RIPKs and this might be of actual importance for aiding local extravasation of tumor cells, but because the amount of tumor cells injected and the majority of them dies, inducing extravasation unrelated overwhelming cytokine response, may vanish the differences that are of relevance to a single tumor cell transmigrating. Therefore, such processes need to be examined at the single-cell level by using flow cytometric analysis in combination with histopathological analysis to assess cellular compartments and cytokine levels. Furthermore, such tumor models that depend on RIPKs need to be assessed in necroptosis deficient *Mlkl*$^{-/-}$ mice.

5.5. Potential cell death independent complex formation with RIPK1 and RIPK3 upon angiogenic signals in endothelial cells

The fact that RIPK1 kinase dead transgenic mice are viable and resistant to necroptosis, while NF-κB signaling was not compromised, it has been established that RIPK1 kinase-independent scaffolding function is essential to inhibit cell death. In addition, if Caspase-8 is inhibited or absent, RIPK1

interacts via the RHIM domain with RIPK3 to form RIPK1/RIPK3 complex which is followed by as series of phosphorylation events on RIPK1 and RIPK3 that leads to the formation of amyloid filamentous structures known as the necrosome [200].

Due to the role of RIPK1 and RIPK3 complex formation during cell death signaling such as the necrosome formation[200], this would suggest that RIPK1 and RIPK3 might work in complex to promote tumor formation in the lung independent of necroptosis. In addition, we hypothesize that such complexes play a role in signaling events that are not related to TNFR1 mediated complex formation. Our observation suggested that vascular permeability related signaling upon VEGF and FGF-b stimulation (e.g. HSP27, ERK) was altered in the RIPK3 deficient endothelial cells (Figure 15a-c, Supplementary Figure 3b). We therefore proposed an important role for RIPK3 in endothelial cells, in which a non-necroptotic role of RIPK3 alters vascular signaling and therefore causing tumor cell induced permeability issues(Figure 14b-d).

To test whether such complexes exist upon VEGF and FGF stimulation, immunoprecipitation experiments need to be performed to test whether RIPK1 and RIPK3 are in complex upon angiogenic stimuli similar to those formed in TNFR1 mediated signaling. For example, other prominent interaction partners of RIPK1 and RIPK3 in TNFR1 cell death signaling such as Caspase-8 and FADD or TAK1 in complex with RIPK1 that is known to mediate survival signaling. It is also possible that the hypothetical complex is consisting of other unknown interaction partners that could be identified by mass spectrometry upon immunoprecipitation of RIPK1 or RIPK3. This should be performed in cells that lack MLKL or Caspase-8, as well as both in order to prove the existence of a complex in the absence of necroptosis- or apoptosis function. Such experiments should resolve whether complex formation is of importance and if RIPK1 and RIPK3 work in concert during necroptosis-independent signaling events upon angiogenic stimuli in endothelial cells.

5.6. The role of posttranslational regulation by ubiquitylation of RIPK3

The ubiquitylation status of RIPK1 has been shown to determine which distinct complexes were formed, which consequently determined whether cells survive, or die by either apoptosis or necroptosis. In contrast to what is known about RIPK1 ubiquitylation, the role of RIPK3 ubiquitylation and how this affects complex formation and signaling is much less defined. For example, it has been observed that the severe skin inflammation in $A20^{-/-}$ mice[52] was rescued upon genetic deletion of RIPK3. A20 is known to have deubiquitylating activity and it was reported to remove ubiquitin chains from RIPK3 at Lys 5, which in turn prevented the interaction of RIPK1 and RIPK3 that was necessary for necroptosis induction[201]. RIPK3 was also shown to be ubiquitylated by cIAPs *in vitro*[202].

We observed that RIPK3 protein levels are increasing at 12h after intravenous tumor cell injection in the majority of the lungs that were assessed (Figure 10b). Increased RIPK3 protein levels were also reported in pancreatic tumors and the adjacent non-tumor tissue[198]. In addition, the levels of p38 activation in the lungs of RIPK3 deficient mice remains poorly activated at two- and six hours after B16F10 injection compared to wildtype (Figure 15c) or decreased activation of HSP27 in RIPK3 deficient endothelial cells after angiogenic stimuli (Figure 15a+b, Supplementary Figure 3b). In order to determine whether posttranslational modifications and not transcriptional activation are involved to elevate RIPK3 protein levels as well as altering signaling events (e.g. decreased p38/HSP27), the expression of RIPK3 mRNA needs to be assessed. If no correlation between mRNA levels and an increase in protein levels is measured, this would strongly suggest that RIPK3 could be protected from degradation due to posttranscriptional modifications. The ubiquitin system is known to mediate proteosomal degradation as well as protein stabilization of a target protein, depending on the type of ubiquitin-linkage to a certain protein. Here, ubiquitylation of RIPK3 by K63- or linear-linked ubiquitin chains is known to often mediate non-degradative complex formation[201,203]. Together, this supports the hypothesis that in the case of

RIPK1 and RIPK3, posttranscriptional modification such as that mediated by K63-linked ubiquitin chain attachment to RIPK3 could be a substantial regulator not only during necroptosis but also during non-cell death related functions or RIPK3 and RIPK1.

In order to detect ubiquitylation on a protein, cultured cells can be transfected with plasmids encoding for the protein of interest (e.g. RIPK1 and RIPK3) and epitope tagged ubiquitin. Immunoprecipitation of RIPK3 will then be tested with respective antibodies to detect ubiquitin after immunoblotting. Ubiquitylation can also be tested *in vitro* by incubating my purified protein with ubiquitin, ubiquitylation E1 and ubiquitylation E2 and then tested using antibodies to detect ubiquitin by immunoblotting[204]. Another approach to detect ubiquitin and ubiquitin attachment sites on the protein of interest could be mass-spectrometry based proteomics[205,206]. Deubiquitylating enzymes (DUBs) can be used to identify how an ubiquitin chain on a protein is build up. This is achieved due to the specificity of different DUB family members to the type of ubiquitin linkage. For example, the DUBs TRABIO and DUBA are known to specifically remove K63-linked ubiquitin from a protein[205,206]. Upon incubation of the ubiquitylated protein of interest with such different DUBs it can be determined how an ubiquitin chain on a protein is build up which then helps to understand where and how a protein is ubiquitylated.

5.7. A potential link between Caspase-8 and RIPK3 in regulating endothelial barrier function via the permeability and cell motility regulator c-Src

In contrast to its role in apoptosis signaling, recent discoveries revealed that Caspase-8 is involved in a number of alternative processes independent of cell death. These findings mainly describe the alternative functions of Caspase-8 to have a role in signaling pathways implicated in cell proliferation, cell migration and cell adhesion[207-212]. Interestingly, Caspase-8 showed to be phosphorylated on Tyr380 by c-Src, which was associated with a decreased activity of Caspase-8[213] that in parallel enhanced its

alternative function to promote cell adhesion, migration and tumor progression[207,210]. The tyrosine kinase Src is known to promote endothelial permeability in normal physiological processes as well as in inflammatory pathologies[214]. Src is part of the canonical pathway induced by VEGF/VEGFR2 that is responsible for metastasis-associated hyperpermeability of endothelial cells[215] and represents a major element in regulating vascular permeability. In this process, Src mediates activation of MLCK/MLC that is responsible for endothelial cell retraction via rearrangement of the cytoskeleton, direct phosphorylation of VE-cadherin, as well as activation of the focal adhesion kinase FAK that is responsible for promoting Calpain/FAK/p42 ERK complex formation where Caspase-8 is also participating in the complex [208,214].

This suggests a link between our observation that RIPK3 promotes vascular permeability and the role of Src signaling via Caspase-8. This may provide new insight by which RIPK3 promotes vascular permeability (Figure 14b-d) by assessing Src-dependent phosphorylation of Caspase-8 in our context, because Caspase-8 activity is also known to directly regulate necroptosis-related complex formation. Vice versa, dominant negative mutant forms of Caspase-8 (e.g. T380A) can be used to determine RIPK3 stability and complex formation, and how does this affect intracellular signaling of endothelial cells upon angiogenic- and permeability factors. It remains to be determined whether RIPK3 similar to Caspase-8 would participate in the focal adhesion complex (Calpain/FAK/p42 ERK), maybe together with Caspase-8 upon VEGF stimulation. Complex formation and protein/protein interaction can be tested by immunoprecipitation experiments, and fluorescence microscopy to define the localization of RIPK3 to certain structures such as tight-junctions, adherens junctions or focal-adhesion complexes.

5.8. The role of RIPK3 in metabolic processes during angiogenic switch

In the past few years, endothelial cell metabolism showed to be crucial regulator of the angiogenic switch[152], which in turn allows for vessel sprouting by inducing quiescent endothelial cells to become highly active, proliferate and migrate in order to form new blood vessels, during normal development as well as tumor related blood vessels[216].

Glycolysis has been implicated as a driving force of vessel sprouting, and upon VEGF signaling endothelial cells double their glycolytic flux. Due to the role of cell metabolism in determining vessel sprouting, and the fact that RIPK3 has been associated with metabolic enzymes during necroptosis signaling such as GLUL, GLUD1 and PYGL[13], this led us hypothesize that the loss of RIPK3 may alter endothelial cell metabolism in the presence of angiogenic factors independent of necroptosis. Our preliminary results indicate that the loss of RIPK3 in normal quiescent endothelial monolayers showed a modest decrease in the potential of elevating oxidative phosphorylation when stressed with inhibitors of mitochondrial respiratory chain (Oligomycin and FCCP), but not in glycolysis (Figure 16a). This proposes that loss of RIPK3 decreases the mitochondrial respiration potential. Surprisingly, when endothelial monolayers were activated for four hours with VEGF-A, we observed a strong dependency on RIPK3 to upregulate the oxygen consumption rate (OCR; measurement for mitochondrial respiration) (Figure 16b). One explanation for the decrease in mitochondrial respiration at basal levels and stressed levels could be that RIPK3 deficient endothelial cells own less mitochondria than wildtype cells do, but this needs to be analyzed by fluorescence microscopy. Moreover, GLUL catalyzes glutamine from glutamate and GLUD1 catalyzes glutamine into α-ketoglutarate. This process has been critical in cancer cells as a source of nitrogen and carbon[216,217], but the relative importance of glutamine metabolism in endothelial cells and how this is affected in the process of tumor cell extravasation and metastasis needs to be determined[216,217].

Interestingly, together with our data this suggests a potential role for RIPK3 in regulating mitochondrial respiration in endothelial cells during VEGF stimulation. But it is not known whether decreased potential in mitochondrial respiration has any functional impact on endothelial cells in to context of the angiogenic switch[152], and whether RIPK3 mediates VEGF-dependent changes in mitochondrial respiration are of relevance to cause permeability and/or allow for tumor cell transmigration in our study (Figure 13b+ca). Therefore, it needs to be further investigated how RIPK3 is related to the metabolism and mitochondrial function in the process of necroptosis-independent function in endothelial cells.

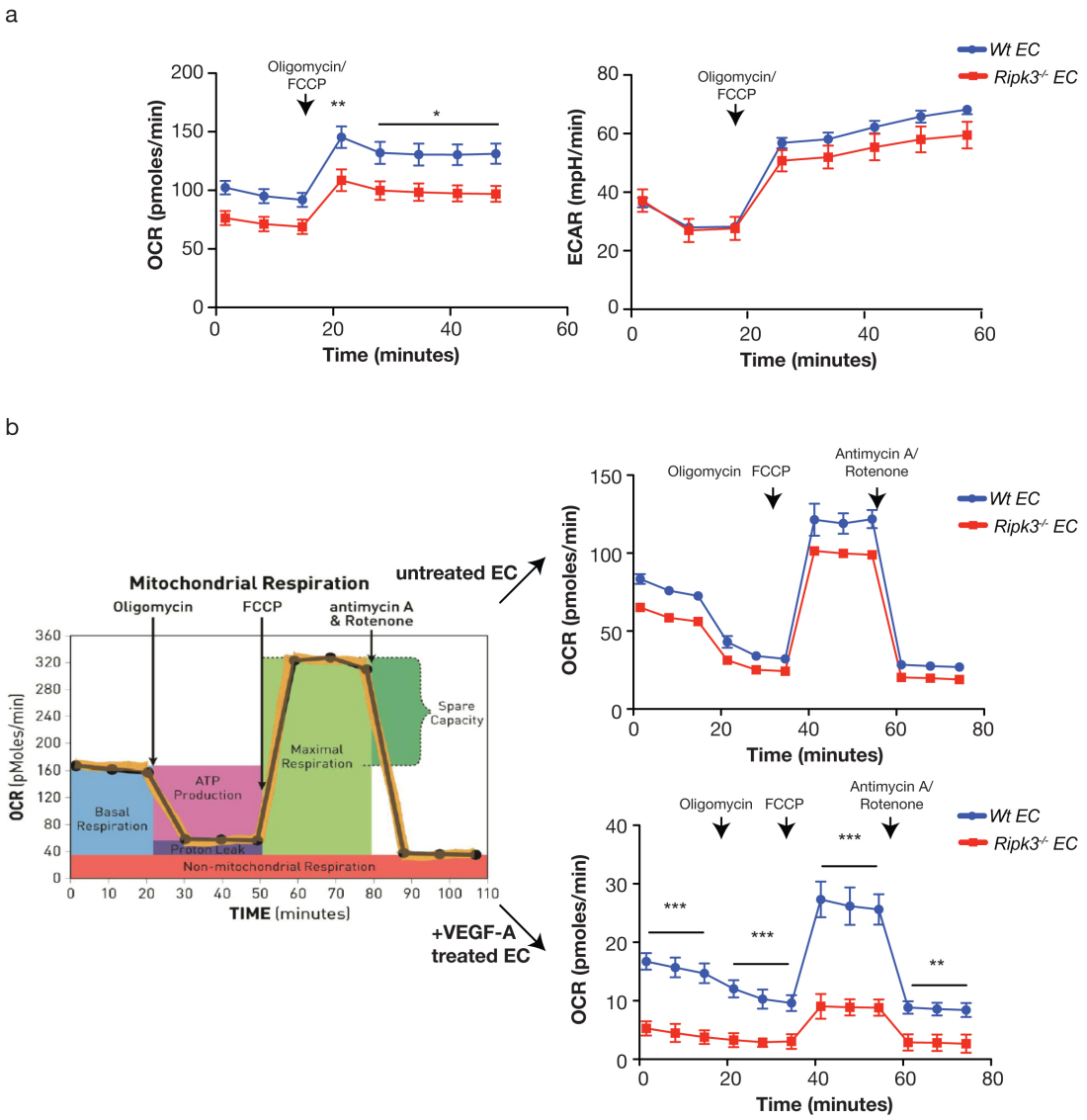

Figure 16: VEGF stimulation induced metabolic changes are reduced in RIPK3 deficient endothelial cells. Using the Seahorse technology, Glycolysis is measured by the

extracellular acidification rate (ECAR) and mitochondrial function by Oxygen consumption rate (OCR). Oligomycin inhibits ATP production by mitochondria, FCCP depolarizes the mitochondrial membrane and drives oxygen consumption rate to restore mitochondrial potential. Rotenone and antimycin A shut down mitochondrial respiration to allow calculation of non-mitochondrial respiration (Image from www.seahorsebio.com). **(a)** Phenotype stress test was performed on endothelial monolayers and **(b)** the mitochondrial stress test was performed on endothelial monolayers in the absence or presence of VEGF for 4h. From this, the seahorse technology allows determining basal respiration rate, ATP production, proton leak, maximal respiration, spare capacity and non-mitochondrial respiration.

5.9. Targeting RIPKs in cancer therapy

Pharmacological inhibitors have been generated in order to block the pro-inflammatory property of necroptosis. RIPK1 kinase inhibition can be achieved by necrostatin-1 (Nec-1) or Nec1s, which is the next generation inhibitor with enhanced specificity and less off targets have been recently developed. GSK'840, GSK'843 and GSK'872 were found to efficiently inhibit RIPK3 kinase activity[218] and necrosulfonamide are described to inhibit MLKL activity[46] to block necroptosis. The fact that Ripk1$^{-/-}$ mice are lethal but the kinase dead mutant mice such as RIPK1$^{K45A/\,K45A}$ or RIPK1$^{D138N/D138N}$ are viable and have no obvious altered phenotype suggests that kinase activity of RIPK1 may provide a save target[47,219,220].

RIPK3$^{-/-}$ or RIPK3 kinase dead (K51A) mice used in our study are viable and fertile[218], while in contrast the mice with inactivated kinase activity via mutation of D161N reveals embryonic lethality due to an elevated apoptosis of the endothelial cells in the yolk sac, which was dependent on RIPK1 and Caspase-8, and it has been suggested by Newton et al., that the kinase mutant D161N may alter structural features that lead to enhanced likelihood of RIPK3/RIPK1 dimerization and cell death signaling via apoptosis[47]. Similar findings were observed using certain RIPK3 kinase inhibitors that support the finding in D161N mice. This suggest that the use of RIPK3 kinase inhibitors for therapy need to be evaluated and it needs to be determined in the context of tumor type whether such inhibitors would have a beneficial effect due to blocking necroptosis or by enhancing apoptosis. Moreover, depletion or downregulation of RIPKs and MLKL in cancer has been associated with bad outcome due to enhanced resistance to cell death induction and contributing to chemotherapeutic resistance. Therefore, inhibition of RIPK1,

RIPK3 or MLKL in cancer therapy would not be advantageous[69,70,74,75]. On the other hand, as my work and others show[198] that ablation of RIPK1 kinase activity or RIPK3 in the TME is able to decrease tumor burden, would make them suitable for cancer therapy. But whether the positive effects of RIPK inhibition in stromal and immune compartment provides beneficial effects over the disadvantageous properties of RIPK or MLKL inhibition in the tumor itself, needs to be addressed in detail in specific tumor models. Necroptosis induction may provide alternative therapeutic strategy to overcome apoptosis-chemoresistance in a subgroup of cancer patients.

5.10. Therapeutic potential of immunogenic cell death via necroptosis

Recent reports identified necroptotic cancer cells as efficient inducers of an adaptive immune response [105,107-109]. However, the role of necroptosis *in vivo* and how it contributes to causing an immune response against tumors is still poorly understood. Moreover, the mechanism and effector molecules have been well described in immunogenic apoptosis with anthracycline agents[101,221], but are not understood yet in terms of necroptosis. As necroptosis was recently reported to occur in lung adenocarcinoma upon treatment with Dasatinib and Paclitaxel, it reveals relevance during cancer treatment, and similar to immunogenic apoptosis, necroptosis could potentially be desired to enhance anti-tumor immunogenicity. Therefore, the ability of necroptosis to induce anti-tumor immunity needs to be evaluated in detail, as necroptosis of the cells in the TME could also have disadvantageous effects[198]. Despite the latter, further studies need to identify chemotherapeutic drug combinations that could enhance necroptosis of tumor cells (e.g. Dasatinib and Paclitaxel)[222], which in turn could be combined with immune checkpoint blockade to unleash anti-tumor immunity.

Whether similar to immunogenic apoptosis, the immunogenicity of necroptotic cells is mediated by the same effector molecules such as HMGMB1 or extracellular DNA or other pathways that contribute to DC activation, needs to be elucidated[25,108]. Correlative evidence of DAMPs and

cytokine release by necroptotic cells and the activation of DCs indicate importance in cancer immunity. However, it is neither determined what the contribution of each factor is, nor is it clear what DC related sensory pathways usually activated upon immunogenic apoptosis, and were of actual importance for necroptosis induced DC maturation. Multiple receptors on DCs have been implicated in the induction of cellular immunity during cancer, including DAMP recognition by toll-like receptors (TLRs), ATP detection by P2RX7, and DNA sensing by cGAS/STING[223-226].

It needs to be evaluated which DAMPs and inflammatory cytokines released from necroptotic cancer cells induce DC maturation *in vitro* and *in vivo*. Cancer cells and DC co-incubation assays can be used to evaluate which pathways are important in mediating DC activation by necroptotic cells. After co-incubation FACS analysis will be performed to measure DC activation by CD80 and CD86. In addition, using the ovalbumin expressing cell lines will also evaluate the ability of DCs to activate naïve T cells, as DC maturation by necroptotic cells does not necessarily correlate with their ability to cross-present antigen.

5.11. Concluding remarks

Taken together, the findings described are of crucial importance, because triggering necroptosis is considered as a promising strategy to overcome apoptosis resistance in cancer therapy. Therefore, this implies that such treatment options need to be validated *in vivo*, because it is not known to which degree necroptosis inducing agents/drug combinations also hit untransformed cells, and therefore any treatment strategy will likely be tumor type specific. To the latter, the fact needs to be taken into account that decreased RIPK3 levels in the tumor correlated with poor prognosis but the loss of RIPKs in the tumor microenvironment can slow down tumor growth, this needs to be assessed in distinct tumor models. In addition, treatment option would only account for established tumors where the inhibition of RIPKs for example would prevent tumor progression, while the goal to

prevent cancer development by preventive administration of drugs would never be feasible.

6. References

1. Salvesen, G. S. & Duckett, C. S. IAP proteins: blocking the road to death's door : Abstract : Nature Reviews Molecular Cell Biology. *Nat Rev Mol Cell Biol* (2002).
2. Silke, J. The anti-apoptotic activity of XIAP is retained upon mutation of both the caspase 3- and caspase 9-interacting sites. *The Journal of Cell Biology* **157,** 115–124 (2002).
3. Van Sant, C., Hagglund, R., Lopez, P. & Roizman, B. The infected cell protein 0 of herpes simplex virus 1 dynamically interacts with proteasomes, binds and activates the cdc34 E2 ubiquitin-conjugating enzyme, and possesses in vitro E3 ubiquitin ligase activity. *Proc. Natl. Acad. Sci. U.S.A.* **98,** 8815–8820 (2001).
4. Bai, L., Smith, D. C. & Wang, S. Small-molecule SMAC mimetics as new cancer therapeutics. *Pharmacology & therapeutics* (2014).
5. Dueber, E. C. *et al.* Antagonists Induce a Conformational Change in cIAP1 That Promotes Autoubiquitination. *Science* **334,** 376–380 (2011).
6. Eckelman, B. P. & Salvesen, G. S. The Human Anti-apoptotic Proteins cIAP1 and cIAP2 Bind but Do Not Inhibit Caspases. *J. Biol. Chem.* **281,** 3254–3260 (2006).
7. Wang, F. *et al.* RIG-I Mediates the Co-Induction of Tumor Necrosis Factor and Type I Interferon Elicited by Myxoma Virus in Primary Human Macrophages. *PLoS Pathog* **4,** e1000099 (2008).
8. Shiozaki, E. N., Chai, J., Rigotti, D. J., Riedl, S. J. & Li, P. Mechanism of XIAP-mediated inhibition of caspase-9. *Molecular Cell* (2003).
9. Degterev, A. *et al.* Identification of RIP1 kinase as a specific cellular target of necrostatins. *Nat Chem Biol* **4,** 313–321 (2008).
10. Holler, N. *et al.* Fas triggers an alternative, caspase-8-independent cell death pathway using the kinase RIP as effector molecule. *Nat Immunol* **1,** 489–495 (2000).
11. Cho, Y. *et al.* Phosphorylation-Driven Assembly of the RIP1-RIP3 Complex Regulates Programmed Necrosis and Virus-Induced Inflammation. *Cell* **137,** 1112–1123 (2009).
12. He, S. *et al.* Receptor Interacting Protein Kinase-3 Determines Cellular Necrotic Response to TNF-&alpha. *Cell* **137,** 1100–1111 (2009).
13. Zhang, D. W. *et al.* RIP3, an Energy Metabolism Regulator That Switches TNF-Induced Cell Death from Apoptosis to Necrosis. *Science* **325,** 332–336 (2009).
14. Sun, X., Yin, J., Starovasnik, M. A., Fairbrother, W. J. & Dixit, V. M. Identification of a Novel Homotypic Interaction Motif Required for the Phosphorylation of Receptor-interacting Protein (RIP) by RIP3. *J. Biol. Chem.* **277,** 9505–9511 (2002).
15. Newton, K., Sun, X. & Dixit, V. M. Kinase RIP3 is dispensable for normal NF-kappa Bs, signaling by the B-cell and T-cell receptors, tumor necrosis factor receptor 1, and Toll-like receptors 2 and 4. *Mol. Cell. Biol.* **24,** 1464–1469 (2004).
16. Feng, S. *et al.* Cleavage of RIP3 inactivates its caspase-independent apoptosis pathway by removal of kinase domain. *Cellular Signalling* **19,** 2056–2067 (2007).
17. Micheau, O. & Tschopp, J. Induction of TNF receptor I-mediated apoptosis

via two sequential signaling complexes. *Cell* **114,** 181–190 (2003).
18. Stanger, B. Z., Leder, P., Lee, T. H., Kim, E. & Seed, B. RIP: a novel protein containing a death domain that interacts with Fas/APO-1 (CD95) in yeast and causes cell death. *Cell* **81,** 513–523 (1995).
19. Chaudhary, P. M. *et al.* Death receptor 5, a new member of the TNFR family, and DR4 induce FADD-dependent apoptosis and activate the NF-kappaB pathway. *Immunity* **7,** 821–830 (1997).
20. Zhang, D., Lin, J. & Han, J. Receptor-interacting protein (RIP) kinase family. *Cell. Mol. Immunol.* **7,** 243–249 (2010).
21. Ashida, H. *et al.* Cell death and infection: a double-edged sword for host and pathogen survival. *The Journal of Cell Biology* **195,** 931–942 (2011).
22. Kroemer, G. *et al.* Classification of cell death: recommendations of the Nomenclature Committee on Cell Death 2009. *Cell Death and Differentiation* **16,** 3–11 (2009).
23. Galluzzi, L. *et al.* Molecular definitions of cell death subroutines: recommendations of the Nomenclature Committee on Cell Death 2012. *Cell Death and Differentiation* **19,** 107–120 (2012).
24. Inoue, H. & Tani, K. Multimodal immunogenic cancer cell death as a consequence of anticancer cytotoxic treatments. *Cell Death and Differentiation* **21,** 39–49 (2013).
25. Wallach, D., Kang, T.-B., Dillon, C. P. & Green, D. R. Programmed necrosis in inflammation: Toward identification of the effector molecules. *Science* **352,** aaf2154 (2016).
26. Ravichandran, K. S. Beginnings of a Good Apoptotic Meal: The Find-Me and Eat-Me Signaling Pathways. *Immunity* **35,** 445–455 (2011).
27. Brenner, D. & Mak, T. W. Mitochondrial cell death effectors. *Curr. Opin. Cell Biol.* **21,** 871–877 (2009).
28. McIlwain, D. R., Berger, T. & Mak, T. W. Caspase functions in cell death and disease. *Cold Spring Harb Perspect Biol* **5,** a008656 (2013).
29. Shiozaki, E. N., Chai, J. & Shi, Y. Oligomerization and activation of caspase-9, induced by Apaf-1 CARD. *Proc. Natl. Acad. Sci. U.S.A.* **99,** 4197–4202 (2002).
30. Kurokawa, M. & Kornbluth, S. Caspases and kinases in a death grip. *Cell* **138,** 838–854 (2009).
31. Riedl, S. J. & Shi, Y. Molecular mechanisms of caspase regulation during apoptosis. *Nat Rev Mol Cell Biol* **5,** 897–907 (2004).
32. Laster, S. M., Wood, J. G. & Gooding, L. R. Tumor necrosis factor can induce both apoptic and necrotic forms of cell lysis. *J. Immunol.* **141,** 2629–2634 (1988).
33. Vercammen, D. *et al.* Inhibition of caspases increases the sensitivity of L929 cells to necrosis mediated by tumor necrosis factor. *J. Exp. Med.* **187,** 1477–1485 (1998).
34. Degterev, A. *et al.* Chemical inhibitor of nonapoptotic cell death with therapeutic potential for ischemic brain injury. *Nat Chem Biol* **1,** 112–119 (2005).
35. Kaiser, W. J. *et al.* Toll-like receptor 3-mediated necrosis via TRIF, RIP3, and MLKL. *J. Biol. Chem.* **288,** 31268–31279 (2013).
36. Thapa, R. J. *et al.* Interferon-induced RIP1/RIP3-mediated necrosis requires PKR and is licensed by FADD and caspases. *Proceedings of the National Academy of Sciences* **110,** E3109–18 (2013).
37. Dillon, C. P., Weinlich, R., Rodriguez, D. A. & Cripps, J. G. RIPK1 Blocks Early Postnatal Lethality Mediated by Caspase-8 and RIPK3. *Cell* (2014).

38. Upton, J. W., Kaiser, W. J. & Mocarski, E. S. DAI/ZBP1/DLM-1 complexes with RIP3 to mediate virus-induced programmed necrosis that is targeted by murine cytomegalovirus vIRA. *Cell Host and Microbe* **11,** 290–297 (2012).
39. Wang, X. *et al.* RNA viruses promote activation of the NLRP3 inflammasome through a RIP1-RIP3-DRP1 signaling pathway. *Nature Publishing Group* **15,** 1126–1133 (2014).
40. Thapa, R. J. *et al.* DAI Senses Influenza A Virus Genomic RNA and Activates RIPK3-Dependent Cell Death. *Cell Host and Microbe* (2016). doi:10.1016/j.chom.2016.09.014
41. Wong, W. W.-L. *et al.* RIPK1 is not essential for TNFR1-induced activation of NF-κB. *Cell Death and Differentiation* **17,** 482–487 (2010).
42. Mildner, A. & Jung, S. Development and function of dendritic cell subsets. *Immunity* **40,** 642–656 (2014).
43. Newton, K. RIPK1 and RIPK3: critical regulators of inflammation and cell death. *Trends Cell Biol.* **25,** 347–353 (2015).
44. Christofferson, D. E., Li, Y. & Yuan, J. Control of life-or-death decisions by RIP1 kinase. *Annu. Rev. Physiol.* **76,** 129–150 (2014).
45. Murphy, J. M. *et al.* The pseudokinase MLKL mediates necroptosis via a molecular switch mechanism. *Immunity* **39,** 443–453 (2013).
46. Hildebrand, J. M. *et al.* Activation of the pseudokinase MLKL unleashes the four-helix bundle domain to induce membrane localization and necroptotic cell death. *Proceedings of the National Academy of Sciences* **111,** 15072–15077 (2014).
47. Newton, K. *et al.* Activity of protein kinase RIPK3 determines whether cells die by necroptosis or apoptosis. *Science* **343,** 1357–1360 (2014).
48. Wang, H. *et al.* Mixed lineage kinase domain-like protein MLKL causes necrotic membrane disruption upon phosphorylation by RIP3. *Molecular Cell* **54,** 133–146 (2014).
49. Dondelinger, Y. *et al.* MLKL compromises plasma membrane integrity by binding to phosphatidylinositol phosphates. *CellReports* **7,** 971–981 (2014).
50. Wong, W. W.-L. *et al.* cIAPs and XIAP regulate myelopoiesis through cytokine production in an RIPK1- and RIPK3-dependent manner. *Blood* **123,** 2562–2572 (2014).
51. Pierdomenico, M. *et al.* Necroptosis is active in children with inflammatory bowel disease and contributes to heighten intestinal inflammation. *Am. J. Gastroenterol.* **109,** 279–287 (2014).
52. Newton, K. *et al.* RIPK3 deficiency or catalytically inactive RIPK1 provides greater benefit than MLKL deficiency in mouse models of inflammation and tissue injury. *Cell Death and Differentiation* (2016). doi:10.1038/cdd.2016.46
53. Lee, T. H., Shank, J., Cusson, N. & Kelliher, M. A. The kinase activity of Rip1 is not required for tumor necrosis factor-alpha-induced IkappaB kinase or p38 MAP kinase activation or for the ubiquitination of Rip1 by Traf2. *THEJOURNALOFBIOLOGICALCHEMISTRY* **279,** 33185–33191 (2004).
54. Kreuz, S., Siegmund, D., Scheurich, P. & Wajant, H. NF-kappaB inducers upregulate cFLIP, a cycloheximide-sensitive inhibitor of death receptor signaling. *Mol. Cell. Biol.* **21,** 3964–3973 (2001).
55. Wertz, I. E. *et al.* De-ubiquitination and ubiquitin ligase domains of A20 downregulate NF-kappaB signalling. *Nature* **430,** 694–699 (2004).
56. Karin, M. & Ben-Neriah, Y. Phosphorylation meets ubiquitination: the control of NF-[kappa]B activity. *Annu. Rev. Immunol.* **18,** 621–663 (2000).
57. Fuchs, Y. *et al.* Sef is an inhibitor of proinflammatory cytokine signaling, acting by cytoplasmic sequestration of NF-κB. *Developmental Cell* **23,** 611–

623 (2012).
58. Wang, L., Du, F. & Wang, X. TNF-α Induces Two Distinct Caspase-8 Activation Pathways. *Cell* **133,** 693–703 (2008).
59. Chan, F. K. M. A Role for Tumor Necrosis Factor Receptor-2 and Receptor-interacting Protein in Programmed Necrosis and Antiviral Responses. *Journal of Biological Chemistry* **278,** 51613–51621 (2003).
60. O'Donnell, M. A. *et al.* Caspase 8 inhibits programmed necrosis by processing CYLD. *Nature Cell Biology* **13,** 1–7 (2011).
61. Declercq, W., Vanden Berghe, T. & Vandenabeele, P. RIP Kinases at the Crossroads of Cell Death and Survival. *Cell* **138,** 229–232 (2009).
62. Micheau, O., Lens, S., Gaide, O., Alevizopoulos, K. & Tschopp, J. NF-kappaB signals induce the expression of c-FLIP. *Mol. Cell. Biol.* **21,** 5299–5305 (2001).
63. Oberst, A. *et al.* Catalytic activity of the caspase-8-FLIPL complex inhibits RIPK3-dependent necrosis. *Nature* 1–6 (2011). doi:10.1038/nature09852
64. Hughes, M. A. *et al.* Co-operative and Hierarchical Binding of c-FLIP and Caspase-8: A Unified Model Defines How c-FLIP Isoforms Differentially Control Cell Fate. *Molecular Cell* **61,** 834–849 (2016).
65. Hanahan, D. & Weinberg, R. A. The hallmarks of cancer. *Cell* **100,** 57–70 (2000).
66. Vaux, D. L., Cory, S. & Adams, J. M. Bcl-2 gene promotes haemopoietic cell survival and cooperates with c-myc to immortalize pre-B cells. *Nature* **335,** 440–442 (1988).
67. Strasser, A., Harris, A. W., Bath, M. L. & Cory, S. Novel primitive lymphoid tumours induced in transgenic mice by cooperation between myc and bcl-2. *Nature* **348,** 331–333 (1990).
68. Brady, C. A. & Attardi, L. D. p53 at a glance. *J. Cell. Sci.* **123,** 2527–2532 (2010).
69. Colbert, L. E. *et al.* Pronecrotic mixed lineage kinase domain-like protein expression is a prognostic biomarker in patients with early-stage resected pancreatic adenocarcinoma. *Cancer* **119,** 3148–3155 (2013).
70. Moriwaki, K., Bertin, J., Gough, P. J., Orlowski, G. M. & Chan, F. K. M. Differential roles of RIPK1 and RIPK3 in TNF-induced necroptosis and chemotherapeutic agent-induced cell death. *Cell Death Dis* **6,** e1636 (2015).
71. Koo, G.-B. *et al.* Methylation-dependent loss of RIP3 expression in cancer represses programmed necrosis in response to chemotherapeutics. *Cell Res* **25,** 707–725 (2015).
72. Geserick, P. *et al.* Absence of RIPK3 predicts necroptosis resistance in malignant melanoma. *Cell Death Dis* **6,** e1884 (2015).
73. Liu, P. *et al.* Dysregulation of TNFα-induced necroptotic signaling in chronic lymphocytic leukemia: suppression of CYLD gene by LEF1. *Leukemia* **26,** 1293–1300 (2012).
74. Nugues, A.-L. *et al.* RIP3 is downregulated in human myeloid leukemia cells and modulates apoptosis and caspase-mediated p65/RelA cleavage. *Cell Death Dis* **5,** e1384 (2014).
75. Fukasawa, T., Shoji, T., Gotoh, H. & Taniwaka, K. [A long-term survivor with stage IV gastric cancer due to postoperative weekly paclitaxel and 5'-DFUR combination therapy]. *Gan To Kagaku Ryoho* **33,** 235–238 (2006).
76. Su, Z., Yang, Z., Xie, L., DeWitt, J. P. & Chen, Y. Cancer therapy in the necroptosis era. *Cell Death and Differentiation* **23,** 748–756 (2016).
77. Imoto, I., Tsuda, H., Hirasawa, A., Miura, M. & Sakamoto, M. Expression of cIAP1, a target for 11q22 amplification, correlates with resistance of cervical

cancers to radiotherapy. *Cancer Research* (2002).
78. Imoto, I., Yang, Z. Q. & Pimkhaokham, A. As a Candidat e Target Gen e within an cIAP1 Identification of. *Cancer Research* (2001).
79. Zender, L. *et al.* Identification and Validation of Oncogenes in Liver Cancer Using an Integrative Oncogenomic Approach. *Cell* **125,** 1253–1267 (2006).
80. Reardon, D. A. *et al.* Extensive genomic abnormalities in childhood medulloblastoma by comparative genomic hybridization. *Cancer Research* **57,** 4042–4047 (1997).
81. Weber-Hall, S. *et al.* Gains, Losses, and Amplification of Genomic Material in Rhabdomyosarcoma Analyzed by Comparative Genomic Hybridization. *Cancer Research* **56,** 3220–3224 (1996).
82. Dai, Z. A comprehensive search for DNA amplification in lung cancer identifies inhibitors of apoptosis cIAP1 and cIAP2 as candidate oncogenes. *Human Molecular Genetics* **12,** 791–801 (2003).
83. Dierlamm, J. *et al.* The apoptosis inhibitor gene API2 and a novel 18q gene, MLT, are recurrently rearranged in the t(11;18)(q21;q21) associated with mucosa-associated lymphoid tissue lymphomas. *Blood* **93,** 3601–3609 (1999).
84. Akagi, T. *et al.* A novel gene, MALT1 at 18q21, is involved in t(11;18) (q21;q21) found in low-grade B-cell lymphoma of mucosa-associated lymphoid tissue. *Oncogene* **18,** 5785–5794 (1999).
85. Cillessen, S. A. G. M. *et al.* Small-molecule XIAP antagonist restores caspase-9 mediated apoptosis in XIAP-positive diffuse large B-cell lymphoma cells. *Blood* **111,** 369–375 (2007).
86. Tamm, I. *et al.* XIAP expression correlates with monocytic differentiation in adult de novo AML: impact on prognosis. *Hematol. J.* **5,** 489–495 (2004).
87. Sung, K. W. *et al.* Overexpression of X-linked inhibitor of apoptosis protein (XIAP) is an independent unfavorable prognostic factor in childhood de novo acute myeloid leukemia. *J. Korean Med. Sci.* **24,** 605–613 (2009).
88. Fulda, S. Smac mimetics as IAP antagonists. *Semin. Cell Dev. Biol.* **39,** 132–138 (2015).
89. Gaither, A. *et al.* A Smac Mimetic Rescue Screen Reveals Roles for Inhibitor of Apoptosis Proteins in Tumor Necrosis Factor- Signaling. *Cancer Research* **67,** 11493–11498 (2007).
90. Geserick, P. *et al.* Cellular IAPs inhibit a cryptic CD95-induced cell death by limiting RIP1 kinase recruitment. *The Journal of Cell Biology* **187,** 1037–1054 (2009).
91. Dougan, M. *et al.* IAP inhibitors enhance co-stimulation to promote tumor immunity. *Journal of Experimental Medicine* **207,** 2195–2206 (2010).
92. Müller-Sienerth, N. *et al.* SMAC Mimetic BV6 Induces Cell Death in Monocytes and Maturation of Monocyte-Derived Dendritic Cells. *PLoS ONE* **6,** e21556 (2011).
93. Srinivasula, S. M. *et al.* A conserved XIAP-interaction motif in caspase-9 and Smac/DIABLO regulates caspase activity and apoptosis. *Nature* **410,** 112–116 (2001).
94. Fulda, S. & Vucic, D. Targeting IAP proteins for therapeutic intervention in cancer. 1–16 (2012). doi:10.1038/nrd3627
95. Satpathy, A. T., Wu, X., Albring, J. C. & Murphy, K. M. Re(de)fining the dendritic cell lineage. *Nat Immunol* **13,** 1145–1154 (2012).
96. Vanden Berghe, T. *et al.* Determination of apoptotic and necrotic cell death in vitro and in vivo. *Methods* **61,** 117–129 (2013).
97. Hashimoto, D., Miller, J. & Merad, M. Dendritic cell and macrophage

heterogeneity in vivo. *Immunity* **35,** 323–335 (2011).
98. Merad, M., Sathe, P., Helft, J., Miller, J. & Mortha, A. The dendritic cell lineage: ontogeny and function of dendritic cells and their subsets in the steady state and the inflamed setting. *Annu. Rev. Immunol.* **31,** 563–604 (2013).
99. Steinman, R. M. & Cohn, Z. A. Identification of a novel cell type in peripheral lymphoid organs of mice. I. Morphology, quantitation, tissue distribution. *J. Exp. Med.* **137,** 1142–1162 (1973).
100. Garg, A. D. *et al.* Molecular and Translational Classifications of DAMPs in Immunogenic Cell Death. *Front Immunol* **6,** 588 (2015).
101. Kroemer, G., Galluzzi, L., Kepp, O. & Zitvogel, L. Immunogenic cell death in cancer therapy. *Annu. Rev. Immunol.* **31,** 51–72 (2013).
102. Kepp, O. *et al.* Molecular determinants of immunogenic cell death elicited by anticancer chemotherapy. *Cancer Metastasis Rev* **30,** 61–69 (2011).
103. Yamazaki, T. *et al.* Defective immunogenic cell death of HMGB1-deficient tumors: compensatory therapy with TLR4 agonists. *Cell Death and Differentiation* **21,** 69–78 (2014).
104. Salmon, H. *et al.* Expansion and Activation of CD103(+) Dendritic Cell Progenitors at the Tumor Site Enhances Tumor Responses to Therapeutic PD-L1 and BRAF Inhibition. *Immunity* **44,** 924–938 (2016).
105. Yatim, N. *et al.* RIPK1 and NF-κB signaling in dying cells determines cross-priming of $CD8^+$ T cells. *Science* **350,** 328–334 (2015).
106. Sánchez-Paulete, A. R. *et al.* Cancer Immunotherapy with Immunomodulatory Anti-CD137 and Anti-PD-1 Monoclonal Antibodies Requires BATF3-Dependent Dendritic Cells. *Cancer Discov* **6,** 71–79 (2016).
107. Aaes, T. L. *et al.* Vaccination with Necroptotic Cancer Cells Induces Efficient Anti-tumor Immunity. *CellReports* **15,** 274–287 (2016).
108. Moreno-Gonzalez, G., Vandenabeele, P. & Krysko, D. V. Necroptosis: A Novel Cell Death Modality and Its Potential Relevance for Critical Care Medicine. *Am J Respir Crit Care Med* **194,** 415–428 (2016).
109. Bracci, L., Schiavoni, G., Sistigu, A. & Belardelli, F. Immune-based mechanisms of cytotoxic chemotherapy: implications for the design of novel and rationale-based combined treatments against cancer. *Cell Death and Differentiation* **21,** 15–25 (2014).
110. Hanahan, D. & Folkman, J. Patterns and emerging mechanisms of the angiogenic switch during tumorigenesis. *Cell* **86,** 353–364 (1996).
111. Pećina-Slaus, N. Tumor suppressor gene E-cadherin and its role in normal and malignant cells. *Cancer Cell Int.* **3,** 17 (2003).
112. Qian, B. *et al.* A distinct macrophage population mediates metastatic breast cancer cell extravasation, establishment and growth. *PLoS ONE* **4,** e6562 (2009).
113. Ruffell, B. *et al.* Macrophage IL-10 blocks CD8+ T cell-dependent responses to chemotherapy by suppressing IL-12 expression in intratumoral dendritic cells. *Cancer Cell* **26,** 623–637 (2014).
114. Qian, B.-Z. *et al.* CCL2 recruits inflammatory monocytes to facilitate breast-tumour metastasis. *Nature* **475,** 222–225 (2011).
115. Teramukai, S. *et al.* Pretreatment neutrophil count as an independent prognostic factor in advanced non-small-cell lung cancer: an analysis of Japan Multinational Trial Organisation LC00-03. *Eur. J. Cancer* **45,** 1950–1958 (2009).
116. Lee, Y.-Y. *et al.* Pretreatment neutrophil:lymphocyte ratio as a prognostic factor in cervical carcinoma. *Anticancer Res.* **32,** 1555–1561 (2012).

117. Gondo, T. *et al.* Preoperative prediction of malignant involvement of resected ureters in patients undergoing radical cystectomy for bladder cancer. *Int. J. Urol.* **20,** 501–506 (2013).
118. Spicer, J. D. *et al.* Neutrophils promote liver metastasis via Mac-1-mediated interactions with circulating tumor cells. *Cancer Research* **72,** 3919–3927 (2012).
119. Huh, S. J., Liang, S., Sharma, A., Dong, C. & Robertson, G. P. Transiently entrapped circulating tumor cells interact with neutrophils to facilitate lung metastasis development. *Cancer Research* **70,** 6071–6082 (2010).
120. Cools-Lartigue, J. *et al.* Neutrophil extracellular traps sequester circulating tumor cells and promote metastasis. *J. Clin. Invest.* (2013). doi:10.1172/JCI67484
121. Kaplan, R. N. *et al.* VEGFR1-positive haematopoietic bone marrow progenitors initiate the pre-metastatic niche. *Nature* **438,** 820–827 (2005).
122. van Niel, G., Porto-Carreiro, I., Simoes, S. & Raposo, G. Exosomes: a common pathway for a specialized function. *J. Biochem.* **140,** 13–21 (2006).
123. Peinado, H., Lavotshkin, S. & Lyden, D. The secreted factors responsible for pre-metastatic niche formation: old sayings and new thoughts. *Seminars in Cancer Biology* **21,** 139–146 (2011).
124. Ratajczak, J., Wysoczynski, M., Hayek, F., Janowska-Wieczorek, A. & Ratajczak, M. Z. Membrane-derived microvesicles: important and underappreciated mediators of cell-to-cell communication. *Leukemia* **20,** 1487–1495 (2006).
125. Xiang, X. *et al.* Induction of myeloid-derived suppressor cells by tumor exosomes. *Int. J. Cancer* **124,** 2621–2633 (2009).
126. Al-Nedawi, K. *et al.* Intercellular transfer of the oncogenic receptor EGFRvIII by microvesicles derived from tumour cells. *Nature Cell Biology* **10,** 619–624 (2008).
127. Hao, N.-B. *et al.* Macrophages in Tumor Microenvironments and the Progression of Tumors. *Clinical and Developmental Immunology* **2012,** 1–11 (2012).
128. Skog, J. *et al.* Glioblastoma microvesicles transport RNA and proteins that promote tumour growth and provide diagnostic biomarkers. *Nature Cell Biology* **10,** 1470–1476 (2008).
129. Hao, S. *et al.* Epigenetic transfer of metastatic activity by uptake of highly metastatic B16 melanoma cell-released exosomes. *Exp. Oncol.* **28,** 126–131 (2006).
130. Strell, C. & Entschladen, F. Extravasation of leukocytes in comparison to tumor cells | Cell Communication and Signaling | Full Text. *Cell* (2008).
131. Aird, W. C. Phenotypic heterogeneity of the endothelium: I. Structure, function, and mechanisms. *Circ. Res.* **100,** 158–173 (2007).
132. Gupta, K., Shukla, M., Cowland, J. B., Malemud, C. J. & Haqqi, T. M. Neutrophil gelatinase-associated lipocalin is expressed in osteoarthritis and forms a complex with matrix metalloproteinase 9. *Arthritis Rheum* **56,** 3326–3335 (2007).
133. Miles, F. L., Pruitt, F. L., van Golen, K. L. & Cooper, C. R. Stepping out of the flow: capillary extravasation in cancer metastasis. *Clin Exp Metastasis* **25,** 305–324 (2008).
134. Sun, Z. *et al.* VEGFR2 induces c-Src signaling and vascular permeability in vivo via the adaptor protein TSAd.
135. Li, X. *et al.* VEGFR2 pY949 signalling regulates adherens junction integrity and metastatic spread. *Nat Commun* **7,** 11017 (2016).

136. van Hinsbergh, V. W. M. & van Nieuw Amerongen, G. P. Intracellular signalling involved in modulating human endothelial barrier function. *J Anat* **200,** 549–560 (2002).
137. Heyder, C. *et al.* Realtime visualization of tumor cell/endothelial cell interactions during transmigration across the endothelial barrier. *J. Cancer Res. Clin. Oncol.* **128,** 533–538 (2002).
138. Strilic, B. *et al.* Tumour-cell-induced endothelial cell necroptosis via death receptor 6 promotes metastasis. *Nature* **536,** 215–218 (2016).
139. Dvorak, H. F. Tumors: wounds that do not heal. Similarities between tumor stroma generation and wound healing. *N. Engl. J. Med.* **315,** 1650–1659 (1986).
140. Schäfer, M. & Werner, S. Cancer as an overhealing wound: an old hypothesis revisited. *Nat Rev Mol Cell Biol* **9,** 628–638 (2008).
141. Hanahan, D. & Coussens, L. M. Accessories to the Crime: Functions of Cells Recruited to the Tumor Microenvironment. *Cancer Cell* **21,** 309–322 (2012).
142. Komohara, Y., Jinushi, M. & Takeya, M. Clinical significance of macrophage heterogeneity in human malignant tumors. *Cancer Sci.* **105,** 1–8 (2014).
143. Lin, E. Y. *et al.* Vascular endothelial growth factor restores delayed tumor progression in tumors depleted of macrophages. *Mol Oncol* **1,** 288–302 (2007).
144. Stockmann, C. *et al.* Deletion of vascular endothelial growth factor in myeloid cells accelerates tumorigenesis. *Nature* **456,** 814–818 (2008).
145. Bergers, G. *et al.* Matrix metalloproteinase-9 triggers the angiogenic switch during carcinogenesis. *Nature Cell Biology* **2,** 737–744 (2000).
146. Nakasone, E. S. *et al.* Imaging Tumor-Stroma Interactions during Chemotherapy Reveals Contributions of the Microenvironment to Resistance. *Cancer Cell* **21,** 488–503 (2012).
147. Powell, D. R. & Huttenlocher, A. Neutrophils in the Tumor Microenvironment. *Trends in Immunology* **37,** 41–52 (2016).
148. Chen, D. S. & Mellman, I. Oncology meets immunology: the cancer-immunity cycle. *Immunity* **39,** 1–10 (2013).
149. Hildner, K. *et al.* Batf3 Deficiency Reveals a Critical Role for CD8 + Dendritic Cells in Cytotoxic T Cell Immunity. *Science* **322,** 1097–1100 (2008).
150. Fuertes, M. B. *et al.* Host type I IFN signals are required for antitumor CD8+ T cell responses through CD8{alpha}+ dendritic cells. *Journal of Experimental Medicine* **208,** 2005–2016 (2011).
151. Broz, M. L. *et al.* Dissecting the tumor myeloid compartment reveals rare activating antigen-presenting cells critical for T cell immunity. *Cancer Cell* **26,** 638–652 (2014).
152. Zecchin, A., Borgers, G. & Carmeliet, P. Endothelial cells and cancer cells: metabolic partners in crime? *Curr. Opin. Hematol.* **22,** 234–242 (2015).
153. Yeh, W. C. *et al.* Early lethality, functional NF-kappaB activation, and increased sensitivity to TNF-induced cell death in TRAF2-deficient mice. *Immunity* **7,** 715–725 (1997).
154. Varfolomeev, E. E. *et al.* Targeted disruption of the mouse Caspase 8 gene ablates cell death induction by the TNF receptors, Fas/Apo1, and DR3 and is lethal prenatally. *Immunity* **9,** 267–276 (1998).
155. Moulin, M. *et al.* IAPs limit activation of RIP kinases by TNF receptor 1 during development. *The EMBO Journal* 1–13 (2012). doi:10.1038/emboj.2012.18
156. Fan, C. *et al.* Lack of FADD in Tie-2 expressing cells causes RIPK3-mediated embryonic lethality. *Cell Death Dis* **7,** e2351 (2016).

157. Forget, M. A. *et al.* Macrophage Colony-Stimulating Factor Augments Tie2-Expressing Monocyte Differentiation, Angiogenic Function, and Recruitment in a Mouse Model of Breast Cancer. *PLoS ONE* **9,** e98623 (2014).
158. Kaiser, W. J. *et al.* RIP3 mediates the embryonic lethality of caspase-8-deficient mice. *Nature* **471,** 368–372 (2011).
159. Aghajanian, A., Wittchen, E. S., Allingham, M. J., Garrett, T. A. & Burridge, K. Endothelial cell junctions and the regulation of vascular permeability and leukocyte transmigration. *J. Thromb. Haemost.* **6,** 1453–1460 (2008).
160. Wolf, M. J. *et al.* Endothelial CCR2 signaling induced by colon carcinoma cells enables extravasation via the JAK2-Stat5 and p38MAPK pathway. *Cancer Cell* **22,** 91–105 (2012).
161. Hoeben, A. *et al.* Vascular endothelial growth factor and angiogenesis. *Pharmacol. Rev.* **56,** 549–580 (2004).
162. Dudek, S. M. & Garcia, J. G. Cytoskeletal regulation of pulmonary vascular permeability. *J. Appl. Physiol.* **91,** 1487–1500 (2001).
163. Eichmann, A. & Simons, M. VEGF signaling inside vascular endothelial cells and beyond. *Curr. Opin. Cell Biol.* **24,** 188–193 (2012).
164. Simons, M., Gordon, E. & Claesson-Welsh, L. Mechanisms and regulation of endothelial VEGF receptor signalling. *Nat Rev Mol Cell Biol* **17,** 611–625 (2016).
165. Xia, P. *et al.* Characterization of vascular endothelial growth factor's effect on the activation of protein kinase C, its isoforms, and endothelial cell growth. *J. Clin. Invest.* **98,** 2018–2026 (1996).
166. Sakurai, Y., Ohgimoto, K., Kataoka, Y., Yoshida, N. & Shibuya, M. Essential role of Flk-1 (VEGF receptor 2) tyrosine residue 1173 in vasculogenesis in mice. *Proc. Natl. Acad. Sci. U.S.A.* **102,** 1076–1081 (2005).
167. Takahashi, T., Yamaguchi, S., Chida, K. & Shibuya, M. A single autophosphorylation site on KDR/Flk-1 is essential for VEGF-A-dependent activation of PLC-gamma and DNA synthesis in vascular endothelial cells. *The EMBO Journal* **20,** 2768–2778 (2001).
168. Takahashi, T., Ueno, H. & Shibuya, M. VEGF activates protein kinase C-dependent, but Ras-independent Raf-MEK-MAP kinase pathway for DNA synthesis in primary endothelial cells. *Oncogene* **18,** 2221–2230 (1999).
169. Wythe, J. D. *et al.* ETS factors regulate Vegf-dependent arterial specification. *Developmental Cell* **26,** 45–58 (2013).
170. Murakami, M. *et al.* FGF-dependent regulation of VEGF receptor 2 expression in mice. *J. Clin. Invest.* **121,** 2668–2678 (2011).
171. De Val, S. *et al.* Combinatorial regulation of endothelial gene expression by ets and forkhead transcription factors. *Cell* **135,** 1053–1064 (2008).
172. Wei, G. *et al.* Ets1 and Ets2 are required for endothelial cell survival during embryonic angiogenesis. *Blood* **114,** 1123–1130 (2009).
173. Lammerts van Bueren, K. & Black, B. L. Regulation of endothelial and hematopoietic development by the ETS transcription factor Etv2. *Curr. Opin. Hematol.* **19,** 199–205 (2012).
174. Jinnin, M. *et al.* Suppressed NFAT-dependent VEGFR1 expression and constitutive VEGFR2 signaling in infantile hemangioma. *Nature Medicine* **14,** 1236–1246 (2008).
175. Ruan, G.-X. & Kazlauskas, A. Axl is essential for VEGF-A-dependent activation of PI3K/Akt. *The EMBO Journal* **31,** 1692–1703 (2012).
176. Carmeliet, P. & Collen, D. in *Vascular Growth Factors and Angiogenesis* **237,** 133–158 (Springer Berlin Heidelberg, 1999).
177. Ju, R. *et al.* Angiopoietin-2 secretion by endothelial cell exosomes:

regulation by the phosphatidylinositol 3-kinase (PI3K)/Akt/endothelial nitric oxide synthase (eNOS) and syndecan-4/syntenin pathways. *J. Biol. Chem.* **289,** 510–519 (2014).
178. Shiojima, I. & Walsh, K. Role of Akt signaling in vascular homeostasis and angiogenesis. *Circ. Res.* **90,** 1243–1250 (2002).
179. Zhao, Y. & Davis, H. W. Endotoxin causes phosphorylation of MARCKS in pulmonary vascular endothelial cells. *J. Cell. Biochem.* **79,** 496–505 (2000).
180. Issbrücker, K. *et al.* p38 MAP kinase--a molecular switch between VEGF-induced angiogenesis and vascular hyperpermeability. *The FASEB Journal* **17,** 262–264 (2003).
181. McMullen, M. E., Bryant, P. W., Glembotski, C. C., Vincent, P. A. & Pumiglia, K. M. Activation of p38 has opposing effects on the proliferation and migration of endothelial cells. *THEJOURNALOFBIOLOGICALCHEMISTRY* **280,** 20995–21003 (2005).
182. Rousseau, S., Houle, F., Landry, J. & Huot, J. p38 MAP kinase activation by vascular endothelial growth factor mediates actin reorganization and cell migration in human endothelial cells. *Oncogene* **15,** 2169–2177 (1997).
183. Liu, F. *et al.* Differential Regulation of Sphingosine-1-Phosphate- and VEGF-Induced Endothelial Cell Chemotaxis. *American Journal of Respiratory Cell and Molecular Biology* **24,** 711–719 (2001).
184. Kawamura, H. *et al.* Neuropilin-1 in regulation of VEGF-induced activation of p38MAPK and endothelial cell organization. *Blood* **112,** 3638–3649 (2008).
185. McMullen, M., Keller, R., Sussman, M. & Pumiglia, K. Vascular endothelial growth factor-mediated activation of p38 is dependent upon Src and RAFTK/Pyk2. *Oncogene* **23,** 1275–1282 (2004).
186. Turner, N. & Grose, R. Fibroblast growth factor signalling: from development to cancer. *Nature Reviews Cancer* **10,** 116–129 (2010).
187. Pepper, M. S., Ferrara, N., Orci, L. & Montesano, R. Potent synergism between vascular endothelial growth factor and basic fibroblast growth factor in the induction of angiogenesis in vitro. *Biochem. Biophys. Res. Commun.* **189,** 824–831 (1992).
188. Presta, M. *et al.* Fibroblast growth factor/fibroblast growth factor receptor system in angiogenesis. *Cytokine Growth Factor Rev.* **16,** 159–178 (2005).
189. Murakami, M. & Simons, M. Fibroblast growth factor regulation of neovascularization. *Curr. Opin. Hematol.* **15,** 215–220 (2008).
190. Seghezzi, G. *et al.* Fibroblast growth factor-2 (FGF-2) induces vascular endothelial growth factor (VEGF) expression in the endothelial cells of forming capillaries: an autocrine mechanism contributing to angiogenesis. *The Journal of Cell Biology* **141,** 1659–1673 (1998).
191. Chen, P.-Y. *et al.* The docking protein FRS2α is a critical regulator of VEGF receptors signaling. *Proceedings of the National Academy of Sciences* **111,** 5514–5519 (2014).
192. Ostrand-Rosenberg, S. Animal models of tumor immunity, immunotherapy and cancer vaccines. *Curr. Opin. Immunol.* **16,** 143–150 (2004).
193. PREHN, R. T. & MAIN, J. M. Immunity to methylcholanthrene-induced sarcomas. *J. Natl. Cancer Inst.* **18,** 769–778 (1957).
194. KLEIN, G., SJOGREN, H. O., KLEIN, E. & HELLSTROM, K. E. Demonstration of resistance against methylcholanthrene-induced sarcomas in the primary autochthonous host. *Cancer Research* **20,** 1561–1572 (1960).
195. OLD, L. J., CLARKE, D. A. & BENACERRAF, B. Effect of Bacillus Calmette-Guerin infection on transplanted tumours in the mouse. *Nature* **184(Suppl 5),** 291–292 (1959).

196. Van Pel, A. & Boon, T. Protection against a nonimmunogenic mouse leukemia by an immunogenic variant obtained by mutagenesis. *… of the National Academy of Sciences* (1982).
197. Höckendorf, U. *et al.* RIPK3 Restricts Myeloid Leukemogenesis by Promoting Cell Death and Differentiation of Leukemia Initiating Cells. *Cancer Cell* **30,** 75–91 (2016).
198. Seifert, L. *et al.* The necrosome promotes pancreatic oncogenesis via CXCL1 and Mincle-induced immune suppression. *Nature* (2016). doi:10.1038/nature17403
199. Rodriguez, D. A. *et al.* Characterization of RIPK3-mediated phosphorylation of the activation loop of MLKL during necroptosis. *Cell Death and Differentiation* **23,** 76–88 (2016).
200. Kang, T.-B., Yang, S.-H., Toth, B., Kovalenko, A. & Wallach, D. Caspase-8 Blocks Kinase RIPK3-Mediated Activation of the NLRP3 Inflammasome. *Immunity* 1–14 (2012). doi:10.1016/j.immuni.2012.09.015
201. Onizawa, M. *et al.* The ubiquitin-modifying enzyme A20 restricts ubiquitination of the kinase RIPK3 and protects cells from necroptosis. *Nat Immunol* **16,** 618–627 (2015).
202. Bertrand, M. J. M. *et al.* cIAP1/2 Are Direct E3 Ligases Conjugating Diverse Types of Ubiquitin Chains to Receptor Interacting Proteins Kinases 1 to 4 (RIP1–4). *PLoS ONE* **6,** e22356 (2011).
203. Chen, Z. J. & Sun, L. J. Nonproteolytic Functions of Ubiquitin in Cell Signaling. *Molecular Cell* **33,** 275–286 (2009).
204. Choo, Y. S. & Zhang, Z. Detection of protein ubiquitination. *JoVE* (2009). doi:10.3791/1293
205. Tran, H., Hamada, F., Schwarz-Romond, T. & Bienz, M. Trabid, a new positive regulator of Wnt-induced transcription with preference for binding and cleaving K63-linked ubiquitin chains. *Genes & Development* **22,** 528–542 (2008).
206. Kayagaki, N. *et al.* DUBA: a deubiquitinase that regulates type I interferon production. *Science* **318,** 1628–1632 (2007).
207. Guttman, J. A. & Finlay, B. B. Tight junctions as targets of infectious agents. *Biochimica et Biophysica Acta (BBA) - Biomembranes* **1788,** 832–841 (2009).
208. Barbero, S. *et al.* Caspase-8 association with the focal adhesion complex promotes tumor cell migration and metastasis. *Cancer Research* **69,** 3755–3763 (2009).
209. Finlay, D. & Vuori, K. Novel noncatalytic role for caspase-8 in promoting SRC-mediated adhesion and Erk signaling in neuroblastoma cells. *Cancer Research* **67,** 11704–11711 (2007).
210. Senft, J., Helfer, B. & Frisch, S. M. Caspase-8 interacts with the p85 subunit of phosphatidylinositol 3-kinase to regulate cell adhesion and motility. *Cancer Research* **67,** 11505–11509 (2007).
211. Torres, V. A., Mielgo, A., Barilà, D., Anderson, D. H. & Stupack, D. Caspase 8 promotes peripheral localization and activation of Rab5. *THEJOURNALOFBIOLOGICALCHEMISTRY* **283,** 36280–36289 (2008).
212. Torres, V. A. *et al.* Rab5 mediates caspase-8-promoted cell motility and metastasis. *Mol. Biol. Cell* **21,** 369–376 (2010).
213. Cursi, S. *et al.* Src kinase phosphorylates Caspase-8 on Tyr380: a novel mechanism of apoptosis suppression. *The EMBO Journal* **25,** 1895–1905 (2006).
214. Kim, M. P., Park, S. I., Kopetz, S. & Gallick, G. E. Src family kinases as

mediators of endothelial permeability: effects on inflammation and metastasis. *Cell Tissue Res.* **335,** 249–259 (2009).
215. García-Román, J. & Zentella-Dehesa, A. Vascular permeability changes involved in tumor metastasis. *Cancer Letters* **335,** 259–269 (2013).
216. De Bock, K., Georgiadou, M. & Carmeliet, P. Role of endothelial cell metabolism in vessel sprouting. *Cell Metab.* **18,** 634–647 (2013).
217. Spolarics, Z., Lang, C. H., Bagby, G. J. & Spitzer, J. J. Glutamine and fatty acid oxidation are the main sources of energy for Kupffer and endothelial cells. *Am. J. Physiol.* **261,** G185–90 (1991).
218. Mandal, P. *et al.* RIP3 induces apoptosis independent of pronecrotic kinase activity. *Molecular Cell* **56,** 481–495 (2014).
219. Kaiser, W. J., Daley-Bauer, L. P. & Thapa, R. J. RIP1 suppresses innate immune necrotic as well as apoptotic cell death during mammalian parturition. in (2014).
220. Berger, S. B. *et al.* Cutting Edge: RIP1 Kinase Activity Is Dispensable for Normal Development but Is a Key Regulator of Inflammation in SHARPIN-Deficient Mice. *The Journal of Immunology* **192,** 5476–5480 (2014).
221. Panaretakis, T. *et al.* The co-translocation of ERp57 and calreticulin determines the immunogenicity of cell death. *Cell Death and Differentiation* **15,** 1499–1509 (2008).
222. Diao, Y. *et al.* Dasatinib promotes paclitaxel-induced necroptosis in lung adenocarcinoma with phosphorylated caspase-8 by c-Src. *Cancer Letters* **379,** 12–23 (2016).
223. Deng, L. *et al.* STING-Dependent Cytosolic DNA Sensing Promotes Radiation-Induced Type I Interferon-Dependent Antitumor Immunity in Immunogenic Tumors. *Immunity* **41,** 843–852 (2014).
224. Corrales, L., McWhirter, S. M., Dubensky, T. W. & Gajewski, T. F. The host STING pathway at the interface of cancer and immunity. *J. Clin. Invest.* **126,** 2404–2411 (2016).
225. Müller, T. *et al.* The purinergic receptor P2Y2 receptor mediates chemotaxis of dendritic cells and eosinophils in allergic lung inflammation. *Allergy* **65,** 1545–1553 (2010).
226. Idzko, M. *et al.* Extracellular ATP triggers and maintains asthmatic airway inflammation by activating dendritic cells. *Nat Med* **13,** 913–919 (2007).

7. Curriculum Vitae

Kay Hänggi

Mühlackerstrasse 15

CH-9436 Balgach, Switzerland

Phone: +41 79 349 62 90

Email: haenggi@immunology.uzh.ch

Swiss nationality

Gender: male

Date of birth: 21.11.1985

Education

July 2012 to present

- *Ph.D. studies at Institute of Experimental Immunology, University of Zurich, Group of Dr. Wei-Lynn Wong*
- *Proposed title of thesis: RIPK3 promotes vascular permeability independent of its kinase activity in the tumor microenvironment*

September 2010 - February 2012

- *MSc in molecular and cellular Biology*
- *Master Thesis work (12 month) in the group of Prof. Dr. Alessandro Sartori, Institute of Molecular Cancer Research, University of Zurich*
- *Title of thesis: Establishing stable, inducible CtIP knockdown cell lines.*

September 2006 - July 2010

- *BSc in Biology, University of Zurich*

August 2002 - July 2006

- *Gymnasium: "Matura" in Economy and Law, Kantonsschule Heerbrugg*

Teaching activity during Ph.D studies

2014 to present

- *Supervision of yearly BIO430 course module "Cell death modalities" (3 days per year)*

September - December 2015

- *Supervision of undergraduate student*

July - August 2014

- *Supervision of undergraduate summer school student*

Fellowships/Awards

- *Candoc, Forschungskredit Universität Zürich 2014 (**54'000 CHF**)*
- *Peter Müller Fellowship 2013 (**40'000 CHF**) awarded from the Ph.D. program in Molecular Life Science Zurich*

Conferences/Talks/Posters

September 2016

- *Swiss apoptosis meeting, Bern (CH); **selected for talk.***

November 2015

- *Cell Death and Immunity, Cell Symposium, Berkeley, CA (USA); Poster presentation*

October 2015

- *ECDO Euroconference, Death Pathways and Beyond, Geneva (Switzerland); **Selected for flash talk** and poster presentation*

September 2015

- *Death Meeting, Cold Spring Harbour Laboratory NY (USA); **Selected for talk** and poster presentation but due to private reasons could not attend the conference.*

June 2015

- *Cancer, Inflammation, and Immunity, Cell Symposium, Sitges (Spain); Poster presentation*

May 2015

- *Conference on Tumor-Host Interaction and Angiogenesis, Ascona (Switzerland); Poster presentation*

January 2015

- *Charles Rudolphe Brupbacher Symposium, Breakthroughs in Cancer Research and Therapy, Zurich (Switzerland); Poster presentation*

November 2014

- *Society for Melanoma Research Congress, Zurich (Switzerland); Poster presentation*

September 2014

- *Swiss Apoptosis Meeting, University of Bern, Bern (Switzerland)*

January 2013

- *Charles Rudolphe Brupbacher Symposium, Breakthroughs in Cancer Research and Therapy, Zurich (Switzerland); Poster presentation*

September 2012

- *Swiss Apoptosis Meeting, University of Bern, Bern (Switzerland)*

Other work experience

2014-2015

- *Member of the "Molecular Life Science Zürich Graduate school" (MLS) steering committee as Ph.D student representative of the University of Zurich*

2014

- *Member of the organizing committee for the MLS Ph.D. retreat in August 2014 (appr. 100 participants)*

2006-2012

- *Every summer semester break I worked for 6-8 weeks in a company for plates and building materials in order to finance my studies; STARK AG 9450 Altstätten*

8. Publication record

- ***Kay Hänggi**, Lazaros Vasilikos, Janin Knop1, Aida Freire Valls, Kristy Rieck, Lisanne Spilgies, Tvisha Misra, John Bertin, Peter J. Gough, Thomas Schmidt, Carmen Ruiz de Almodovar, W. Wei-Lynn Wong; RIPK3 promotes vascular permeability via VEGF/p38 axis to allow tumor cell extravasation independent of its necroptotic function. **(In review at Cell Death and Disease**).*

- *Najoua Lalaoui[1,2], **Kay Hänggi**[3*], Gabriela Brumatti[1,2*], Diep Chau[1,2], Nhu-Y N. Nguyen[4,5], Lazaros Vasilikos[3], Lisanne Spilgies[3], Denise A. Heckmann[1,2], Chunyan Ma[1,2], Margherita Ghisi[6*], Jessica M. Salmon[6*], Geoff Matthews[6], Elisha de Valle[7], Donia Moujalled[4,5], Manoj B. Menon[8], Sukhdeep Spall[1,2], Stefan P. Glaser[1,2], Jennifer Richmond[9], Richard B. Lock[9], Lenka Munoz[10], Stephen M. Condon[11] Raffi Gugasyan[7], Matthias Gaestel[8], Mark Guthridge[4,5], Ricky W Johnstone[6], Andrew Wei[4,5], Paul G. Ekert[1,2,12], David L. Vaux[1,2], W. Wei-Lynn Wong[3] and John Silke[1,2#]; Targeting p38 or MK2 enhances the anti-leukemic activity of Smac-mimetics. **Cancer Cell** (Impact factor 23.5), February 2016 (Cited 1 time)*

- *Olga Murina, Christine von Aesch, Ufuk Karakus, Lorenza P. Ferretti, Hella A. Bolck**, K. Hänggi** and Alessandro A. Sartori1,3;*
  *FANCD2 and CtIP cooperate in the repair of DNA interstrand crosslinks. **Cell Rep** (Impact factor 8.3). 2014 May 22;7(4):1030-8. doi: 10.1016/j.celrep.2014.03.069. Epub 2014 May 1. (Cited 13 times)*

- *M. Steger, O. Murina, D. Hühn, L.P. Feretti, R. Walser, **K. Hänggi**, L. Lafranchi, C. Neugebauer, S. Paliwal, P. Janscak, B. Gerrits, G. Del Sal, O. Zerbe, and A.A. Sartori; Prolyl isomerase PIN1 regulates DNA double strand break repair by counteracting DNA end resection. Molecular Cell (Impact factor 14.0), vol. 50, no. 3, pp.333-343, May 2013. (Cited 24 times)*